Alois Herzog, BSc

Process monitoring of a fluidized bed pellet coating process via optical coherence tomography

MASTER'S THESIS

to achieve the university degree of

Diplom-Ingenieur

Master's degree programme: Chemical and Process Engineering

submitted to

Graz University of Technology

Supervisor

Univ.-Prof. Dipl.-Ing. Dr.techn. Johannes Khinast

Institute of Process and Particle Engineering

Dr. Daniel Markl
Research Center Pharmaceutical Engineering GmbH

Graz, October 2015

AFFIDAVIT

I declare that I have authored this thesis independently, that I have not used other than the declared sources/resources, and that I have explicitly indicated all material which has been quoted either literally or by content from the sources used. The text document uploaded to TUGRAZonline is identical to the present master's thesis dissertation.

12.10.2015

Date

Herzog Alois

Signature

Acknowledgement

First of all, i want to thank the members of the Research Center Pharmaceutical Engineering and the Institute of Process and Particle Engineering, which have supported me by creating this master thesis. Especially i want to thank my supervisor Dr. Daniel Markl for the outstanding support. Also, i want to thank Prof. Dr. Johannes Khinast for assessing the thesis. Last but not least my gratitude goes to my girlfriend Judith, to my family and friends.

Abstract

In the pharmaceutical industry pellets are often covered with a thin film applied by the fluidized bed technique. The covering also called “coating” typically aims to influence different properties of solid dosage forms such as taste, colour or the disintegration and dissolution behaviour in the human body. The determination of thickness and homogeneity of the coating layer are key factors for a successful and economic manufacturing. This thesis describes the characterisation of the coating of pellets produced by a fluidized bed coater. Optical coherence tomography (OCT) is used to perform the analysis of the coating thickness and homogeneity. In addition, an algorithm is developed and applied to evaluate the off- and in-line OCT data automatically. The measurement system and the algorithm are tested with two different test series (laboratory scale) to prove this new method for process monitoring.

Kurzfassung

In der pharmazeutischen Industrie werden Pellets häufig mit dem Wirbelschichtverfahren beschichtet. Die Beschichtung auch „coating“ genannt beeinflusst dabei verschiedenste Faktoren des pharmazeutischen Endproduktes, wie zum Beispiel den Geschmack, die Farbe oder die kontrollierte Wirkstofffreisetzung im menschlichen Körper. Die Bestimmung der Schichtdicke und die Gleichmäßigkeit der Coatingschicht sind somit wichtige Qualitätsmerkmale für eine erfolgreiche und wirtschaftliche Produktion. Ziel dieser Diplomarbeit ist die kontinuierliche Aufzeichnung der Coatingschichtdicke in einem Wirbelschichtcoater. Als Messverfahren wurde hierfür die optische Kohärenztomografie ausgewählt. Zusätzlich wurde ein Algorithmus für die automatisierte off- und in-line Datenauswertung implementiert. Mit zwei unterschiedlichen Testreihen (Labormaßstab) wurden das Messverfahren und der Algorithmus getestet, um die Eignung dieser neuen Methode für die Prozesskontrolle zu prüfen.

Table of Contents

List of Figures

List of Tables

Nomenclature

Symbol	Unit	Description
a	$[\sqrt{s}]$	Variable fitted with the automatic evaluated data (model from Turton)
Ar	[-]	Archimedes number
c_r	[g/min]	Spray rate of the coating (dry substance)
ct	[s]	Circulating time
cv	[%]	Relative standard deviation
cv_{sample}	[%]	Relative standard deviation of the mean coating thickness
d	[µm]	OCT measured coating thickness
d_{coat}	[µm]	Coating thickness theoretical growth model
$d_{coat+sample}$	[µm]	Coating thickness theoretical growth model with sampling
d_p	[µm]	Particle size
D	[µm]	True coating thickness
DS	[%]	Dry substance
g	[m/s^2]	Gravitation
i	[-]	Sample index
m_{coat}	[g]	Coating mass of one pellet
$m_{coat,i}$	[g]	Applied coating mass on the pellets
$m_{coating}$	[g]	Total mass of the coating material for one batch
m_{core}	[g]	Mass of one pellet without coating

Symbol	Unit	Description
$m_{pellets,0}$	[g]	Total mass of the pellets for one batch without coating
$m_{pellets,i}$	[g]	Mass of the pellets without coating for sample i
$m_{pellets+coat,i}$	[g]	Total mass of the pellets with coating for sample i
$m_{sample,coat,i}$	[g]	Coating mass for sample i
$m_{sample,i}$	[g]	Mass of the sampling weighed with a balance
n	[-]	Sum of the A-scan
n_a	[-]	Refractive index of air
n_c, n_{coat}	[-]	Refractive index of coating
n_i	[-]	Number of thickness measurements per sample
N	[-]	Number of the detected pellets per sample
N_{sample}	[-]	Number of the samples taken during the coating process
q	[%]	Ratio of the applied coating mass onto the pellets
q_{fit}	[%]	Loss of coating material during the process fitted with the automatic evaluated coating thickness
r, r_{core}	[mm]	Radius of one pellet
$r_{particle}$	[mm]	Particle radius of the pellet with coating
t	[min]	Process time
T_{coat}	[min]	Coating process time
$T_{sample,i}$	[min]	Point of time for sample i
U, U_0	[m/s]	Superficial gas velocity

Symbol	Unit	Description
U^*	[-]	Dimensionless superficial gas velocity
V	[m^3]	Total volume
V_H	[m^3]	Void volume
V_S	[m^3]	Solid volume
x	[g]	Mass of coating per pass through the spray zone
$\Delta T_{sample,i}$	[min]	Time interval between the samples
Δx	[nm]	Distance between the A-scans
ΔX	[µm]	Measuring position
ΔY	[µm]	Displacement of an OCT image
$\Delta\lambda$	[nm]	Spectral bandwidth
δ_{max}	[Pixel]	Hard constraint
ε	[-]	Factor for the porosity
θ_i	[°]	Angle of refraction
θ_j	[°]	Incident angle
λ_c	[nm]	Wavelength of the light source
μ_{ct}	[s]	Mean circulating time
$\mu_{cv,sample}$	[%]	Mean of RSD of the coating thickness
μ_f	[Pa·s]	Dynamic viscosity of the fluid
μ_i	[µm]	Measured coating thickness

Symbol	Unit	Description
μ_p	[µm]	Mean coating thickness detected pellet
μ_{sample}	[µm]	Mean coating thickness for the respective sample
μ_{tot}	[g]	Mean value of the coating mass on a particle
ρ_{coat}	[g/cm^3]	Density of the coating material
$\rho_{coat,m}$	[g/cm^3]	Medium density of the coating layer
ρ_{core}	[g/cm^3]	Density of the pellet
ρ_f	[g/cm^3]	Density fluid phase
ρ_g	[g/cm^3]	Density gas phase
ρ_p	[g/cm^3]	Density solid particles
σ_p	[µm]	Standard deviation detected pellet
σ_{sample}	[µm]	Standard deviation for the respective sample
σ_{tot}	[g]	Standard deviation of the coating mass on a particle
Ψ	[-]	Sphericity degree (average)

Abbreviations

API	Active pharmaceutical ingredient
B	Batch
BS	Bulk beam splitter
CCD	Charged coupled device
DC	Directional coupler
DG	Diffraction grating
FC	Fibre collimator
FDA	Food and drug administration
GM	Galvanometer mirror
L	Lens
M	Mirror
MRI	Magnetic resonance imaging
NIR	Near-infrared
OCT	Optical coherence tomography
PAT	Process analytical technology
PLC	Programmable logic controller
RSD	Relative standard deviation
SEM	Scanning electron microscopy
TPI	Terahertz pulse imaging

1 Introduction

The main task of the coating process is to cover the final pharmaceutical product against environmental condition and to influence different properties of the solid dosage form: taste, colour, surface properties or the location of disintegration and dissolution in the human body. Therefore, the method of coating for pharmaceutical products (e.g. tablets or pellets) becomes more important in the pharmaceutical industry. There are three basic coating processes: sugar coating, film coating and press coating. Sugar coating is a suitable application for thick coating layer and for masking the taste. Film coating is an effective method to manipulate the product characteristic. Press coating uses compression to form a coat around a preformed core and is generally used to separate chemically incompatible materials (Kumpugdee-Vollrath & Krause 2011).

1.1 Coating of Pharmaceutical Products

1.1.1 Coating Process

The coating solution is sprayed onto a moving bed of the solid dosage form using a special designed nozzle and atomizing air, as schematically illustrated in Fig. 1.1. In the spray zone the coating solution wets the surface of the moving particles. Outside of the spray zone, the particles are dried with a warm gas stream. The performance of the coating process is controlled by the movement of particles into and out of the spray zone (Turton 2008).

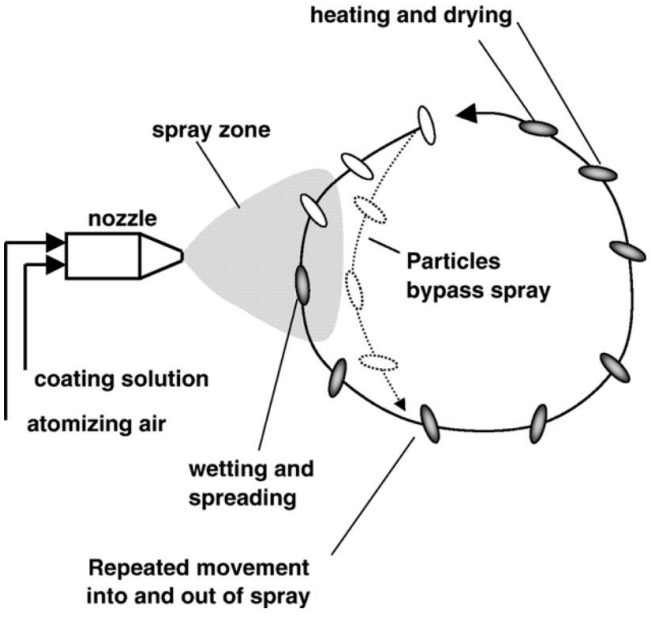

Fig. 1.1. Schematic of the coating process (Turton 2008).

The coating process depends on three phases: spraying, wetting and drying as shown in Fig. 1.2. At first, the droplets from the coating solution impact the surface and wet the particle. Then the particle is dried with a warm gas stream. Ideally, the drying of the particle is finished before reaching the spray zone again. Otherwise the particles can stick together or the surface is inhomogeneous. During the coating process, ideally each particle passes through the spray zone several times. Fig. 1.2 additionally illustrates an image from a typically film-coated tablet. This image was recorded by SEM (scanning electron microscopy) and shows the inhomogeneity of the coating layer (Suzzi et al. 2010).

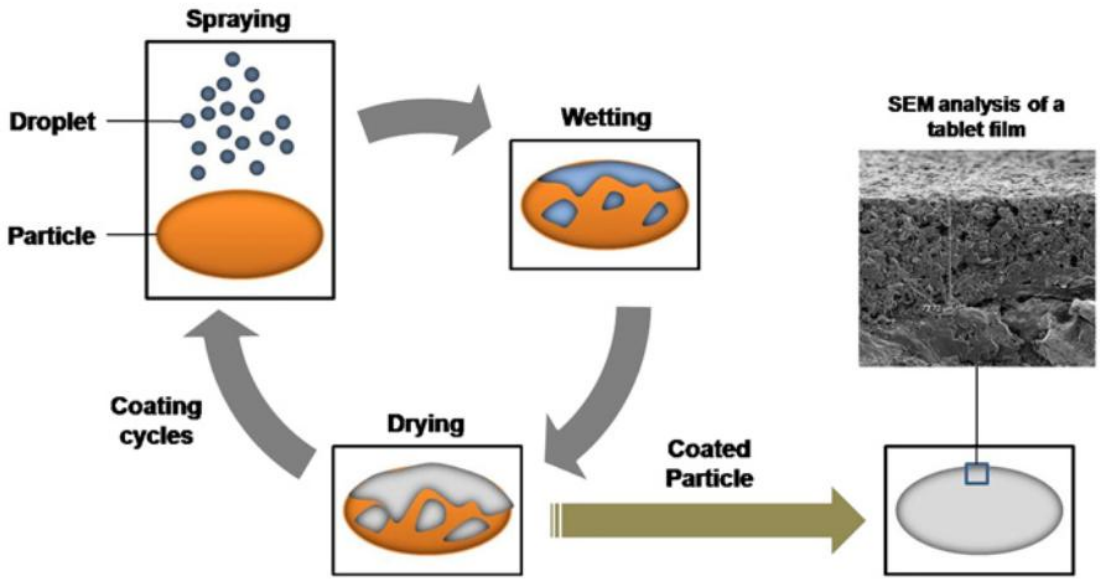

Fig. 1.2. Phases of the coating process (Suzzi et al. 2010).

1.1.2 Types of Pharmaceutical Coatings

Generally, there exist three types of coating for solid dosage forms. At first, non-functional coatings are for the design of the tablets, easier intake and swallowing. Functional coatings are applied to protect the API (active pharmaceutical ingredient) for example against the acid environment of the stomach or to mask a bad taste of the solid dosage form. The third type contains active coatings; the coating layer includes an API for example to combine different release behaviours. Tablets are typically coated in (perforated) drums or pans and pellet coating is performed in a fluid bed (Knop & Kleinebudde 2013).

1.1.3 Drum Coater

In a rotating drum (also referred to as a pan) coater, large solid forms (tablets) are moving through the spray zone. The nozzles bring in the coating solution with the atomizing air and with increasing process time the thickness of the coating layer is growing. Outside the spray zone, the particles are dried by a warm airflow through the perforated drum. The drum or pan coater is the classical method for the coating of pharmaceutical products and is frequently used. A schematic of a drum coater process is illustrated in Fig. 1.3 and a picture of a drum coater is shown in Fig. 1.4 (Glatt GmbH 2011).

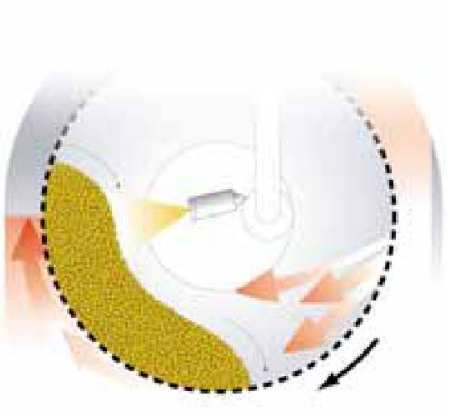

Fig. 1.3. Schematic of a drum coating process (Glatt GmbH 2011).

Fig. 1.4. Drum coater (Glatt GmbH 2011)

1.1.4 Fluidized Bed Coater

The particles (pellets) in this coating system are fluidized with a gas stream and the coating solution is sprayed on the moving bed of the particles. There are three different configurations for this type of coating process.

Fig. 1.5 illustrates the top spray coating process. The nozzle is placed over the moving bed of the particles and sprays the coating liquid against the airflow. The coating liquid is dried on the surface of the particle by the airflow. A low viscosity and the small droplets from the coating solution guarantee a uniform distribution of the coating layer.

Fig. 1.5. Top spray coating (Glatt GmbH 2014)

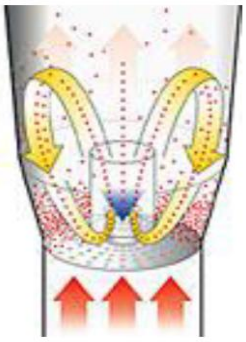

The bottom spray coating process is shown in Fig. 1.6. The nozzle is installed on the bottom of the coater. A special designed cylinder (Wurster) and a base plate with different perforation effects a circular product flow. With this method, a high quality of the pharmaceutical product is possible.

Fig. 1.6. Bottom spray coating (Glatt GmbH 2014)

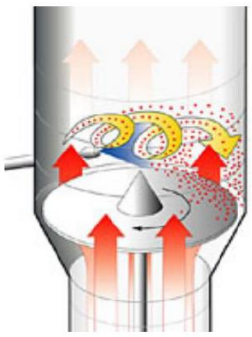

In the tangential spray coating process (Fig. 1.7), a rotating base plate sets the particles into a spiral motion. The spray nozzle is installed tangential to the rotor. Very thin coating layers are possible with this technique and it is ideal for coatings with high solid content (Glatt GmbH 2014).

Fig. 1.7. Tangential spray coating (Glatt GmbH 2014)

The critical process parameters for a fluidized bed coater are droplet size, coating solution spray rate, relative humidity, atomization air pressure, inlet and bed temperature and the drying time.

1.1.5 Fluidized Beds

The fluidized bed is an important industrial operation and is based on a multiphase flow. A gas stream is rising up through the bed and suspends the particles. This process is also called fluidization. The mixture of the particles is homogeneous because of the fluidization. In addition, an optimal mass- and heat-transport is reached between particle and gas flow. Therefore, the fluidized beds are used in combustion technology, coal gasification, exhaust gas treatment and for many other chemical processes. Fig. 1.8 illustrates the different flow regimes of fluidization depending on the superficial gas velocity (U).

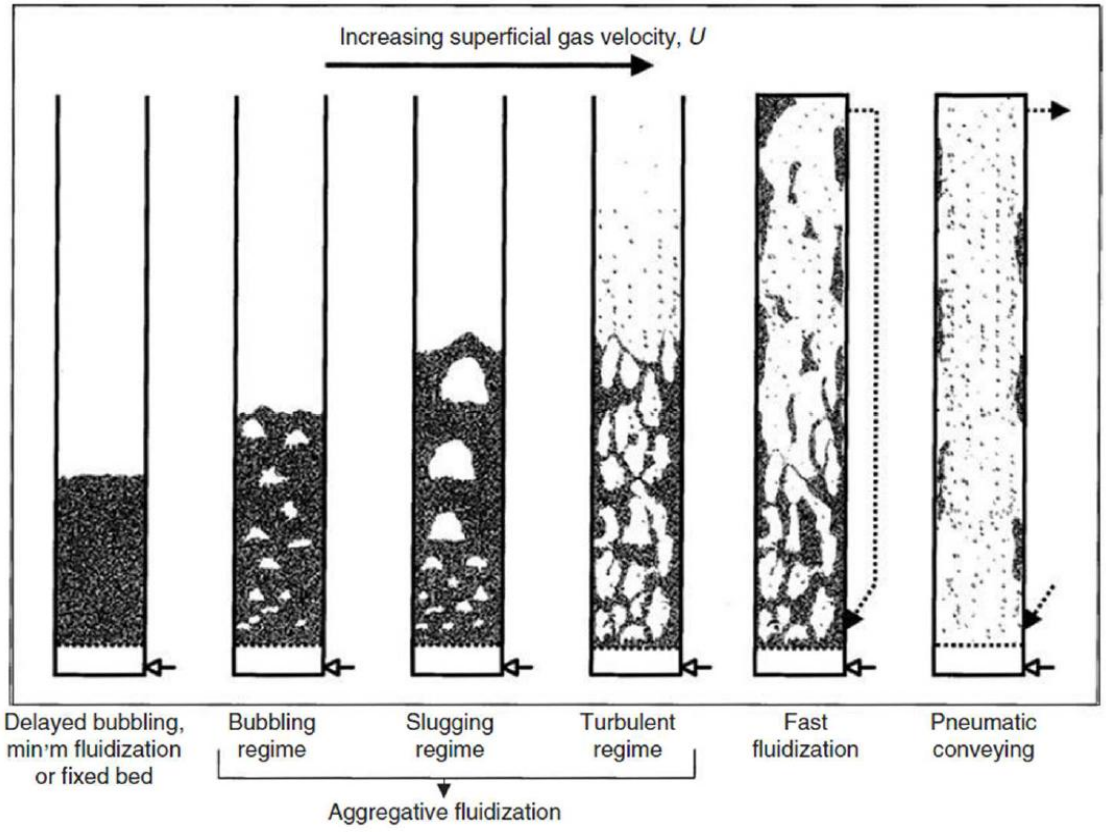

Fig. 1.8. The different flow regimes of fluidization (Clayton T. Crowe 2006).

The different flow regimes of the fluidization as shown in Fig. 1.8 are classified into the following groups:

- *Fixed bed:*

  Particles do not move leading to a poor energy transport through the bed, also referred to as delayed bubbling or minimum fluidization.

- *Moving bed:*

  Particles are moving as a whole through the reactor and the energy transport is also poor. The intersection between delayed bubbling and the bubbling regime.

- *Stationary fluidized beds:*

  The velocity of the gas stream is very low and thus only bubbles effect the fluidization, is also called bubbling or slugging regime.

- *Circulating fluidized beds:*

  The gas velocity is typically higher than the settling velocity of the particles. The particles transported out of the fluidized bed (as shown Fig. 1.8: the turbulent regime and fast fluidization) and with a separation device (cyclone) traced back to the reactor. The performance of the mass- and heat-transfer is much better than in stationary fluidized beds (Clayton T. Crowe 2006).

For all processes where particles are mixed with a fluid the Geldart classification is relevant. The Geldart diagram as shown in Fig. 1.9 is used for the classification of granular materials in fluidized beds. Test condition for the gas stream was dry air at ambient pressure and temperature. Classifications of the groups are depending on the particle size (d_p) and the relative density difference between the solid particles (ρ_p) and the gas phase (ρ_g).

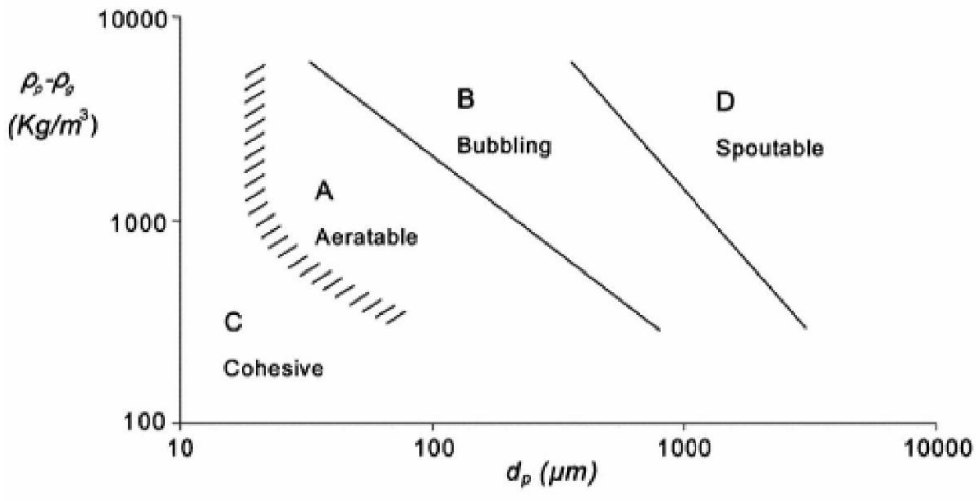

Fig. 1.9. Geldart's diagram (J.M. Valverde Millan 2013)

The diagram (Fig. 1.9) shows the following four groups:

- *Group A (aeratable):*

  This granular material has a small particle size and/or low particle density. The particle density is smaller than 1.4 g/cm^3 and this group of materials fluidizes easily.

- *Group B (bubbling):*

  The particle mean size is between 40 and 500 µm and the density is between 1.4 and 4.0 g/cm^3. A typical material of this group is sand. There is a small effect of cohesive forces between the particles.

- *Group C (cohesive):*

  The fluidization of these materials is very difficult due to the small particle size. The interparticle forces prevent the fluidization and thus for example, a mechanical stirrer is needed.

- *Group D (spoutable):*

  In this group of material, the particle mean size is large and the particles have high densities. A homogenous fluidization over the whole cross section is not possible (Geldart 1973) (J.M. Valverde Millan 2013).

A rough dimensioning of the fluidizing regime can be realized with the diagram from Grace (Fig. 1.10). The Archimedes number (Ar) can be calculated by Eq. (1.1) and is a function of gravitation (g), density fluid phase (ρ_f), density solid particles (ρ_p), particle size (d_p) and the dynamic viscosity of the fluid (μ_f) (Clayton T. Crowe 2006).

$$Ar = \frac{g \cdot \rho_f \cdot (\rho_p - \rho_f) \cdot d_p^3}{\mu_f^2} \tag{1.1}$$

The dimensionless superficial gas velocity (U^*) can be determine with the Archimedes number and the Grace diagram (Fig. 1.10). The superficial gas velocity (U_0) can be calculated by rearranging Eq. (1.2) (Clayton T. Crowe 2006).

$$U^* = \sqrt[3]{\frac{\rho_f^2}{(\rho_p - \rho_f) \cdot g \cdot \mu_f}} \cdot U_0 \tag{1.2}$$

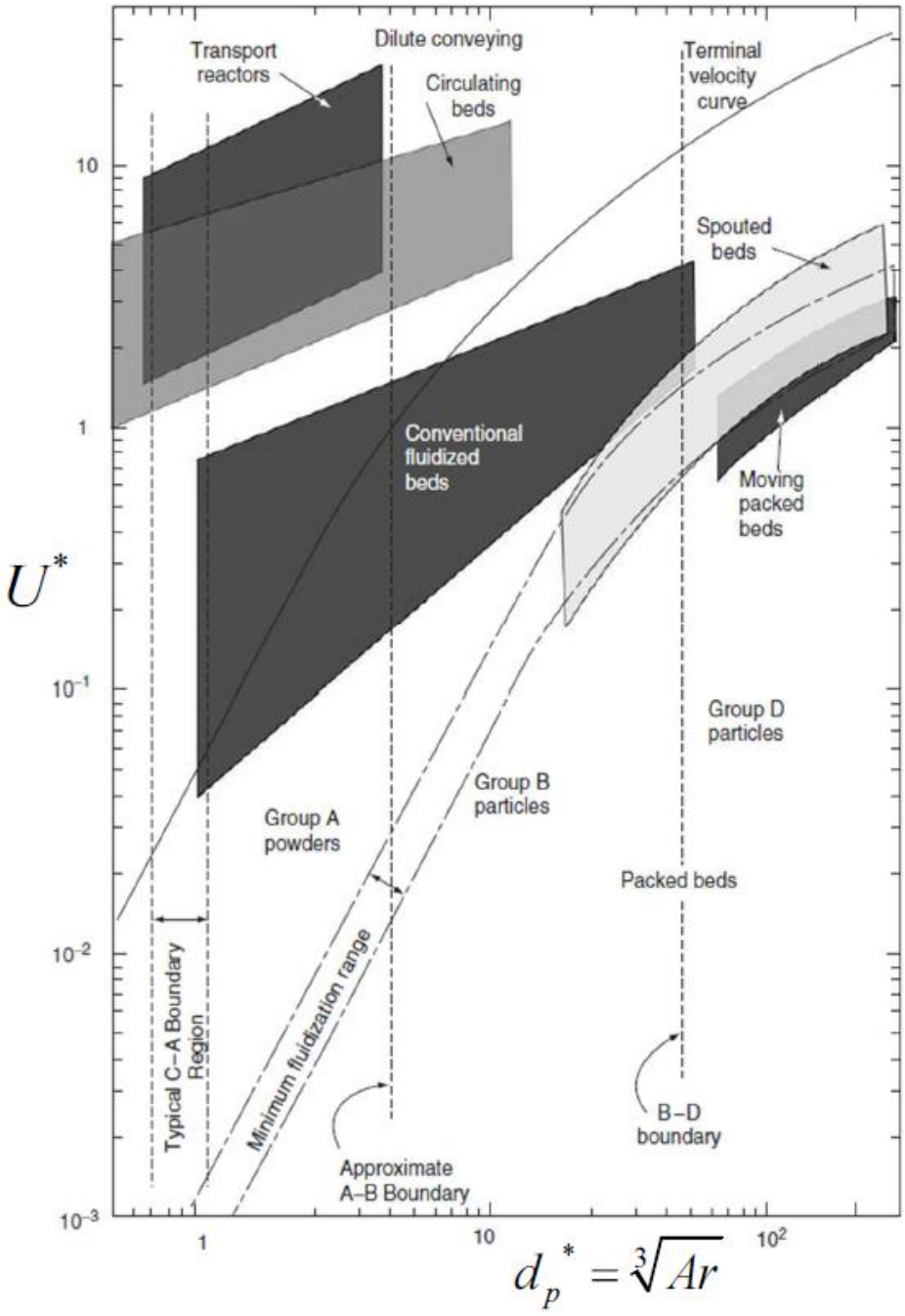

Fig. 1.10. Dimensionless flow regime map from Grace (Clayton T. Crowe 2006).

1.2 Process Analytics for Coating Processes

The U.S. FDA (food and drug administration) has defined a guideline for the improvement of the pharmaceutical development, manufacturing and quality assurance by using process analytical technology (PAT). PAT describes different methods for the analysing and the optimization of chemical processes. Main aim of this guideline is process automation, facilitating continuous processing, improving material and energy use. Also the reduction of production cycle times by using in-line control and measurement is a long term goal (FDA 2004).

Specifically, one of the most important quality parameters in pharmaceutical coating technologies are the thickness and the uniformity of the coat. Therefore, the direct or indirect determination of the coating thickness is essential. The homogeneity of the coating thickness of one single particle and between particles is described by the intra- and inter-particle variability. The different methods of sampling are illustrated in Fig. 1.11. The in-line sampling method measures directly at the product stream and the on-line method uses a bypass. The at-line method uses sampling and the analysis is close to the line. On the other hand, the off-line method is a discontinuous sampling and the analysis is executed in an extern laboratory. In this thesis, the in-line method is used for the determination of the coating thickness during the coating process and additional the sampling is analysed off-line with the optical coherence tomography system.

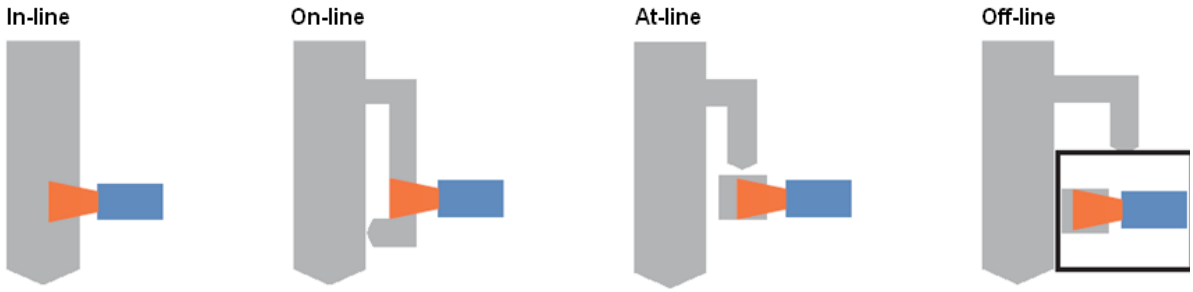

Fig. 1.11. Methods of sampling (Kessler 2006)

1.2.1 Methods for Measuring the Coating Thickness

The main task of this thesis is the in-line determination of the coating thickness during the process in a fluidized bed coater. Therefore, destructive methods, for example SEM, are not qualified (Ruotsalainen et al. 2003). Non-destructive analysis methods are spectroscopic techniques, such as NIR (near-infrared) and Raman spectroscopy. These methods have been successfully tested for the off- and in-line product characterization (Cahyadi et al. 2010). The main disadvantage of the spectroscopic techniques is that a calibration based on primary measurements (SEM) is necessary to predict the coating thickness. Therefore, the precision of the measured coating thickness depends on the calibration. Alternatives are tomographic techniques for example magnetic resonance imaging (MRI), terahertz pulse imaging (TPI) and optical coherence tomography (OCT). These methods allow the direct measurement of the coating thickness (Zeitler & Gladden 2008). TPI and OCT fulfil the requirements for the determination of the coating thickness during processing. The disadvantages of the TPI system are the long measurement times, high purchase price and the transversal and axial spatial resolutions are limited to 50 µm and 40 µm. On the other hand, OCT has a short measurement time, high axial (1-10 µm) and transversal (1-10 µm) resolutions. Also the easy handling, low costs, the separation of the sensor head and processing module make it to a promising technology for in-line process monitoring. Therefore, this thesis describes the process monitoring of a fluidized bed pellet coating process using an OCT sensor. The selected OCT system is described in detail in chapter 1.2.2 (Markl, Hannesschläger, et al. 2014).

1.2.2 OCT System

OCT is a non-destructive, contact and calibration free measuring system. It is a high-resolution imaging technique based on low-coherence interferometry (Fercher 2010) (Wojtkowski 2010). The OCT system was developed for the field of biomedicine, for example cardiology (Bezerra et al. 2009), dermatology (Sattler et al. 2013) and endoscopy (Adler et al. 2009). Recently the OCT system is also used in the material science and the quality control.

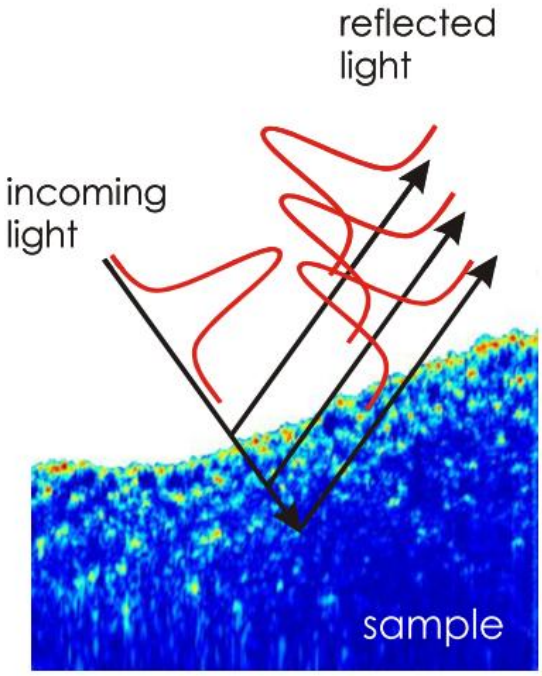

Fig. 1.12. Detection scheme of OCT (Recendt GmbH 2002)

The detection scheme of an OCT system is illustrated in Fig. 1.12. The physically method of OCT is the interferometric superposition of a reference light wave (in the range of infrared) with the back-reflected light wave from the different layers in the sample. The back-reflected light wave contains the depth information of the sample by detecting the intensity and the travelling time. Thus, OCT allows the generation of cross-sectional, depth-resolved, two- and three-dimensional images of translucent materials (Recendt GmbH 2002).

An off-line OCT image of a commercially available tablet (Thrombo ASS®) with enteric coating is illustrated in Fig. 1.13. Image contrast and penetration depth of the tablets strongly depend on the different operating wavelengths of the light source, optical properties of the coating layer and the tablet or the pellet core (Markl, Hannesschläger, et al. 2014).

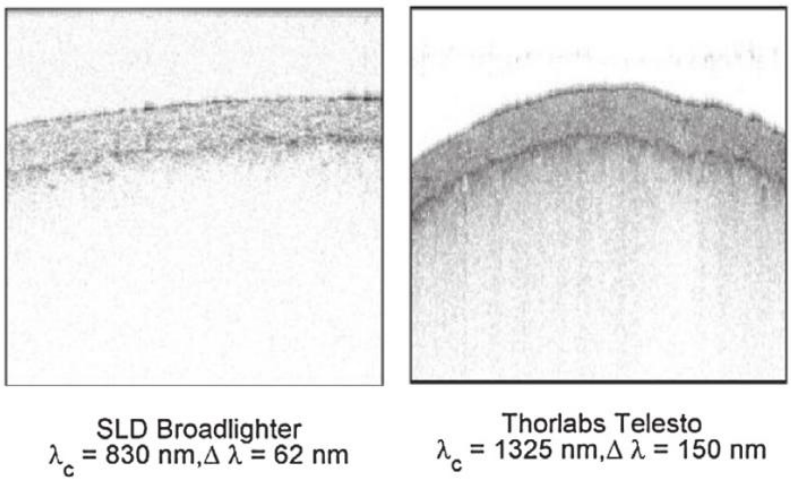

Fig. 1.13. OCT images of Thrombo ASS® with different wavelengths (Markl, Hannesschläger, et al. 2014).

Fig. 1.14 shows a schematic of the experimental design of an OCT system. The spectrometer includes a charged coupled device (CCD), a lens (L3), a diffraction grating (DG) and a fibre collimator (FC). The light beam generated from the light source passes a directional coupler (DC). The 3-D sensor head consist of a fibre collimator (FC), a bulk beam splitter (BS), a lens (L2) and the reference arm with a gold coated mirror (M). The BS splits the light into a probe and a reference beam. The 3-D sensor additionally includes two galvanometer mirrors (GM1 and GM2), and a lens (L1). The GMs are in synchrony with the camera read out. A 3-D sensor can be used as a 2-D sensor by turning off one galvanometer mirror and as a 1-D sensor by turning off both galvanometer mirrors (Markl, Hannesschläger, Sacher, Buchsbaum, et al. 2015).

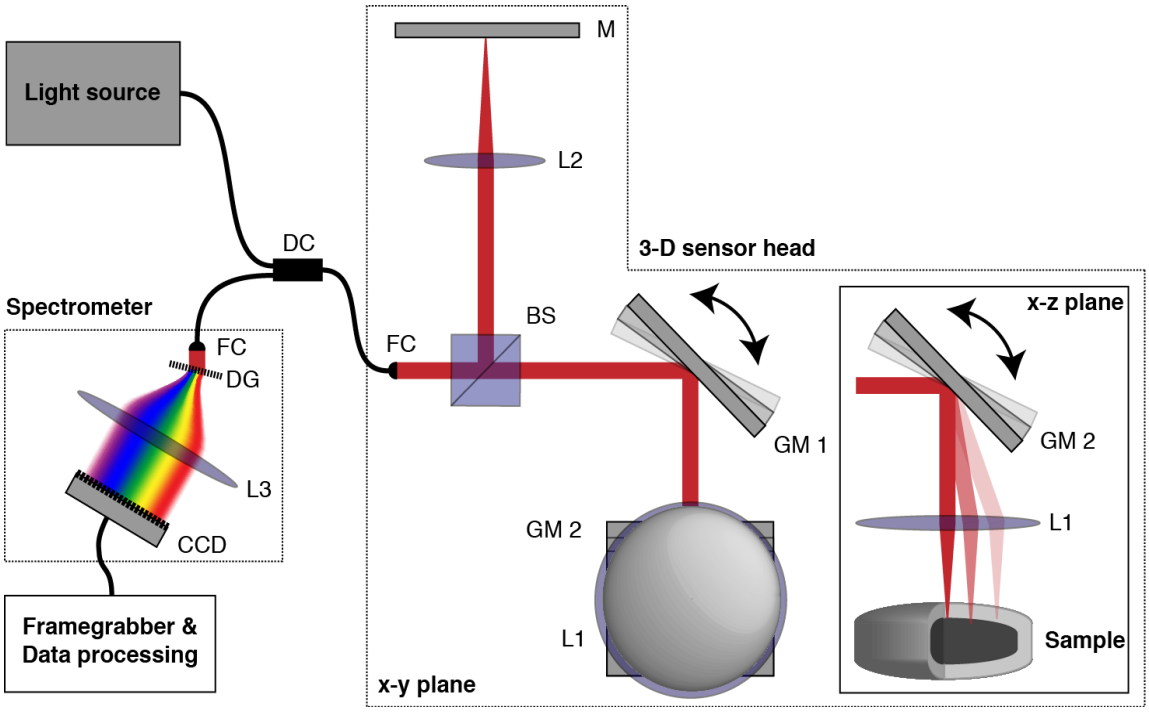

Fig. 1.14. Schematic of the OCT (experimental design). The sensor head can be exchanged easily (Markl, Hannesschläger, Sacher, Buchsbaum, et al. 2015). CCD-charged coupled device, L-lenses, DG-diffraction grating, FC-fibre collimator, DC-directional coupler, BS-bulk beam splitter, M-mirror, GM-galvanometer mirrors.

The OCT system with the 3D sensor head for the off-line measurement is illustrated in Fig. 1.15.

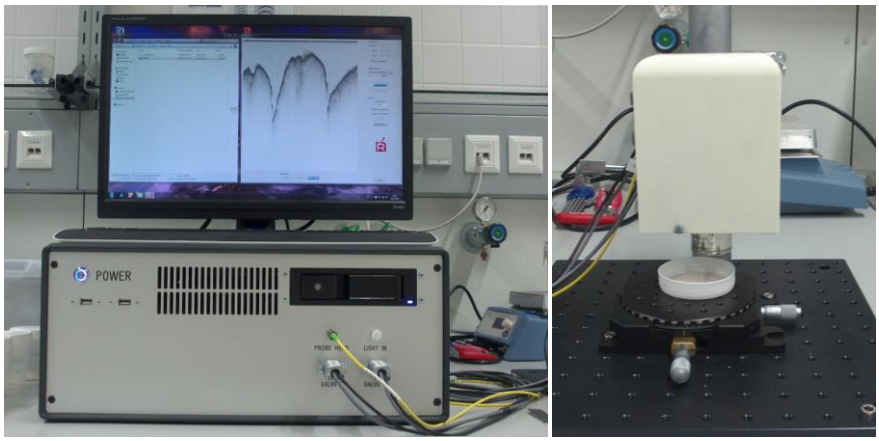

Fig. 1.15. OCT system with the 3D sensor head for the off-line measurement.

Such a 1-D sensor generates single depth profiles, so-called A-scans. A B-scan as illustrated in Fig. 1.16 is a cross-sectional image generated by scanning the incident optical beam transversely. A B-scan can be generated with a 2-D sensor (off-line) or by moving the sample in transverse direction relative to the sensor head (in-line). The 1-D sensor is suitable for the in-line monitoring and the 3-D sensor is for the off-line monitoring.

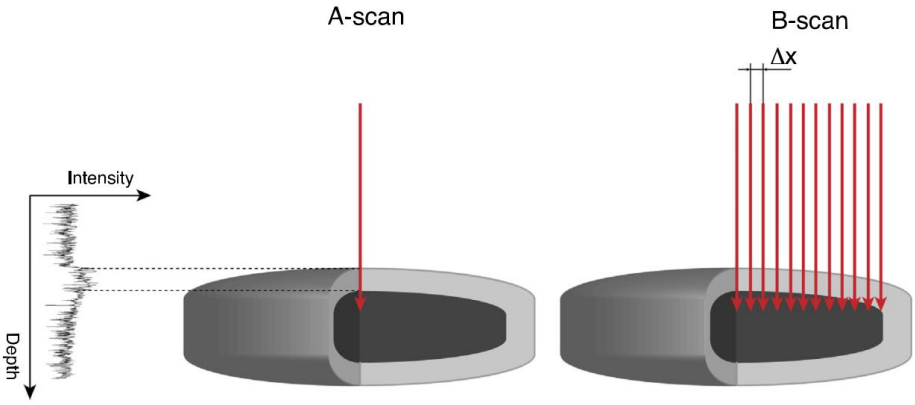

Fig. 1.16. A-scan and B-scan (Markl, Hannesschläger, et al. 2014).

In addition, an off-line 3D volumetric image from a sample can be generated with the OCT system. For example, a 3D volumetric image of a film-coated tablet measured by OCT is illustrated in Fig. 1.17. The volume of the film-coated tablet is composed by several hundred B-scans in y direction.

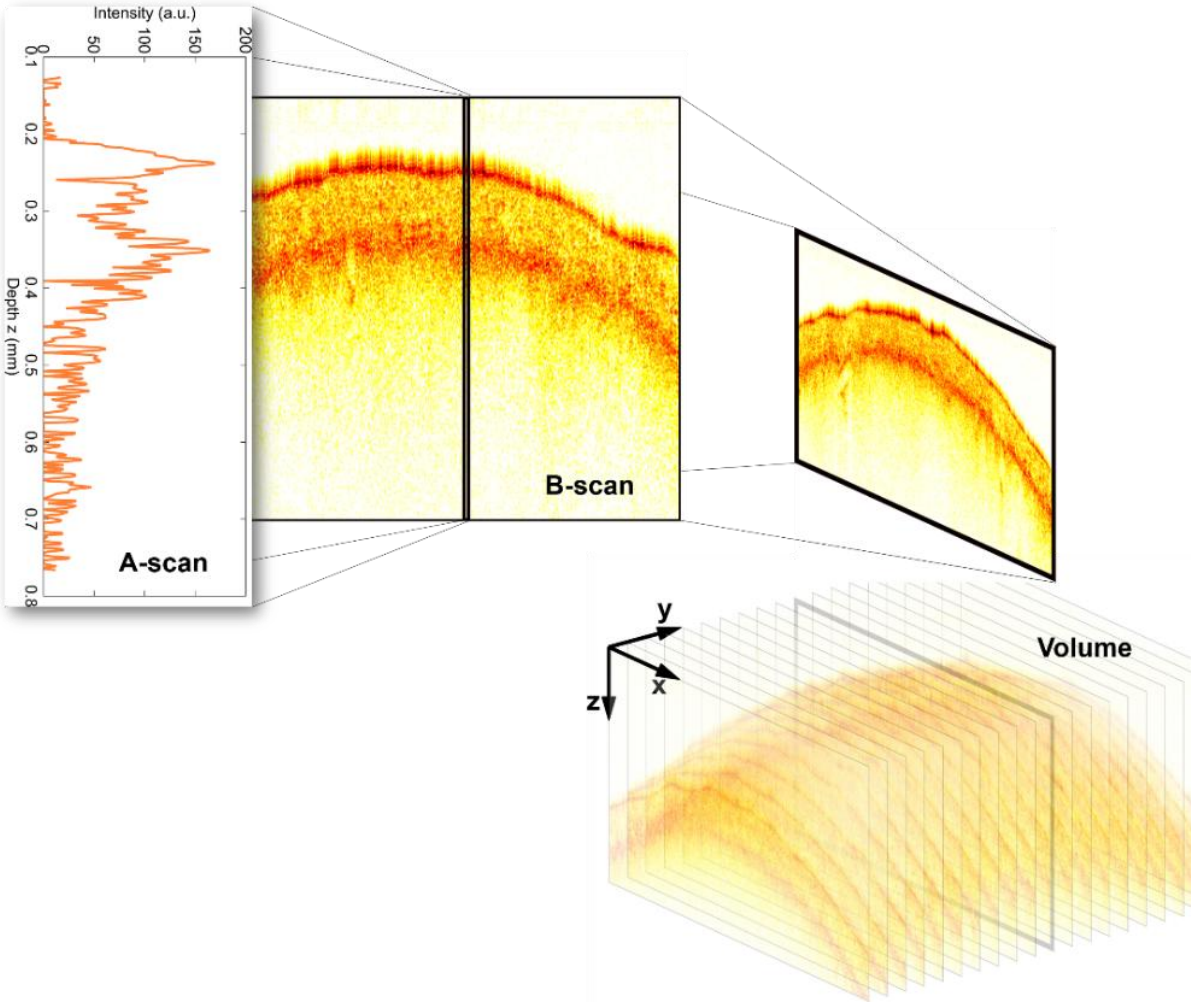

Fig. 1.17. 3D volumetric image of a film-coated tablet composed by B-scans. A-scan=single-depth scan and B-scan=cross-section (Markl, Hannesschläger, Sacher, Buchsbaum, et al. 2015).

1.3 Scope of this Work

In the literature, many different methods of measuring the coating thickness of pharmaceutical products are available. This work should describe the process monitoring of a fluidized bed pellet coating process using OCT. The OCT system fulfils the requirements for the determination of the coating thickness during the process in a fluidized bed coater. The determination of the thickness and the homogeneity of the layer are key factors for the quality of the final product. First, experiments are designed, including material and process parameter selection. After that, the experiments and comparison measurements are conducted. The main part of this work is the automated evaluation of the off-line OCT data.

1.3.1 Experimental Setup

The experimental setup for the measuring of the coating thickness during the coating process is illustrated in Fig. 1.18. An airflow technology coater (INNOJET® VENTILUS 2.5 / 1), an OCT system and a data processing unit is used in this work. An inspection window is located at the spray zone of the fluid bed coater. A thin plastic protection foil is fixed between the sensor head from the OCT system and the spray zone (Markl, Zettl, et al. 2014).

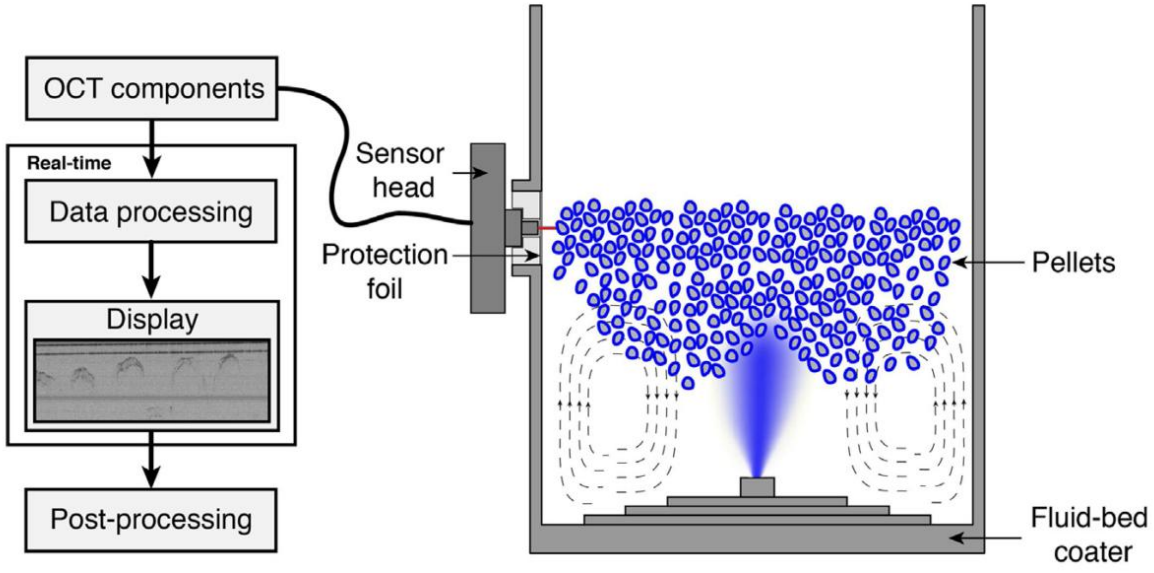

Fig. 1.18. Schematic of the fluid bed coater and the OCT system (Markl, Zettl, et al. 2014).

1.3.2 Measurement Errors

At the determination of the coating thickness, the following measurement errors occur with the OCT system. In the fluidized bed coater, the imaging plane from the OCT system might be displaced from the center of the pellet. Fig. 1.19 illustrates the displacement (ΔY) of the OCT image, which introduces a thickness measurement error (Markl, Zettl, et al. 2014).

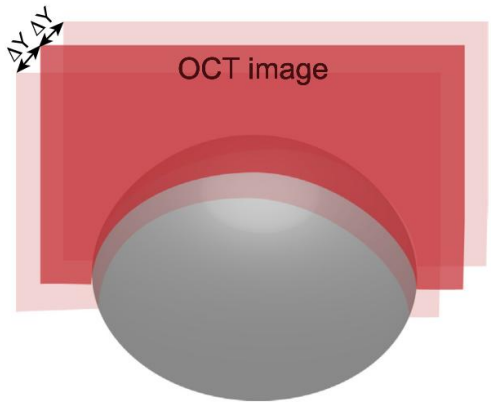

Fig. 1.19. Displacement (ΔY) of an OCT image (Markl, Zettl, et al. 2014).

In case of the in-line monitoring, the velocity of the pellets at the inspection window (Fig. 1.18) is unknown causing a horizontal stretching of the pellets in the OCT image. The curvature of the pellets also affects a measurement error as shown in Fig. 1.20. The red arrows indicate the thickness measurements on different measuring positions (ΔX). In addition, one path of the optical beam is illustrated in detail. The optical beam is retracted by the air/coating interface, which introduce the OCT measured coating thickness (d). According to the Snell's law described in Eq. (1.3) the true coating thickness (D) by measuring normal to the pellet surface can be determined. Snell's law describes the relation between the incident angle (θ_j) and the angle of refraction (θ_i). The refractive indices of air and coating is denoted by n_a and n_c (Markl, Zettl, et al. 2014).

$$n_a \cdot \sin\theta_j = n_c \cdot \sin\theta_i \tag{1.3}$$

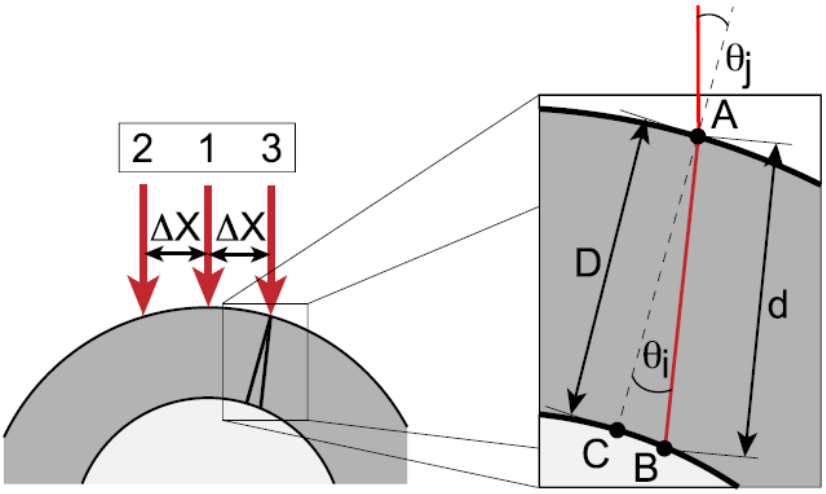

Fig. 1.20. Cross section model of a pellet. ΔX-measuring position, θ_j-incident angle, θ_i-angle of refraction, d-OCT measured coating thickness, D-true coating thickness (Markl, Zettl, et al. 2014).

1.3.3 Minimization of the Measurement Errors

The measurement error induced by the velocity of the pellets could be corrected by the following approach (see Fig. 1.21): The material for the coating process has a defined ideal spherical distribution. In Fig. 1.21(a), one ideal spherical pellet with the blue cycle is illustrated and the grey ellipse shows one image from the OCT system. The pellet contour in the OCT image is similar to an ellipse due to the velocity of the pellet. The coordinates of the ellipse (x_1 and z_1) can be calculated with an algorithm. This algorithm transforms the pellet contour to a circle (Fig. 1.21(b)) enabling the determination of the true coating thickness (D).

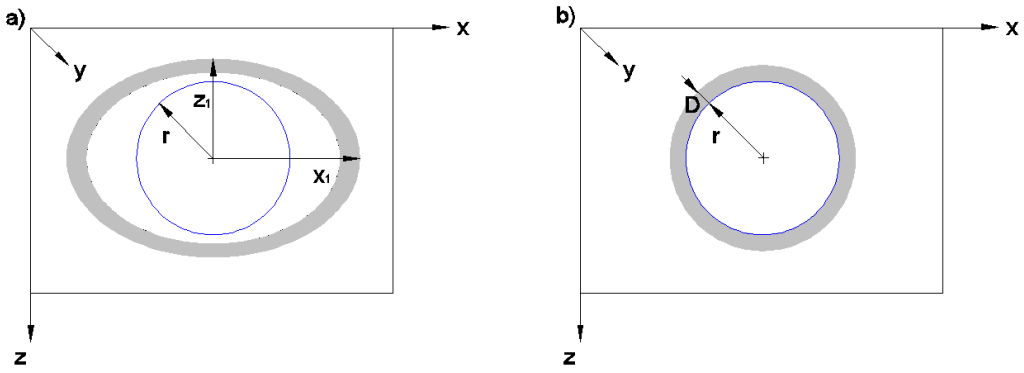

Fig. 1.21. Method for the data evaluation. (a) illustrates one ideal spherical pellet (blue) with the radius (r) and the OCT image (grey) with the coordinates (x_1 and z_1). A proper transformation of the OCT image from (a) to (b) allows the determination of the true coating thickness (D).

1.3.4 Theoretical Growth Model

The theoretical coating thickness as a function of the process time can be calculated with the following theoretical growth model. The simplifications for the growth model are:

- The pellets have an ideal spherical shape with the same diameter and without pores.
- During the process the number of particles does not change; abrasion, breakage of the particles and agglomeration of several particles does not occur.
- The coating material is sprayed uniformly on all pellets (Kumpugdee-Vollrath & Krause 2011).

The mass of one pellet m_{core} without coating is defined in Eq. (1.4), where r_{core} is the radius and ρ_{core} the density of the pellet.

$$m_{core} = \frac{4 \cdot \pi}{3} \cdot r_{core}^3 \cdot \rho_{core} \tag{1.4}$$

The coating layer is similar to a spherical shell and the coating mass of one pellet as a function of the process time $m_{coat}(t)$ can be calculated with Eq. (1.5) with $r_{particle}(t)$ as the particle radius of the pellet with coating and ρ_{coat} as the density of the coating material.

$$m_{coat}(t) = \left[\frac{4 \cdot \pi}{3} \cdot r_{particle}^3(t) - \frac{4 \cdot \pi}{3} \cdot r_{core}^3\right] \cdot \rho_{coat} \tag{1.5}$$

In Eq. (1.6) $r_{particle}(t)$ is defined as the sum of r_{core} and the coating thickness $d_{coat}(t)$.

$$r_{particle}(t) = r_{core} + d_{coat}(t) \tag{1.6}$$

Inserting $r_{particle}(t)$ into the function $m_{coat}(t)$ results in Eq. (1.7).

$$m_{coat}(t) = \frac{4 \cdot \pi}{3} \cdot \left[\left(r_{core} + d_{coat}(t)\right)^3 - r_{core}^3\right] \cdot \rho_{coat} \tag{1.7}$$

Using the weight gain of the coating, i.e. the ratio of $m_{coat}(t)$ and m_{core}, the coating thickness $d_{coat}(t)$ can be calculated (see Eq. (1.8)). The mass of the pellets for one batch without coating is defined by $m_{pellets,0}$ and $c_r(t)$ describes the spray rate (dry substance) of the coating.

$$\frac{m_{coat}(t)}{m_{core}} = \frac{c_r . t}{m_{pellets,0}} \tag{1.8}$$

The ratio of $m_{coat}(t)$ and m_{core} using Eq. (1.4) and (1.7) is defined in Eq. (1.9).

$$\frac{m_{coat}(t)}{m_{core}} = \left[\frac{\left(r_{core} + d_{coat}(t)\right)^3}{r_{core}^3} - 1\right] \cdot \frac{\rho_{coat}}{\rho_{core}} \tag{1.9}$$

Inserting Eq. (1.9) into Eq. (1.8), the coating thickness $d_{coat}(t)$ as a function of the process time t can be calculated as seen in Eq. (1.10).

$$d_{coat}(t) = r_{core} \cdot \left(\left(\frac{c_r . t}{m_{pellets,0}} \cdot \frac{\rho_{core}}{\rho_{coat}} + 1\right)^{\frac{1}{3}} - 1\right) \tag{1.10}$$

Eq. (1.10) needs to be adapted to consider the sampling for the off-line measurement. The time interval $\Delta T_{sample,i}$ between the samples as a function of the sample index i ($i = 1, \dots, N_{sample}$) is defined in Eq.(1.11). N_{sample} is the number of the samples taken during the coating process and the point of time is described with $T_{sample,i}$.

$$\Delta T_{sample,i} = \begin{cases} T_{sample,i} & \text{if } i = 1 \\ T_{sample,i} - T_{sample,i-1} & \text{otherwise} \end{cases} \tag{1.11}$$

The total mass of the pellets with coating $m_{pellets+coat,i}$ is defined in Eq. (1.12). The variable $m_{pellets,i}$ describes the mass of the pellets without coating and $m_{coat,i}$ considers the already applied coating mass on the pellets (see Eq. (1.15)).

$$m_{pellets+coat,i} = m_{pellets,i-1} + c_r \cdot \Delta T_{sample,i} + m_{coat,i-1} \tag{1.12}$$

The coating mass for sample i is defined as $m_{sample,coat,i}$ and can be calculated with Eq. (1.13). The mass of the sample is described with $m_{sample,i}$ and were weighed with a balance.

$$m_{sample,coat,i} = \frac{m_{sample,i}}{m_{pellets+coat,i}} \cdot \left(c_r \cdot \Delta T_{sample,i} + m_{coat,i-1}\right) \tag{1.13}$$

The mass of the pellets without coating $m_{pellets,i}$ as a function of the sample index i is expressed in Eq (1.14).

$$m_{pellets,i} = m_{pellets,i-1} - \left[m_{sample,i} - m_{sample,coat,i}\right] \tag{1.14}$$

$$m_{coat,i} = \begin{cases} 0 & \text{if } i = 1 \\ m_{coat,i-1} - m_{sample,coat,i} + c_r \cdot \Delta T_{sample,i} & \text{otherwise} \end{cases} \tag{1.15}$$

The Eq. (1.10) can be split into two functions $func(r,k)$ and $K(t)$ as illustrated in Eq. (1.16) and Eq. (1.17). The variable q describes the loss of coating material during the process, for example on the wall of the product container or on the filter bags. This variable can be fitted by the measured coating thickness from the OCT data.

$$func(r,K) = r \cdot \left(\left(K \cdot \frac{\rho_{core}}{\rho_{coat}} + 1 \right)^{\frac{1}{3}} - 1 \right) \tag{1.16}$$

$$K(t) = q \cdot \frac{c_r \cdot t}{m_{pellets,i}} \tag{1.17}$$

The coating thickness under consideration of the sampling (used for off-line measurement) $d_{coat+sample}(t)$ can be calculated by inserting Eq. (1.16) into Eq. (1.18).

$$d_{coat+sample}(t) = \begin{cases} func(r,K) & \text{if } i = 1 \\ d_{coat+sample}\left(T_{sample,i-1}\right) + func\left(r + d_{coat+sample}\left(T_{sample,i-1}\right), K\right) & \text{otherwise} \end{cases} \tag{1.18}$$

2 Materials

This thesis presents the coating of pellets using a fluid bed process. Pellets are spherical particles with a mean particle size between 400 and 2000 µm. Pellets can be produced by different ways: for example in a fluidized bed rotor chamber or with extrusion and a following spheronization process. Pellets are usually film coated to manipulate the product characteristic. The final pellets can be either taken orally in form of tablets or as capsules (Šibanc et al. 2013).

On the market a broad range of pellets is available. A defined ideal spherical distribution of the pellets is preferable for the experiments and the data evaluation. In this thesis, two different kinds of pellets and coating material were selected. First, calcium stearate pellets were coated with Dynasan® 118. Three experiments (referred to as B01, B02, and B03) were operated with these materials and under exactly the same process conditions. Second, Cellets® were coated with Eudragit® L 30 D-55, which is henceforth referred to as experiment B04.

2.1 Pellets: Calcium Stearate

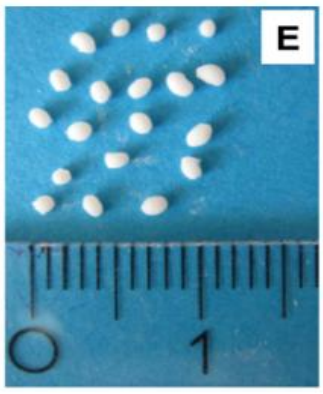

Fig. 2.1. Calcium stearate pellets (Roblegg et al. 2011)

The pellets (Fig. 2.1) are composed of a matrix carrier with calcium stearate 75% (w/w), the API is paracetamol 20% (w/w), the plasticizer is glycerol monostearate 5% (w/w) and were manufactured from the Research Center Pharmaceutical Engineering GmbH, Graz, Austria (Roblegg et al. 2011). The material data from the used calcium stearate pellets is listed in Table 2.1 (Markl, Zettl, et al. 2014).

2.2 Pellets: Cellets®

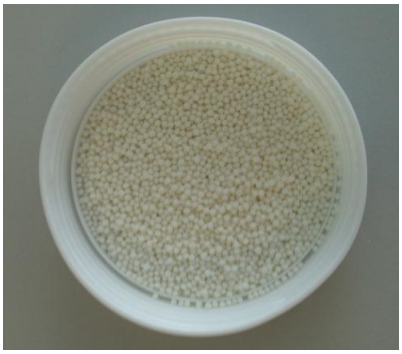

Fig. 2.2. Cellets® pellets

The Cellets® as shown in Fig. 2.2 consist of microcrystalline cellulose. The chosen particle size distribution is about 1000-1400 µm and it is produced by Pharmatrans-Sanaq AG, Allschwil, Switzerland (Pharmatrans Sanaq AG 2008). The material data from the used Cellets® pellets in detail is listed in Table 2.1 (Pharmatrans Sanaq AG 2013).

2.3 Coating Material: Dynasan® 118

The coating material Dynasan® 118 is a glyceryl tristearate, produced by Sasol Germany GmbH, Witten, Germany. The melting point is at 70-73 °C. This coating material is used in the pharmaceutical and cosmetic industry for example in tablets as lubricant or in cosmetic sticks to improve the solidification process (Sasol Germany GmbH 2007). The refractive index n_{coat} from Dynasan® 118 is 1.4385 and the material data is listed in Table 2.1 (Markl, Zettl, et al. 2014).

2.4 Coating Material: Eudragit® L 30 D-55

The coating material Eudragit® L 30 D-55 (Methacrylic Acid - Ethyl Acrylate Copolymer) is an enteric coating with talc as anti-tacking agent, produced by Evonik Industries AG, Darmstadt, Germany. The material data for the coating Eudragit® L 30 D-55 is listed in Table 2.1 (Evonik Industries AG 2014). The refractive index n_{coat} from the coating material Eudragit® L 30 D-55 is 1.48 (Koller et al. 2011).

Table 2.1. Pellet and coating materials data for the experiments

	B01/B02/B03	B04
Pellet material	Calcium stearate	Cellets®
$m_{pellets,0}$	450.0 g	300.0 g
ρ_{core}	1.1105 g/cm^3	0.84 g/cm^3
Ψ	0.92	0.97
r_{core}	0.7113 mm	0.6 mm
Coating material	Dynasan® 118	Eudragit® L 30 D-55
$m_{coating}$	218.0 g	800.46 g
ρ_{coat}	1.056 g/cm^3	1.585 g/cm^3
DS	100 %	20 %
n_{coat}	1.4385	1.48

The coating composition is soluble in the intestine above a pH of 6 and is listed in Table 2.2.

Table 2.2. Coating composition for pellet coating

Function	Ingredient	Quantity	Weighing	Dry substance		Density
		[g]	[g]	[g]	[%]	[g/cm^3]
Polymer	Eudragit® L30 D-55	333.4	333.30	100.00	62.28	1.067[1]
Plasticizer	Triethyl citrate	10.0	10.10	10.10	6.29	1.135[2]
Anti-tacking	Talc	50.0	50.47	50.47	31.43	2.700[3]
Diluent	Water	406.6	406.59	--	--	--
	Total	800.0	800.46	160.57	100.00	$\rho_{coat} = 1.585$

[1](Evonik Industries AG 2014), [2](IFA 2015b), [3](IFA 2015a)

The coating components were weighed with the precision balance New Classic ML from Mettler-Toledo GmbH, Wien, Austria. According to the coating composition (Table 2.2) the excipient suspension as shown in Fig. 2.3 can be generated. At first, talc and triethyl citrate are homogenized in water by using a mixer for 10 minutes. On the next step, the excipient suspension is slowly filled into the Eudragit® L 30 D-55 dispersion while stirring gently. Finally, the spray suspension is passed through a 0.5 mm sieve as illustrated in Fig. 2.4.

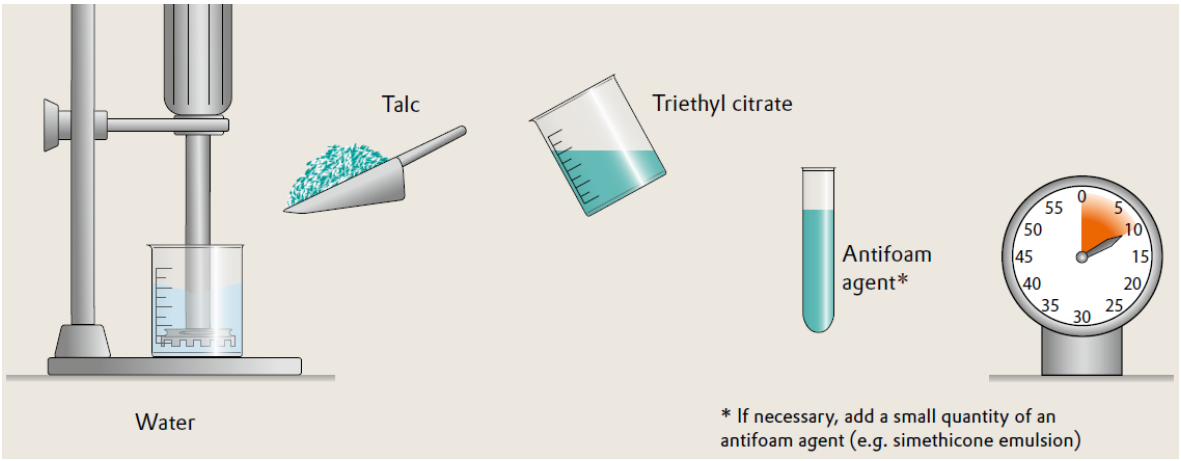

Fig. 2.3. Excipient suspension (Evonik Industries AG 2011)

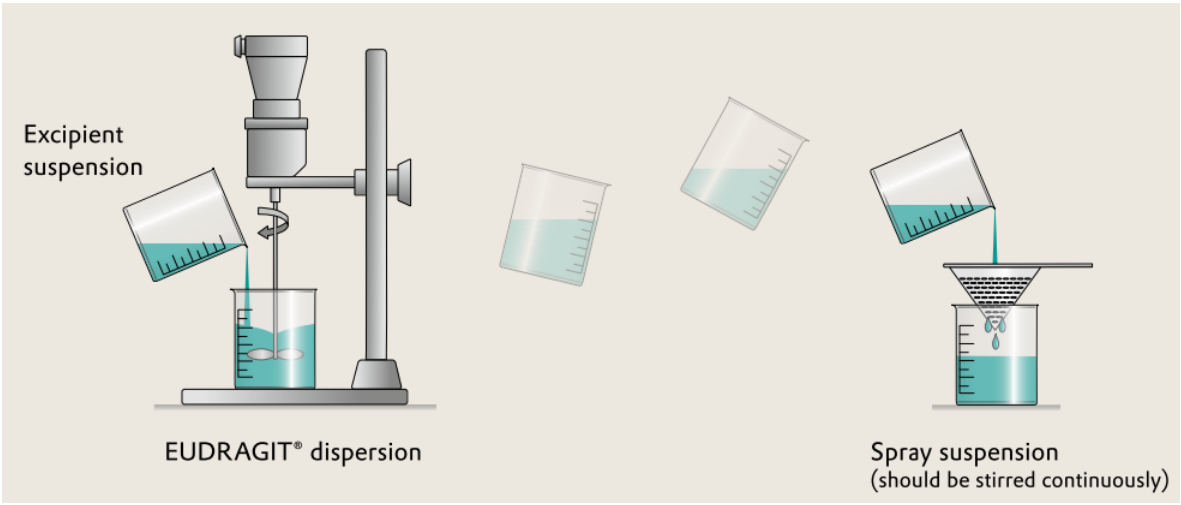

Fig. 2.4. Spray suspension (Evonik Industries AG 2011)

3 Experimental Equipment

Fig. 3.1. VENTILUS 2.5 / 1 (INNOJET® Herbert Hüttlin 2008)

The INNOJET® VENTILUS 2.5 / 1 (Fig. 3.1) is a laboratory equipment for granulate, coating and drying processes. The materials can be powders, crystals, pellets or tablets. The pellets are fluidized with a warm air stream and the coating solution is sprayed on the moving bed of the particles. In the spray zone the coating solution wets the surface of the moving pellets. Outside of the spray zone, the pellets are dried with the warm air stream. Therefore, the coating layer is growing with the process time. The laboratory equipment consists of the processing unit, supply air area, exhaust air area, spray system and the control system as illustrated in Fig. 3.2. The general technical data from the VENTILUS 2.5 / 1 is listed in Table 3.1 (INNOJET® Herbert Hüttlin 2008).

Table 3.1. General technical data VENTILUS 2.5 / 1 (INNOJET® Herbert Hüttlin 2008)

Parameter	Quantity
Width	860 mm
Height	2080 mm
Depth	860 mm
Weight	About 450 kg
Input supply voltage	400 V, 50 Hz
Power input	4.0 kW
Process airflow	Max. 100 m^3/h
Supply air temperature	Max. 90 °C
Spray rate	1-30 g/min
Spray nozzle rotation	About 50 rpm
System pressure	Min. 6 bar
Volume product container	0.4-2.5 l

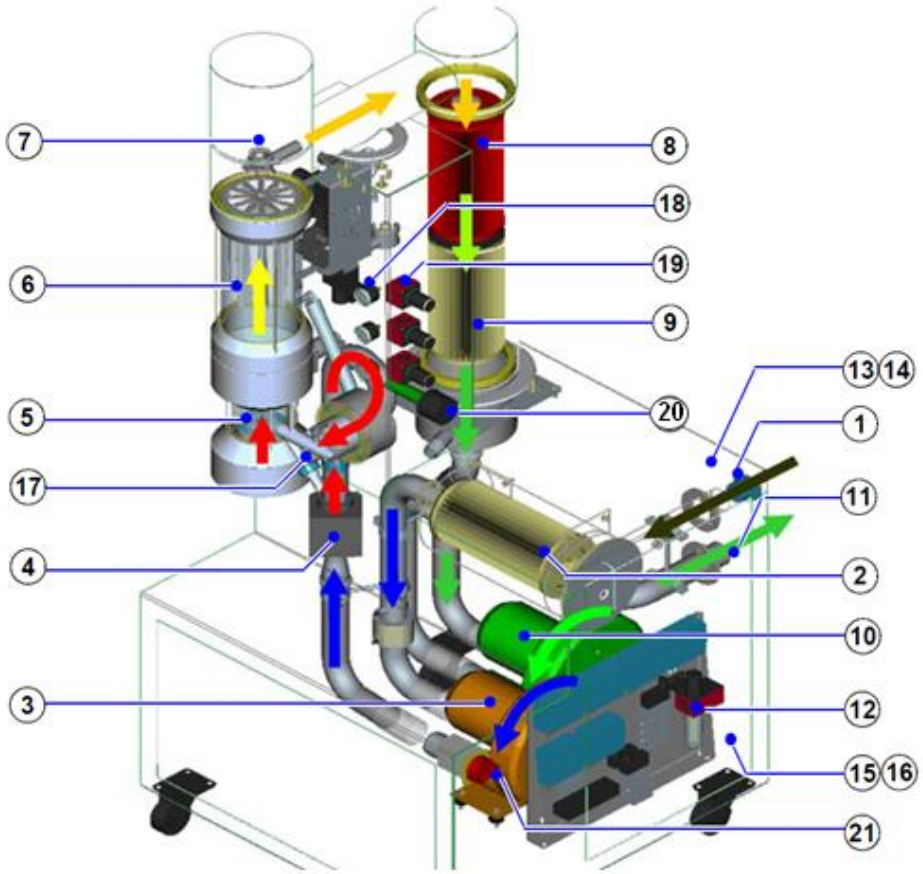

Fig. 3.2. Schema VENTILUS 2.5 / 1 (INNOJET® Herbert Hüttlin 2008)

1. Supply air connection (DN 50 mm)
2. F9 filter supply air (in filter box)
3. Ventilator supply air
4. Air heater
5. Product tank with propelling charge IBO150 and spray nozzle INR2/ IHN2
6. Filter exhaust air Sepajet IRS/ Sepasieve ISS
7. Powder recirculation system
8. F6 filter exhaust air (in filter box)
9. F9 filter exhaust air (in filter box)
10. Ventilator exhaust air
11. Exhaust air connection (DN 50 mm)
12. Inlet pressure controller (normal pressure 6 bar)
13. Network connection – RJ45 (Data Logger)
14. 2x 230V – 50Hz power outlets
15. Power supply – 400V / 50Hz
16. Compressed air supply (6 bar)
17. Sampling, product infrared sensor
18. Manometer spray air
19. Nozzle pressure adjustment
20. Dosing system for spray fluid
21. Emergency stop switch

Fig. 3.3. INNOJET® Hot Melt Device (IHD1) (INNOJET® Herbert Hüttlin 2012b)

The INNOJET® Hot Melt Device (IHD1) as shown in Fig. 3.3 is used for the hot melt coating experiments. The range of application of the hot melt system is to mask the taste and the smell. For example fat or wax as coating material can be used with this system. The coating material is molten in the furnace crucible on a heater with a magnetic stirrer. A heated piston pump ensures a constant flow of the molten coating material to the spray nozzle. The hose pipe with the molten coating is heated by hot air (INNOJET® Herbert Hüttlin 2012b).

The Hot Melt Spray Nozzle type IHN-2 is used (Fig. 3.4) for all experiments. The spray nozzle is located in the middle of the bottom of the product container and has two connections, one for the atomizing pressure and one for the coating material. For the experiment B04 a peristaltic pump ensures a constant flow of the spray suspension to the spray nozzle.

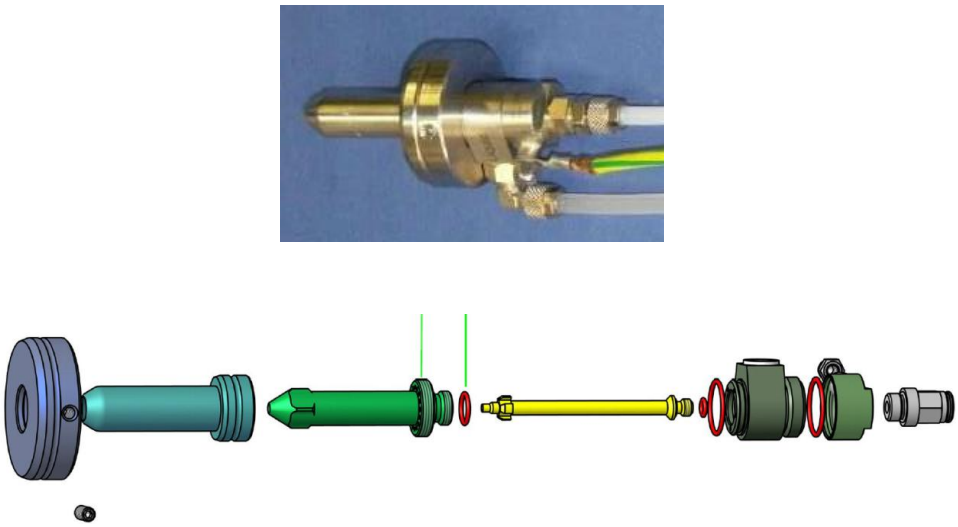

Fig. 3.4. Hot Melt Spray Nozzle type IHN-2 (INNOJET® Herbert Hüttlin 2012a)

The control system from the VENTILUS 2.5 / 1 is a programmable logic controller (PLC) made by WAGO and is visualised with a touch screen display (Fig. 3.5). Process parameters can be easily changed with the touch panel. The set point is marked with the blue box and the actual value with the green box (INNOJET® Herbert Hüttlin 2008).

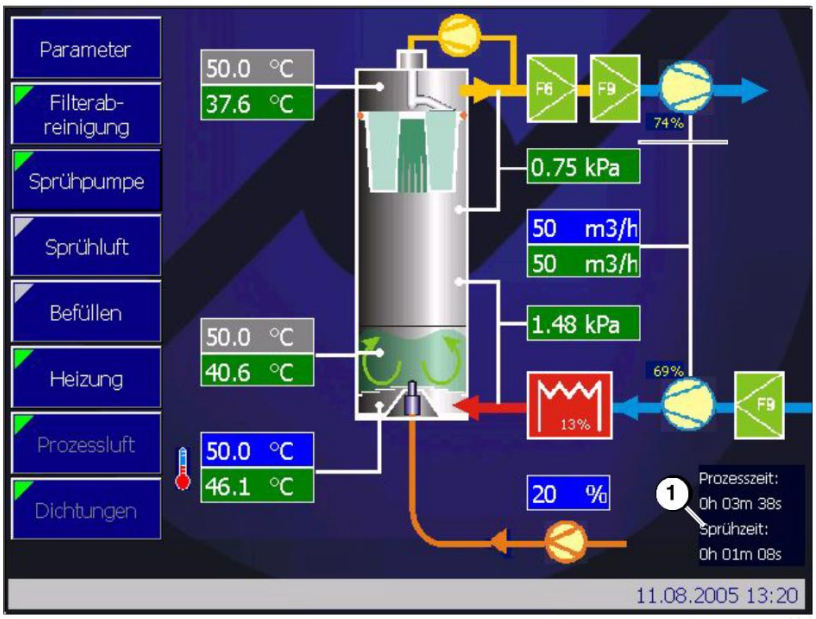

Fig. 3.5. Touch screen display from the VENTILUS 2.5 / 1 (INNOJET® Herbert Hüttlin 2008)

The record protocol from the INNOJET® Data Logger with the different process conditions for the experiment B04 is illustrated in Fig. 3.6. The process air, spray rate and the product temperature was constant during the process. Due to the evaporating of the diluent (water) in the spray solution the inlet air temperature is fluctuating during the process.

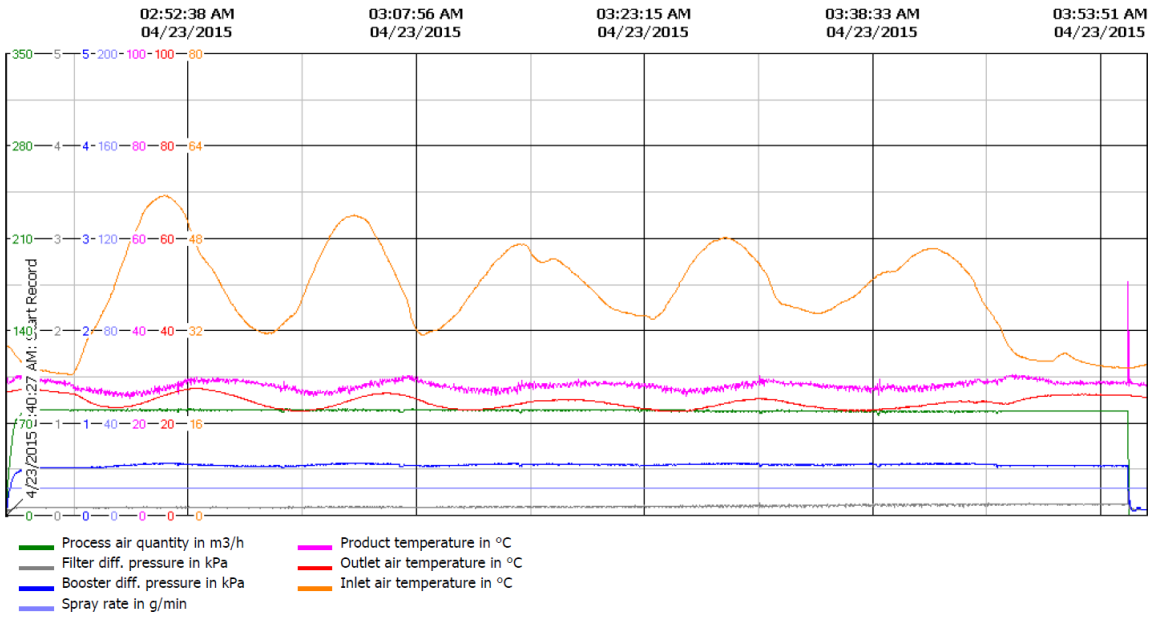

Fig. 3.6. Record protocol from the experiment B04

The handling with the INNOJET® VENTILUS 2.5 / 1 and the Hot Melt Device (IHD1) is described in detail in the user manuals (INNOJET® Herbert Hüttlin 2008; INNOJET® Herbert Hüttlin 2012b; INNOJET® Herbert Hüttlin 2012a). For the experiments B01, B02 and B03 the INNOJET® VENTILUS 2.5 / 1 and the Hot Melt Device (IHD1) as shown in Fig. 3.3 are used (Markl, Zettl, et al. 2014). Furthermore, for the experiment B04 only the INNOJET® VENTILUS 2.5 / 1 as shown in Fig. 3.1 is needed. The process conditions for the experiments are listed in Table 3.2.

Table 3.2. Process conditions for the experiments

	B01/B02/B03	B04
Spray rate	7.0 g/min	12.0 g/min
Atomizing pressure	1.5 bar	1.0 bar
Process air	60 m^3/h	80 m^3/h
Product temperature	35 °C	28 °C
Process time	32 min	64 min
Sample time	4, 6, 6, 6, 6, 4 min	Every 8 min
Number of samples	6	8

4 Off-line OCT Characterisation of Pellets

The samples from all experiments (B01 – B04) were analysed off-line with the OCT system as shown in Fig. 1.14 and Fig. 1.15. A 2D sensor was used to generate the cross-sectional images for the analysis of the samples from B01/B02/B03. A 3D sensor was applied for the experiment B04 and the cross-sectional images were generated by turning off one galvanometer mirror.

4.1 Data Evaluation of Off-line OCT Data

The following chapter describes the algorithm for the determination of the coating thickness with the off-line OCT data. The algorithm was implemented in MATLAB® R2013a. The data flow diagram of the algorithm is shown in Fig. 4.1.

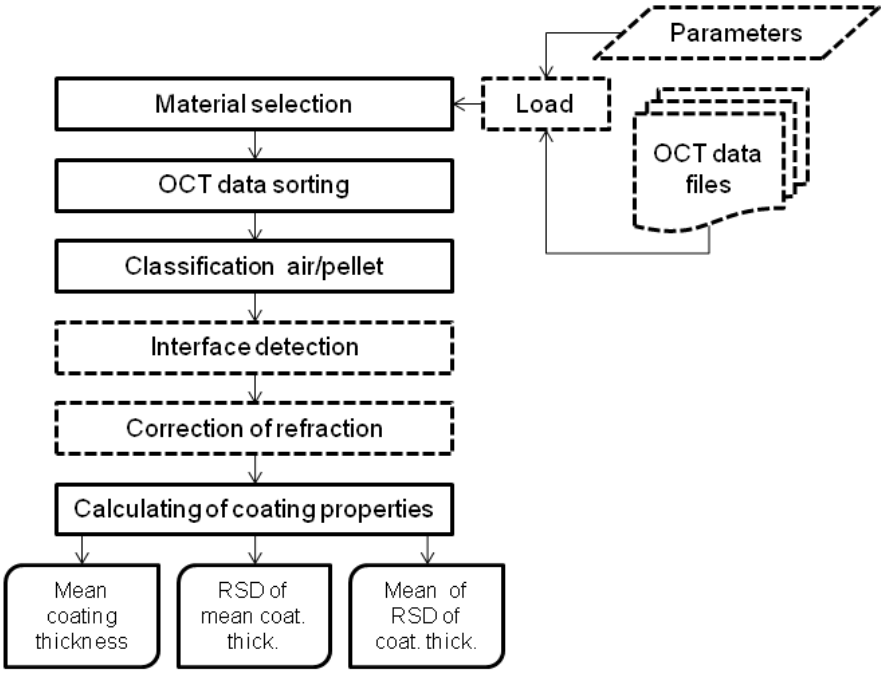

Fig. 4.1. Data flow diagram of the off-line coating thickness evaluation algorithm. The dotted line indicates the existing code.

The first part “material selection” loads the parameters and the OCT data files (.raw or .bmp) into the workspace of the MATLAB® program. A raw image file includes the data from the CCD camera (without any processing). An OCT image is calculated from raw-files and stored as a bitmap image. The OCT data files are sorted depending on their timestamp. The function “classification” calculates the mean value for each A-scan. A threshold is then applied on this mean value enabling the differentiation between air and pellet. Finally, a shortest path algorithm detects the air/coating and coating/pellet core interfaces as shown in Fig. 4.2. The hard constraint δ_{max} describes the maximum axial deviation of neighbouring pixels. The green nodes show the optimal path of the coating layer contour using a δ_{max} of two pixels. On the other hand the red nodes show an incorrect path of the coating layer contour using a δ_{max} of one pixel.

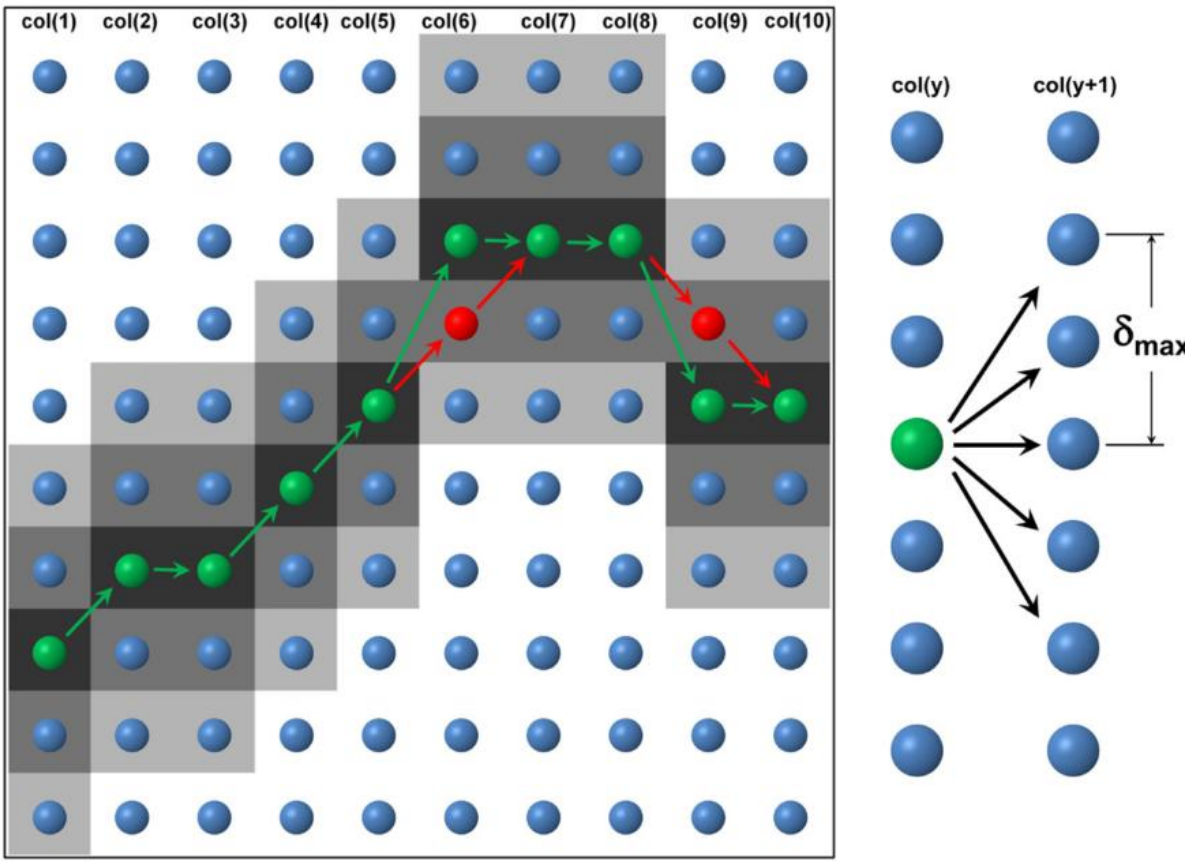

Fig. 4.2. Detection of the contour of the coating layer. The green nodes show the optimal and the red nodes an incorrect path of the coating layer contour (Markl, Hannesschläger, Sacher, Leitner, et al. 2015).

Fig. 4.3 illustrates the different steps of the coating thickness evaluation algorithm from one detected pellet (a). The interface detection identifies first the air/coating interface (b) and then the coating/pellet core interface (c). The curvature of the pellets induces a measurement error as shown in Fig. 1.20. The optical beam is refracted by the air/coating interface, which introduces the OCT measured coating thickness. The correction of refraction is performed by fitting a circle (d) in the air/coating interface.

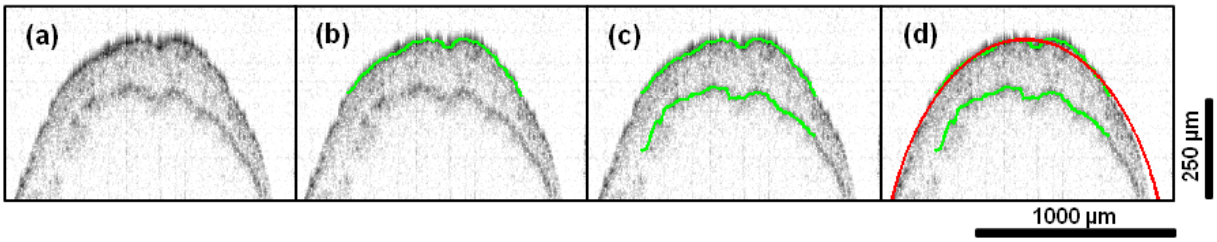

Fig. 4.3. Steps of the coating thickness evaluation algorithm for one pellet (B01, Sample 5). (a) OCT image, (b) detection air/coating interface, (c) detection coating/pellet core interface and (d) correction of refraction. Image dimensions (in air) are 1.47 x 0.49 mm^2 (500 x 200 pixels).

Finally, the following coating properties can be calculated. At first the mean coating thickness μ_P per detected pellet (see Eq. (4.1)) was estimated, with the measured coating thickness μ_i and the number of thickness measurements n.

$$\mu_P = \frac{1}{n} \cdot \sum_{i=1}^{n} \mu_i \tag{4.1}$$

In a similar manner the standard deviation σ_P per detected pellet was calculated with Eq. (4.2).

$$\sigma_P = \sqrt{\frac{1}{n-1} \cdot \sum_{i=1}^{n} (\mu_i - \mu_P)^2} \tag{4.2}$$

Now the mean coating thickness for the respective sample μ_{sample} can be calculated with Eq. (4.3). The variable N describes the number of the detected pellets per sample.

$$\mu_{sample} = \frac{1}{N} \cdot \sum_{i=1}^{N} \mu_{P,i} \tag{4.3}$$

The standard deviation for the respective sample σ_{sample} is defined by Eq. (4.4).

$$\sigma_{sample} = \sqrt{\frac{1}{N-1} \cdot \sum_{i=1}^{N} (\mu_{P,i} - \mu_{sample})^2} \tag{4.4}$$

The relative standard deviation (RSD) cv_{sample} of the mean coating thickness is defined by Eq.(4.5). The inter-pellet coating uniformity is represented by the cv_{sample} as a function of process time.

$$cv_{sample} = \frac{\sigma_{sample}}{\mu_{sample}} \tag{4.5}$$

In addition, the mean of the relative standard deviation of the coating thickness can be calculated by Eq.(4.6). The intra-pellet coating uniformity is represented by the $\mu_{cv,sample}$ as a function of process time.

$$\mu_{cv,sample} = \frac{1}{N} \cdot \sum_{i=1}^{N} \frac{\sigma_{P,i}}{\mu_{P,i}} \tag{4.6}$$

Another program was developed for the data evaluation and for the generation of the diagrams as illustrated by the data flow diagram in Fig. 4.4. At first, the part “material selection” loads the data material, process parameters and the determined coating properties into the workspace of the MATLAB® program. Then the program calculates the theoretical coating thickness according to Eq. (1.10) and the theoretical coating thickness under consideration of the sampling (see Eq.(1.18)). Finally, the different diagrams for the mean coating thickness, RSD of mean coating thickness and the mean of RSD of coating thickness are generated automatically. The MATLAB® code for the off-line OCT characterisation of pellets is in appendix C.

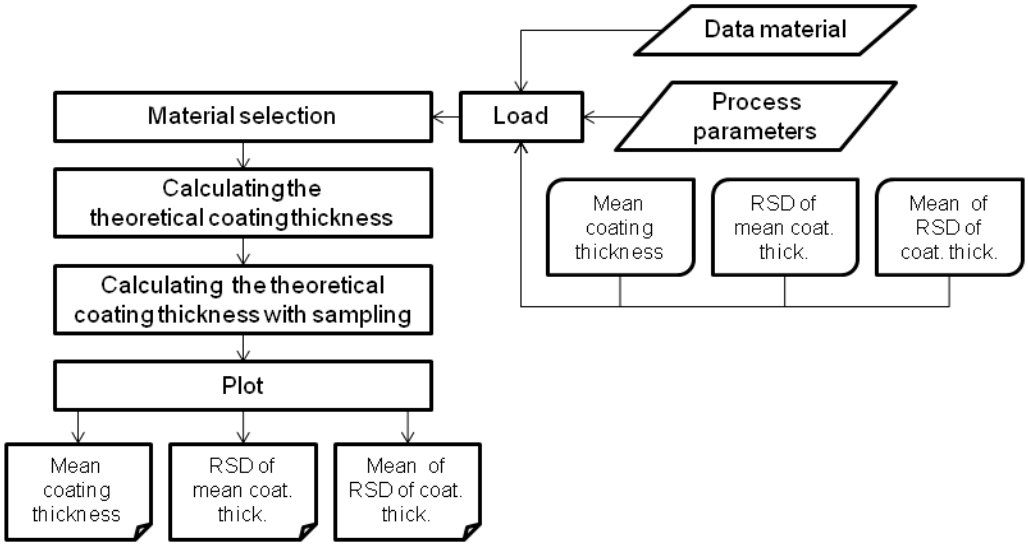

Fig. 4.4. Data flow diagram of the data evaluation.

4.2 Results and Discussion

Fig. 4.5 shows the OCT images from pellets (calcium stearate 75% (w/w), paracetamol 20% (w/w) and monostearate 5% (w/w)) with the coating material Dynasan® 118. The images show samples taken at different process times. Each sample consists ten different pellets for the further data evaluation (Markl, Zettl, et al. 2014). The air/coating and the coating/pellet core interface of the coating layer is clearly specifiable and an automatic data evaluation with the algorithm is possible.

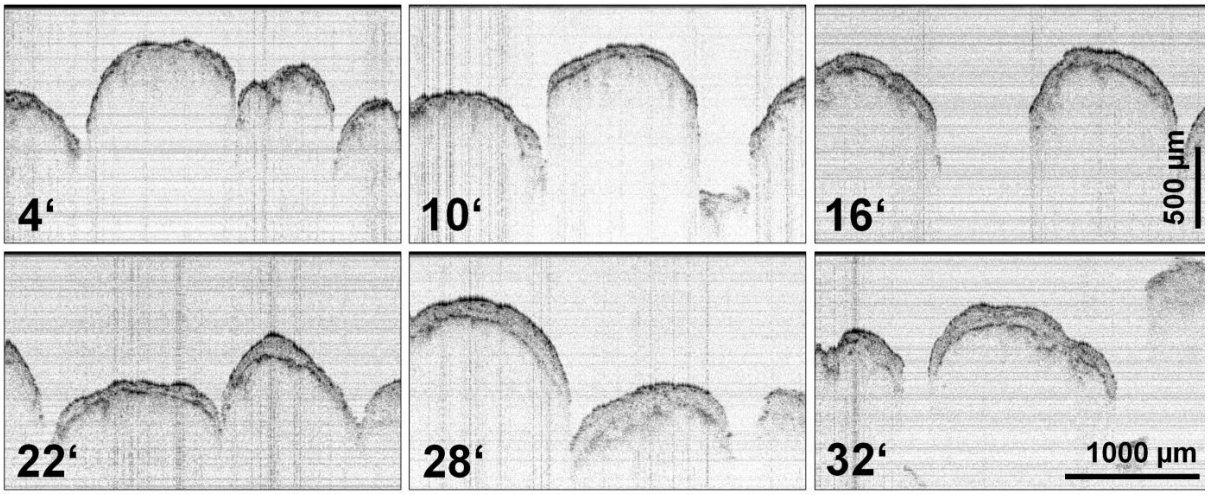

Fig. 4.5. Off-line OCT images of film-coated pellets with Dynasan® 118 at different process times (in minutes). Image dimensions (in air) are 2.94 x 1.46 mm^2 (1000 x 600 pixels) (Markl, Zettl, et al. 2014).

Fig. 4.6 illustrates the coating thickness as a function of the process time of B02. The green line indicates the theoretical growth model (see Eq. (1.10)). It is assumed that the pellets have an ideal spherical shape with the same diameter and without pores. During the process, the number of particles does not change and the coating material is sprayed uniformly on all pellets. The blue dotted line shows the theoretical growth model considering the sampling for the off-line measurement as defined in Eq.(1.18). The loss of coating mass (q) during the process is unknown; therefore, this variable q was fitted by a non-linear least-squares fitting algorithm. For the B02, 71 % from the input coating mass was applied onto the pellets fitted with the automatic evaluated data. Based on the loss of coating (for example on the wall of the product container or the filter bags) the growth model with sampling deviate under the ideal growth model.

The automatic evaluated data is illustrated with the red crosses and the error bars. Error bars show the standard deviations from the mean coating thickness. The manual data was measured by hand with three data points per pellet and is denoted by the black circles (Markl, Zettl, et al. 2014). The particle size analysis (Qicpic) is illustrated with the magenta squares. The measurement system from the Qicpic particle analyser (Sympatec GmbH, Germany) is based on dynamic image analysis. The Qicpic particle analyser was therefore used to estimate the mean volume diameter of the uncoated pellets and of every taken sample. The coating thickness is half of the difference between the mean volume diameters of the coated pellets and the product substrate (Markl, Zettl, et al. 2014). The automatic evaluated data with the algorithm deviates slightly from the theoretical growth models. Until a process time of 10 minutes, the automatic evaluated coating thickness is less than the theoretical coating thickness due to the limited axial resolution (10 µm) of the OCT system (Markl, Zettl, et al. 2014). In Table 4.3 the number of the detected pellets (N) and the number of thickness measurements (n_i) per sample of the automatic evaluated data are listed.

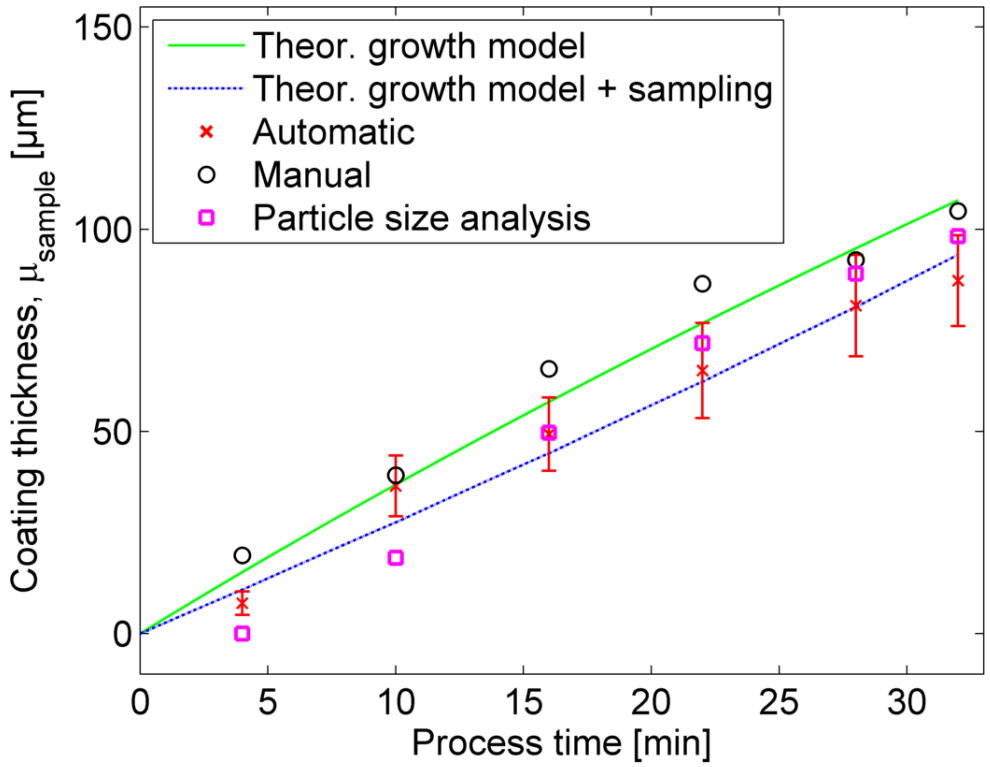

Fig. 4.6. Coating thickness as a function of the process time for B02.

Fig. 4.7 shows the inter-pellet coating uniformity represented by the RSD of the mean coating thickness (see Eq. (4.5)) as a function of the process time for B02. The automatic evaluated data is illustrated with the red crosses and the manual evaluated data is displayed with black circles (Markl, Zettl, et al. 2014). Both streams of data are proportional to $\sqrt{1/t}$ and the RSD of mean coating thickness is sinking by the process time t. This trend can be explained with the model from Turton, as a ratio from the standard deviation σ_{tot} and the mean value μ_{tot} of the coating mass on a particle (see Fig. 4.8). The subscript ct in the Turton model refers to the circulation time and x to the mass of coating per pass through the spray zone. A long process time T_{coat} compared to the mean circulating time μ_{ct} leads to a low value cv_{sample} as shown in Fig. 4.7. Therefore frequently passes of the pellets through the spray zone decreases cv_{sample} (Turton 2008).

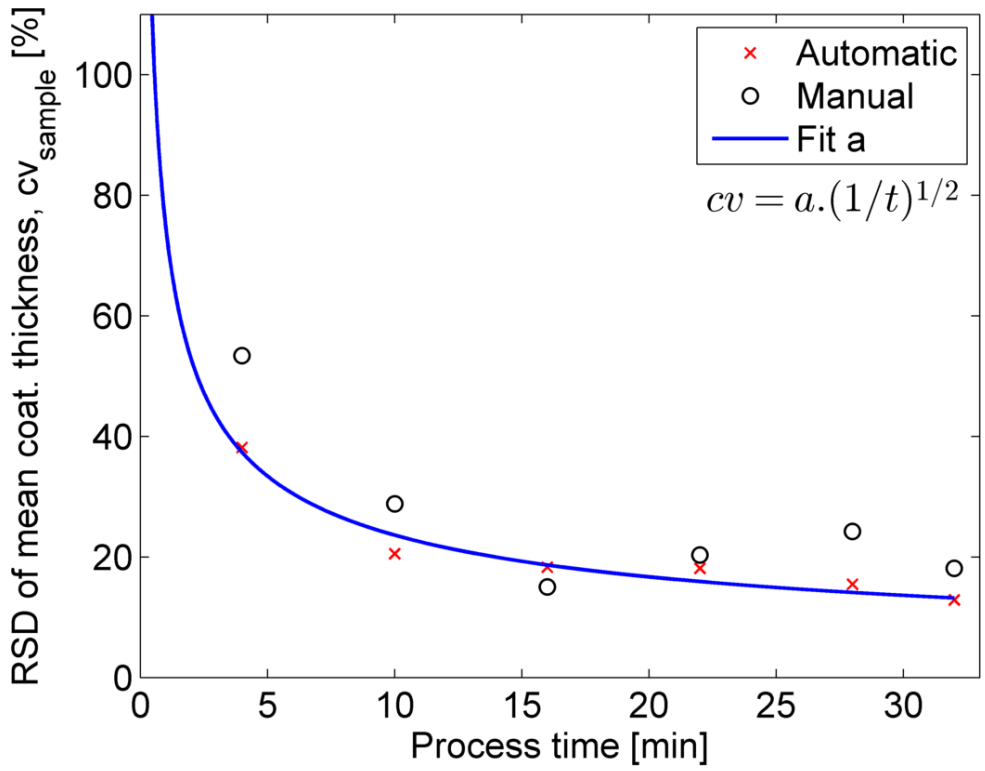

Fig. 4.7. Inter-pellet coating uniformity for B02. The variable a for the blue curve was fitted with the automatic evaluated data.

The variable a for the blue curve was fitted with the automatic evaluated data using a non-linear least-squares fitting algorithm. Decreasing the variable a causes a lower RSD of mean coating thickness as explained in Fig. 4.8.

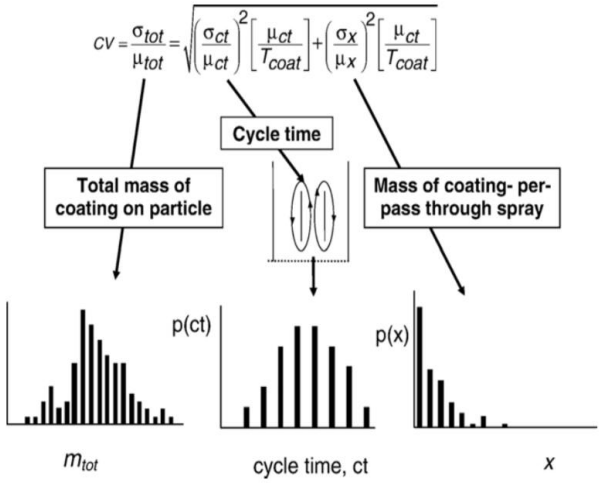

Fig. 4.8. Model for the coating uniformity (Turton 2008)

The intra-pellet coating uniformity represented by the mean of RSD of coating thickness (see Eq.(4.6)) as a function of the process time for B02 is illustrated in Fig. 4.9. The automatic evaluated data is illustrated with the red crosses and the manual evaluated data is displayed with black circles (Markl, Zettl, et al. 2014). The automatic evaluated data with the algorithm deviates clearly from the manual evaluated data at the beginning of the coating process. The reason is the algorithm evaluates much more data points per pellet for the coating thickness (see Table 4.3) and thus provides statistics that are more reliable. In case of the manual measurements, the coating thickness was measured only on three different positions on the pellet.

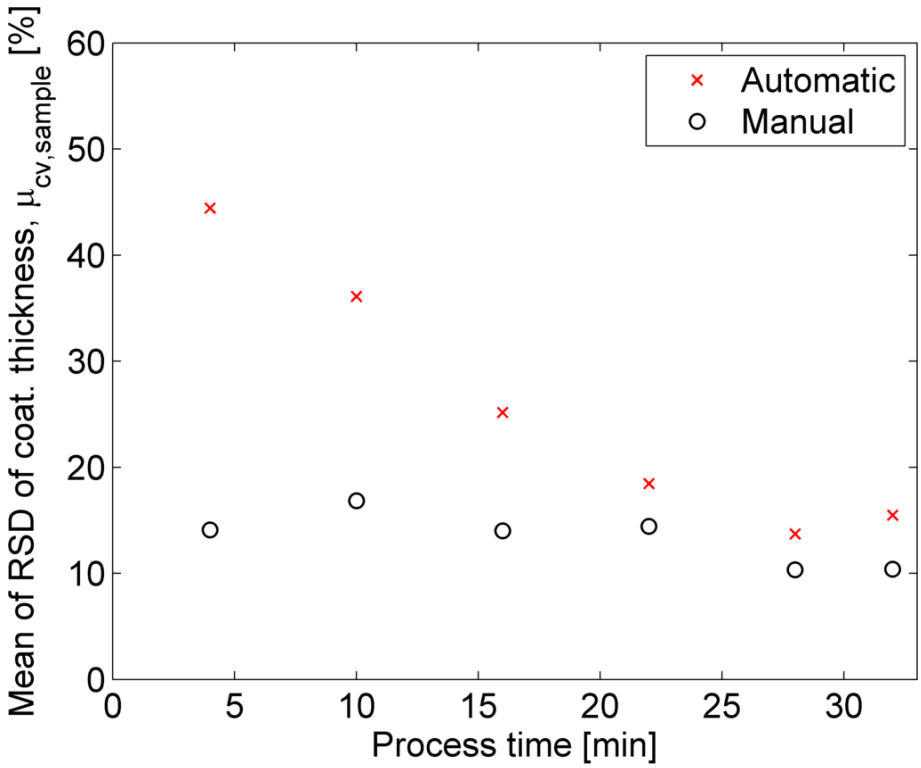

Fig. 4.9. Intra-pellet coating uniformity for B02.

In Fig. 4.10 the coating thickness as a function of the process time for all three automatic evaluated batches is illustrated. The experiments referred to as B01 (red square), B02 (magenta circle) and B03 (black plus) were operated under exactly the same process conditions (Markl, Zettl, et al. 2014). All three batches showed a similar trend between the theoretical growth model (green line) and the theoretical growth model with sampling for the off-line measurement (blue dotted line). The loss of coating mass (q) during the process is unknown; therefore, this variable q was fitted with the automatic evaluated data from experiment B02. For B01, B02 and B03, 79 %, 71 % and 76 % from the input coating mass was applied onto the pellets. Table 4.3 lists the number of the detected pellets (N) and the number of thickness measurements (n_i) per sample for all three automatic evaluated batches.

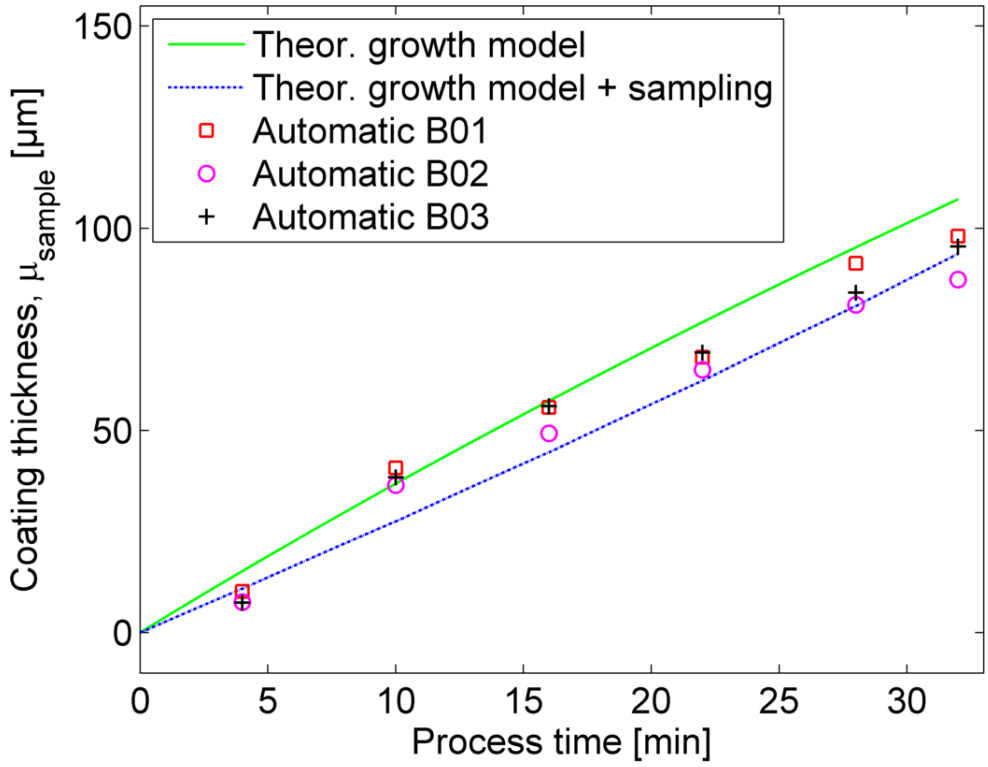

Fig. 4.10. Coating thickness as a function of the process time for all three experiments (B01 B02 and B03).

The results of all three batches (for the process end) are summarised in Table 4.1. The standard deviation from the automatic evaluated data with the algorithm is clearly lower than the manual evaluated data.

Table 4.1. Summary of the results for the coating thickness (B01, B02 and B03)

	Process end						
	Mean coating thickness Qicpic [µm]	Mean coating thickness Manual [µm]	Standard deviation Manual [µm]	Mean coating thickness Automatic [µm]	Standard deviation Automatic [µm]	Theor. growth model [µm]	Theor. growth model +sampling [µm]
B01	99.34	104.00	22.20	98.06	10.53	107.20	104.10
B02	98.26	104.51	18.96	87.28	11.24	107.20	93.68
B03	74.23	105.62	22.96	95.48	9.35	107.20	100.70

In addition, the mass of the sampling (B01, B02 and B03) was weighed with the precision balance New Classic ML from Mettler-Toledo GmbH, Wien, Austria and is listed in Table 4.2.

Table 4.2. Mass of the sampling (B01, B02 and B03)

Sample index i [-]	Process time t [min]	B01 $m_{sample,i}$ [g]	B02 $m_{sample,i}$ [g]	B03 $m_{sample,i}$ [g]
1	4	4.1	5.4	6.1
2	10	5.9	2.9	7.3
3	16	7.2	5.6	8.7
4	22	7.8	12.2	9.8
5	28	4.8	10.7	5.6
6	32	4.5	7.0	10.3

Table 4.3 lists the number of the detected pellets (N) and the number of thickness measurements (n_i) per sample for all three automatic evaluated batches.

Table 4.3. Number of the automatic evaluated pellets per sample (B01, B02 and B03)

Sample index	B01		B02		B03	
i	N	n_i	N	n_i	N	n_i
[-]	[-]	[-]	[-]	[-]	[-]	[-]
1	15	679	9	624	9	934
2	10	1325	11	810	11	989
3	6	1155	10	963	12	745
4	6	648	9	697	7	1165
5	6	807	8	948	8	722
6	6	1275	8	801	10	398

Fig. 4.11 shows the inter-pellet coating uniformity represented by the RSD of the mean coating thickness as a function of the process time for all three batches. The automatic evaluated data for the three batches are proportional to $\sqrt{1/t}$ and the RSD of mean coating thickness is sinking with the process time t. The variable a for the blue curve was fitted with the automatic evaluated data of B02 using a non-linear least-squares fitting algorithm.

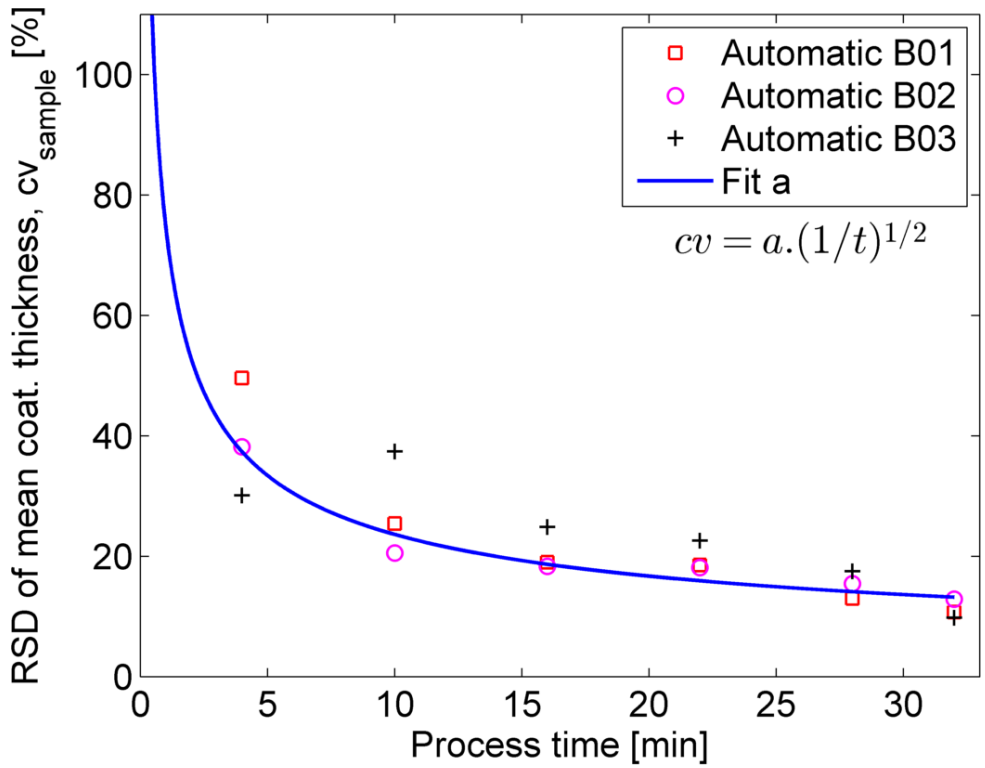

Fig. 4.11. Inter-pellet coating uniformity for all three replication experiments. The variable a for the blue curve was fitted with the automatic evaluated data of B02.

In Table 4.4 the summary of the results is listed for the inter-pellet coating uniformity at the process end. The RSD of the mean coating thickness from the automatic evaluated data with the algorithm is clearly lower than the manual evaluated data, as explained in Fig. 4.9. The experiment B02 has the best coating uniformity of all three replication experiments, indicated by the low value of a.

Table 4.4. Summary of the results for the inter-pellet coating uniformity (B01, B02 and B03)

	Process end		
	RSD of mean coat. thickness Manual [%]	RSD of mean coat. thickness Automatic [%]	Model from Turton a $[\sqrt{s}]$
B01	21.35	10.73	677.16
B02	18.14	12.87	578.69
B03	21.74	9.79	634.13

In addition, the intra-pellet coating uniformity represented by the mean of RSD of coating thickness as a function of the process time for all three batches is illustrated in Fig. 4.12. The three automatic evaluated data with the algorithm deviate slightly from each other.

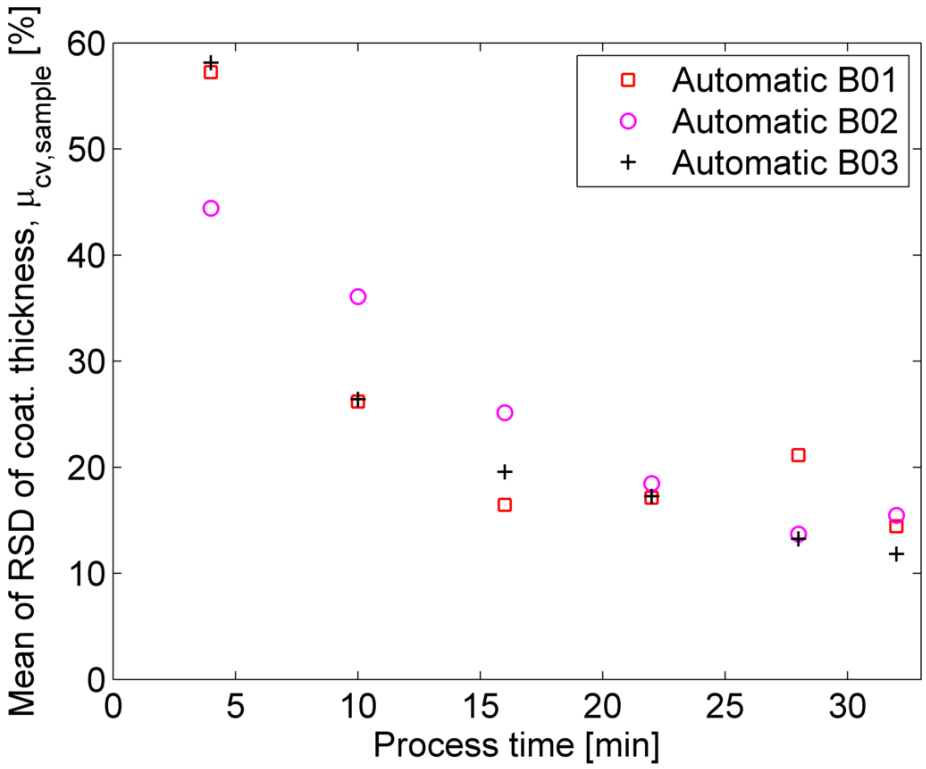

Fig. 4.12. Intra-pellet coating uniformity for all three replication experiments.

Table 4.5 summarises the results for the intra-pellet coating uniformity at the process end. The diagrams from the data evaluation for B01 and for B03 are illustrated in appendix A. In addition, the summary of the results for B01, B02 and B03 is listed in appendix B.

Table 4.5. Summary of the results for the intra-pellet coating uniformity (B01, B02 and B03)

	Process end	
	Mean of RSD of coat. thickness Manual [%]	Mean of RSD of coat. thickness Automatic [%]
B01	9.14	14.42
B02	10.39	15.47
B03	11.67	11.81

Fig. 4.13 illustrates the OCT images from the Cellets® with the coating material Eudragit® L 30 D-55. The images are illustrated at different process times and every sample has at least twenty different pellets for the further data evaluation (see Table 4.8). The air/coating and the coating/pellet core interfaces of the coating layer is not clearly specifiable as a result of the porous coating layer.

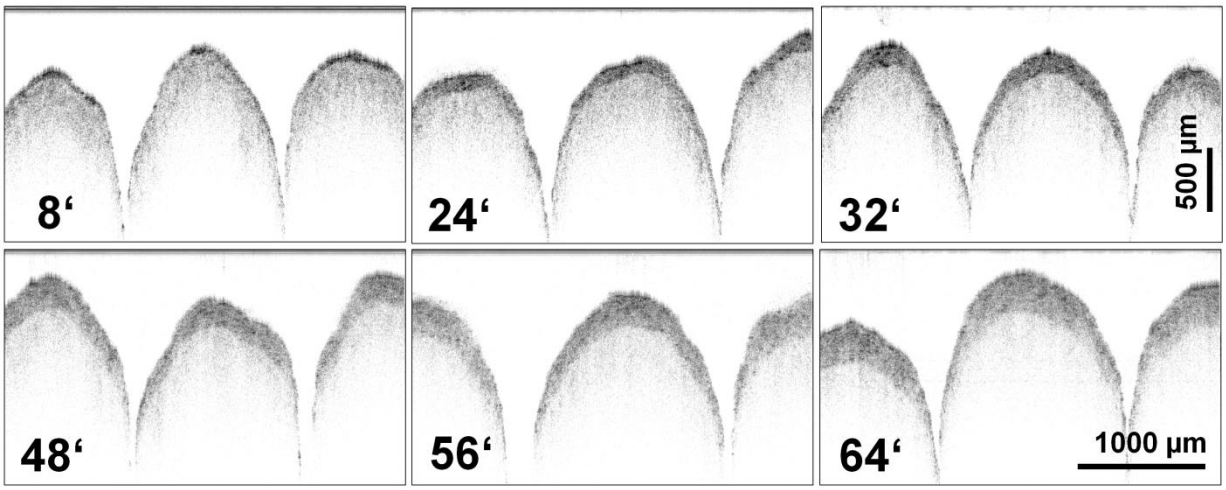

Fig. 4.13. Off-line OCT images of film-coated pellets with Eudragit® L 30 D-55 at different process times (in minutes). Image dimensions (in air) are 3.13 x 1.83 mm^2 (1024 x 600 pixels).

Fig. 4.14 illustrates the coating thickness as a function of the process time for B04. The green line indicates the theoretical growth model (see Eq. (1.10)). The blue dotted line shows the theoretical growth model considering the sampling for the off-line measurement as defined in Eq.(1.18). The coating layer as shown in Fig. 4.13 is very porous, which is considered by a factor ε for the porosity. In Eq. (4.7) V_H is the void volume, V_s the solid volume and V the total volume.

$$\varepsilon = \frac{V_H}{V} = 1 - \frac{V_s}{V} \tag{4.7}$$

The loss of coating mass during the process is unknown and this q_{fit} was fitted with a non-linear least-squares fitting algorithm. The data for the fitting algorithm was the automatic evaluated coating thickness. The variable q describes the ratio of the applied coating mass onto the pellets and was assumed to be between 60% to 70% based on the previous experiments (B01, B02 and B03).

The factor for the porosity ε can be calculated by Eq. (4.8) and is for the experiment B04 0.71.

$$q_{fit} = q \cdot \frac{1}{(1-\varepsilon)} \tag{4.8}$$

Finally, the medium density of the coating layer $\rho_{coat,m}$ can be determined using Eq. (4.9) (Stieß 2009).

$$\rho_{coat,m} = \rho_{coat} \cdot (1-\varepsilon) \tag{4.9}$$

The automatic evaluated data is illustrated in Fig. 4.14 with the red crosses and the error bars. Error bars show the standard deviations from the mean coating thickness. Until a process time of 10 minutes, the automatic evaluated coating thickness is less than the theoretical coating thickness, as explained in Fig. 4.6. After a process time of 10 minutes, the automatic evaluated data with the algorithm deviates slightly from the theoretical growth models. The high standard deviation at process end is caused by the porous coating layer of the pellets and leads to an incorrect interface detection. The summary of the results is listed in Table 4.6 for B04. Table 4.8 lists the number of detected pellets (N) and the number of thickness measurements (n_i) per sample.

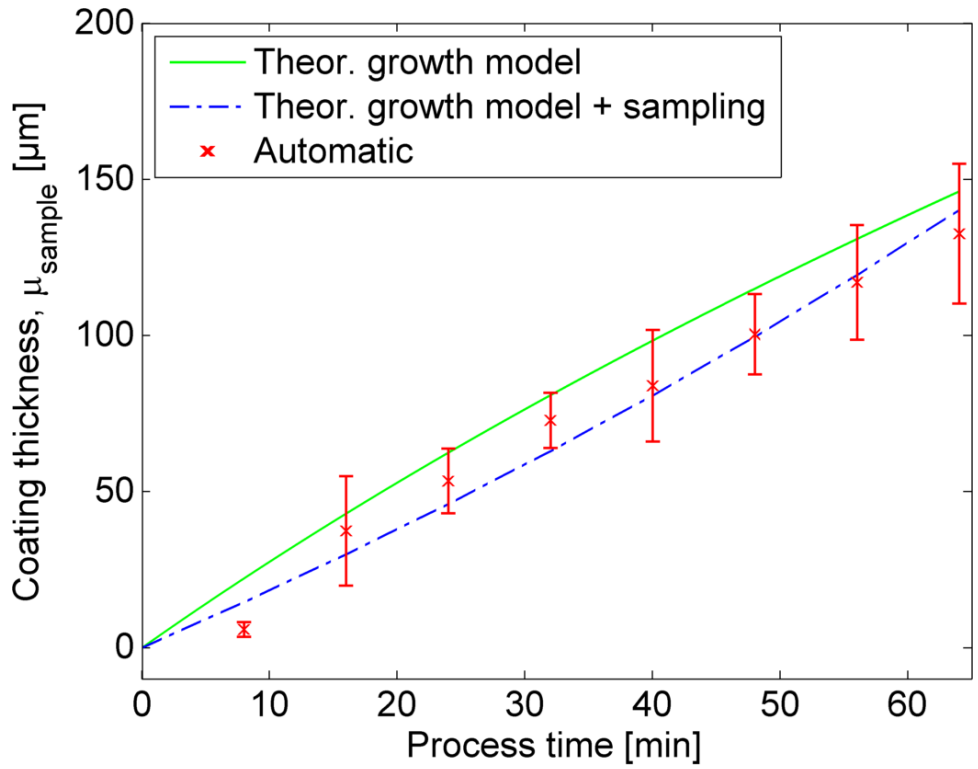

Fig. 4.14. Coating thickness as a function of the process time for B04.

Fig. 4.15 shows the inter-pellet coating uniformity represented by the RSD of the mean coating thickness (see Eq. (4.5)) as a function of the process time for B04. The red crosses denote the automatic evaluated data. This data is proportional to $\sqrt{1/t}$ and the RSD of mean coating thickness decreases with increasing process time t. The variable a for the blue curve was fitted by a non-linear least-squares fitting algorithm and is for B04 943.64 $\sqrt{s}$.

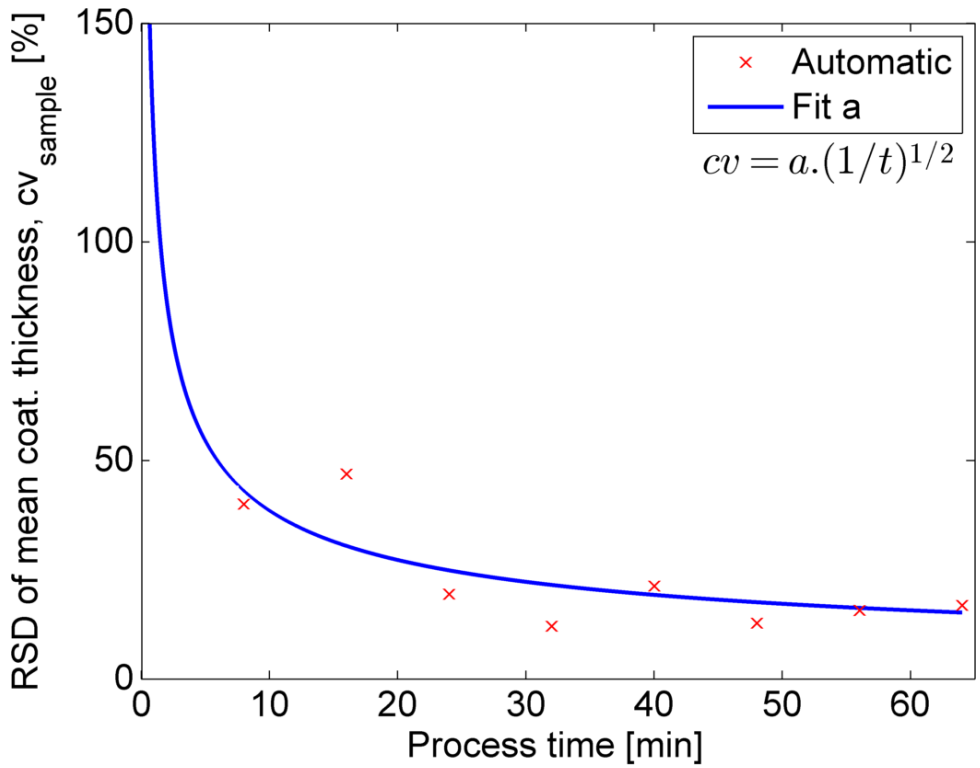

Fig. 4.15. Inter-pellet coating uniformity for B04. The variable a for the blue curve was fitted with the automatic evaluated data.

The intra-pellet coating uniformity represented by the mean of RSD of coating thickness (see Eq.(4.6)) as a function of the process time is illustrated in Fig. 4.16 for B04. At the beginning of the coating process, the mean of RSD is high. A reason for that is at this point of time only a few pellets pass the spray zone. Therefore, a high amount of the measured pellets did not pass the spray zone. Table 4.6 lists the results for B04 at the process end.

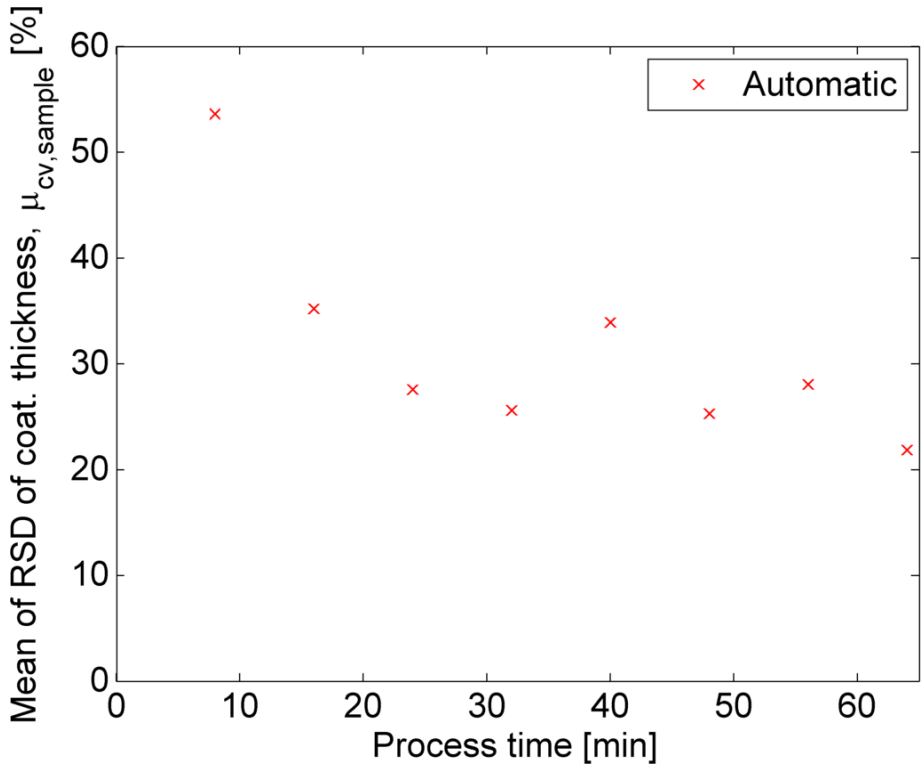

Fig. 4.16. Intra-pellet coating uniformity for B04.

Table 4.6. Summary of the results for the coating thickness (B04)

	Process end					
	Mean coating thickness Automatic [µm]	Standard deviation Automatic [µm]	Theor. growth model [µm]	Theor. growth model +sampling [µm]	RSD of mean coat. thickness Automatic [%]	Mean of RSD of coat. thickness Automatic [%]
B04	132.56	22.36	146.10	140.10	16.87	21.86

In addition, the mass of the sampling for B04 was weighed with the precision balance New Classic ML from Mettler-Toledo GmbH, Wien, Austria and is listed in Table 4.7.

Table 4.7. Mass of the sampling (B04)

Sample index i [-]	Process time t [min]	B04 $m_{sample,i}$ [g]
1	8	7.6
2	16	8.0
3	24	9.2
4	32	8.9
5	40	9.7
6	48	8.9
7	56	8.6
8	64	11.0

In Table 4.8 the number of the detected pellets (N) and the number of thickness measurements (n_i) per sample of the automatic evaluated data are listed. In addition, the summary of the results for experiment B04 is listed in appendix B.

Table 4.8. Number of the automatic evaluated pellets per sample (B04)

Sample index	B04	
i [-]	N [-]	n_i [-]
1	54	2230
2	58	2746
3	43	2298
4	32	1329
5	25	1720
6	28	1582
7	22	1542
8	27	1717

Fig. 4.17 shows different views of 3D OCT data of film-coated pellets from B04 (at process end). The acquisition of 3D volumetric images with the OCT system is described in detail in Fig. 1.17.

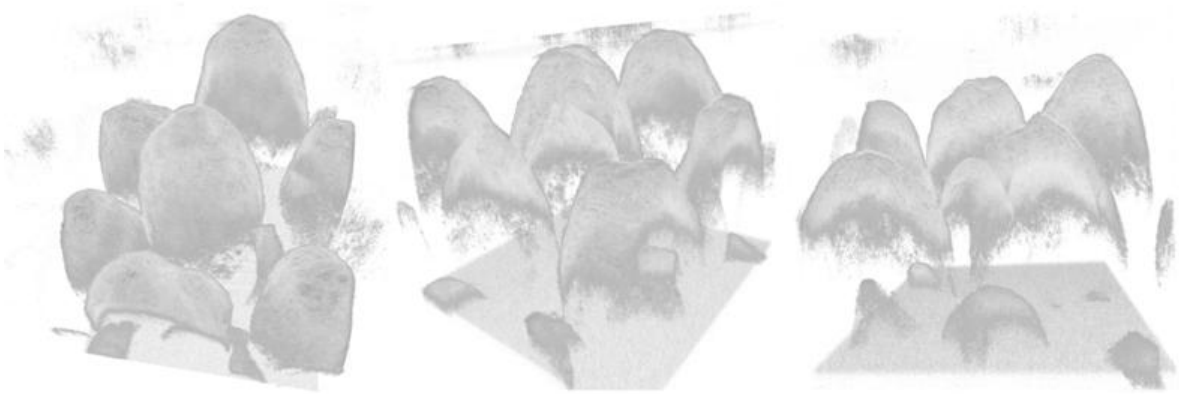

Fig. 4.17. 3D volumetric images of film-coated pellets (B04) at the process end.

In addition, the cross-sectional images of the 3D volumetric data (B04) at the process end are illustrated in Fig. 4.18.

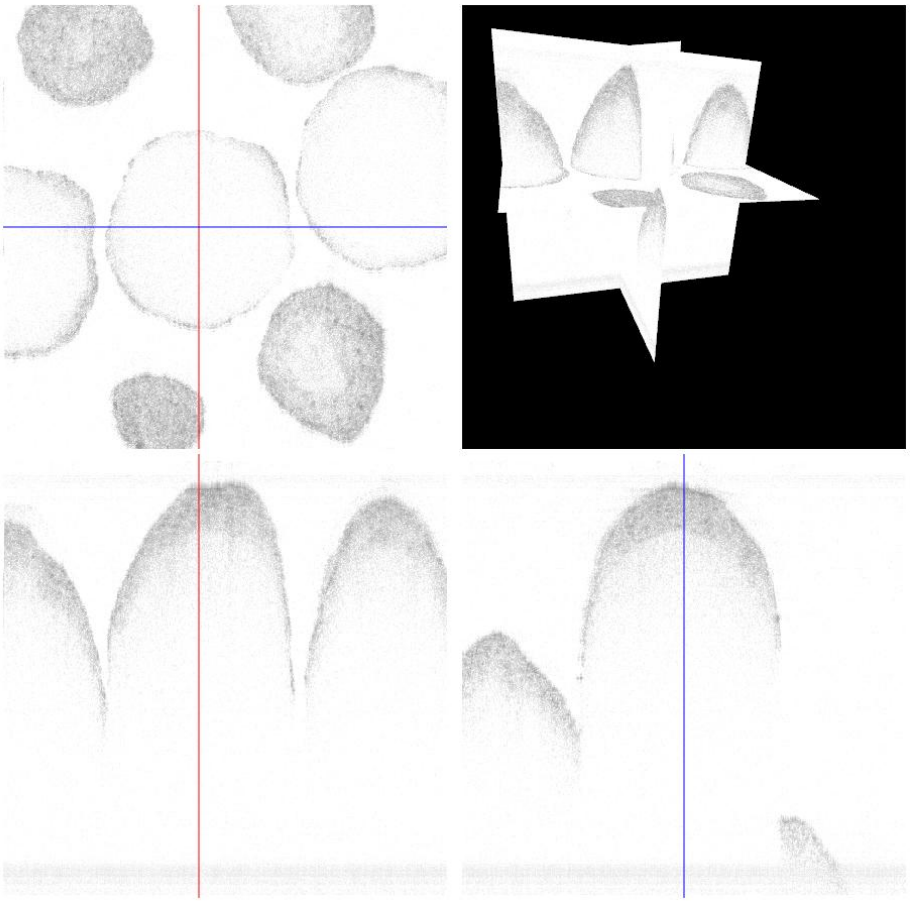

Fig. 4.18. Cross-sectional images of film-coated pellets (B04) at the process end.

5 In-line OCT Characterisation of Pellets

The determination of the coating thickness and the analysis of the homogeneity of the coating layer are key factors for the quality of the final product. With the OCT system, the determination of the coating thickness during the process is possible and it is described in the following chapter.

5.1 OCT Sensor Integration

For the measurement with the OCT system during the fluid bed coating process an insert was required for the inspection window of the product container. The insert for the OCT sensor was designed in 3D with the software PTC® Creo and manufactured by a 3D printer. Fig. 5.1 shows the insert for the OCT sensor integration in detail. A thin plastic foil is fixed on the insert to protect the OCT sensor from the spray droplets and the randomly moving pellets. A high reflection of the protection foil influences the measuring result with the OCT system. Therefore, the selection of the material of the protection foil is important.

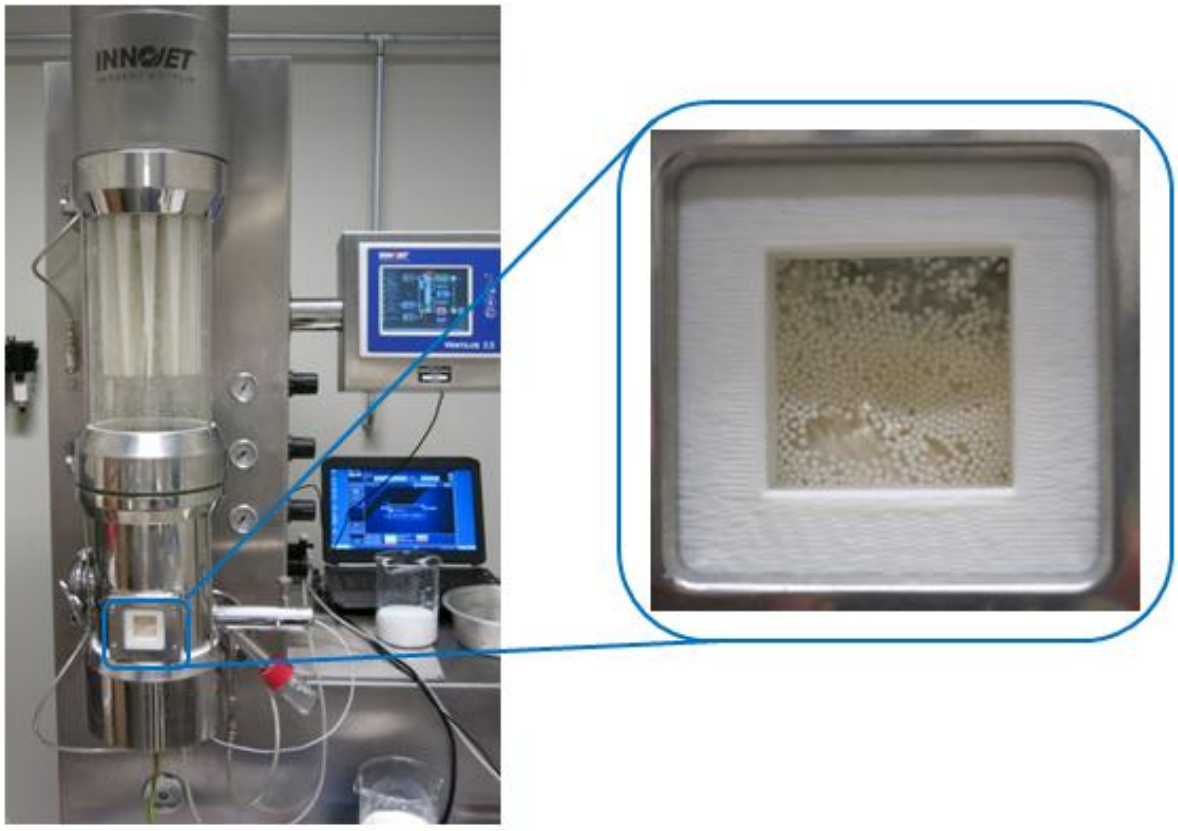

Fig. 5.1. Inspection window for the OCT sensor integration.

In Fig. 5.2 the insert for the inspection window designed in 3D with the software PTC® Creo is illustrated.

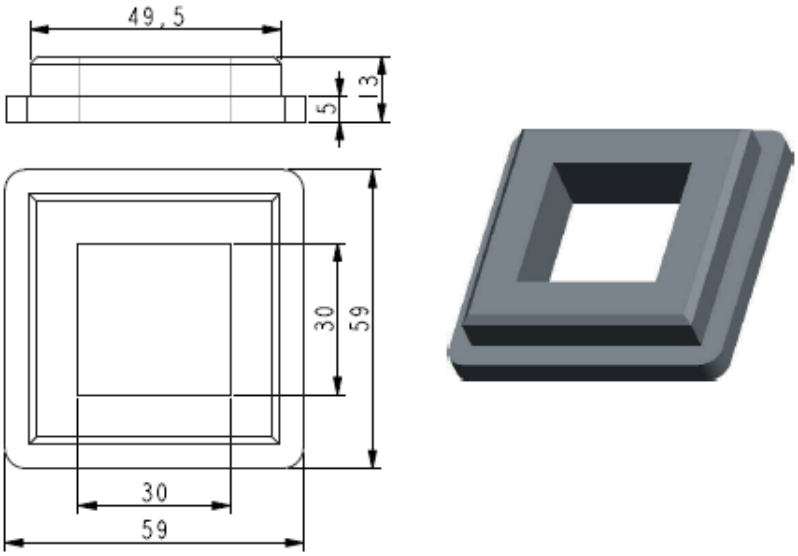

Fig. 5.2. Insert for the inspection window. The dimensions of the insert are in mm.

The window of the insert has the dimension 30 x 30 mm (as shown in Fig. 5.2). It is important to detect the moving pellets with the OCT sensor. The pellet movement enables the generation of cross-section images of a pellet. Sometimes the pellets sticks to the protection foil (see Fig. 5.1), which causes that the OCT system measures only one position of the pellet. Also important for the measurement is the focus distance (25.1 mm) between the moving pellets and the lens of the OCT sensor.

Fig. 5.3. Positioning of the OCT sensor

At the experiments B01, B02, and B03 a 2D sensor was used to generate the cross-sectional images (Markl, Zettl, et al. 2014). A 3D sensor was applied for the experiment B04. The galvanometer mirrors were turned off, so the cross-sectional images were generated by moving the pellets in transverse direction relative to the sensor head. The settings of the OCT system for the experiments are listed in Table 5.1.

Table 5.1. Settings of the OCT system

	B01/B02/B03		B04	
Sensor head	2D		3D	
	[mm]	[pixel]	[mm]	[pixel]
Displacement x direction	2.94	1000	3.13	1024
Displacement z direction	1.46	600	3.13	1024
Light source wavelength		830 nm		832 nm
Spectral bandwidth		62 nm		75 nm
Axial resolution		4.90 µm		4.07 µm

5.2 Data Evaluation of In-line OCT Data

The following chapter describes the algorithm for the determination of the coating thickness from in-line OCT data. The algorithm is implemented in MATLAB® R2013a. The data flow diagram of the algorithm is shown in Fig. 5.4. The algorithm for the in-line coating thickness evaluation uses the same functions as described in chapter 4.1 for the off-line evaluation. Additional the function “region of interest” detects the protection foil on the OCT image with an autocorrelation function. This function correlates a signal with itself having a time shift. Therefore, the autocorrelation function is a simple method for pattern recognition (Radl 2013). A threshold is then applied on the output of the autocorrelation function to detect the protection foil on the OCT image. Appendix C contains the MATLAB® code for the in-line OCT characterisation of pellets.

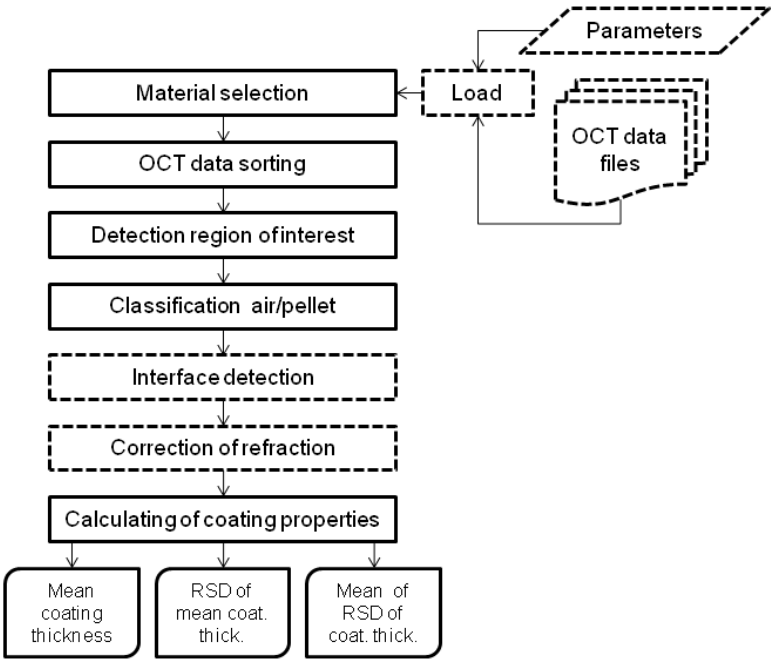

Fig. 5.4. Data flow diagram of the in-line coating thickness evaluation algorithm. The dotted line indicates the existing code.

5.3 Results and Discussion

Fig. 5.5 shows the in-line monitoring of a fluid bed coater with the OCT system. The experimental setup was the same as shown in Fig. 1.18. The top two horizontal lines indicate the protection foil. The vibration during the coating process is partly responsible for the bad image quality. Most of the OCT images show only half of the pellets due to the attenuation of the optical beam in the coating layer and the pellet core (Markl, Zettl, et al. 2014).

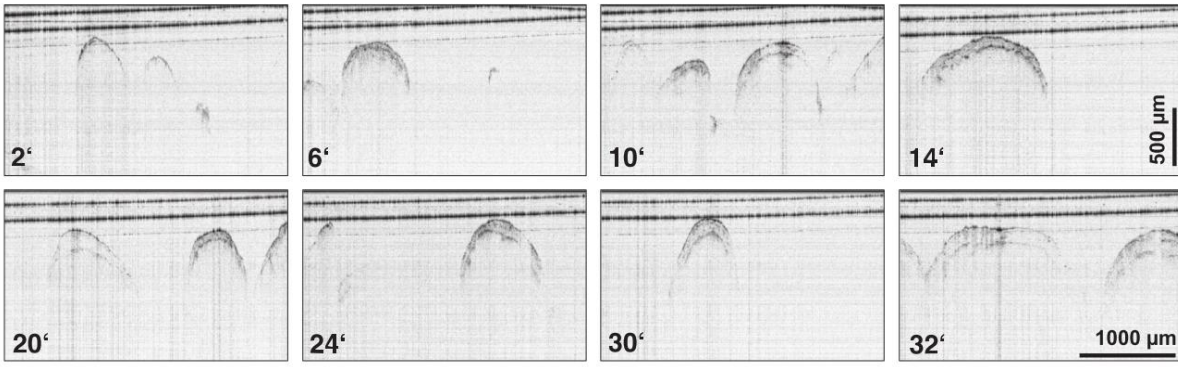

Fig. 5.5. In-line OCT images of film-coated pellets with Dynasan® 118 at different process times (in minutes). Image dimensions (in air) are 2.94 x 1.46 mm^2 (1000 x 600 pixels) (Markl, Zettl, et al. 2014).

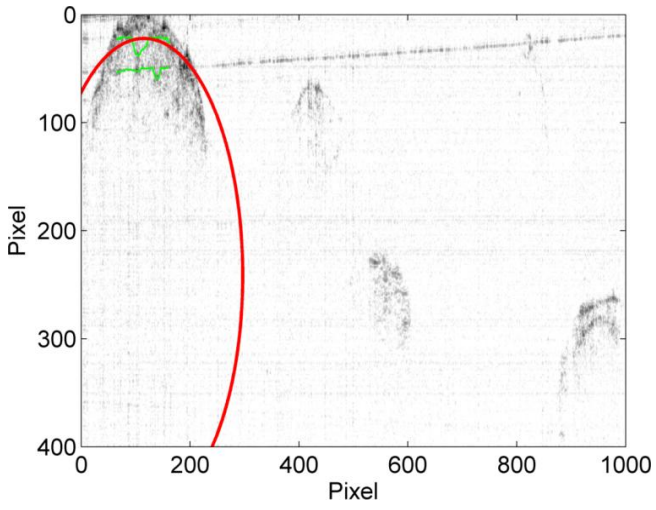

Fig. 5.6. Detected pellet (B01) with the algorithm at a process time of 10 min. Image dimensions (in air) are 2.94 x 0.97 mm^2 (1000 x 400 pixels).

One automatic detected pellet with the algorithm is illustrated in Fig. 5.6. The two green lines indicate the air/coating and the coating/pellet core interface of the coating layer. The correction of refraction is performed by fitting a circle (red) in the air/coating interface. The air/coating interface cannot be detected clearly, because of the bad image quality. As a result of the reflection of the protection foil one horizontal line is displayed in the OCT image.

The algorithm detects this line as the coating/pellet core interface of the coating layer. Based on the reflection of the protection foil and the bad image quality of the in-line OCT images, an automatic data evaluation for the experiments B01-B03 is not possible.

The in-line OCT images of film-coated pellets from B04 at different process times is illustrated in Fig. 5.7. The top two horizontal lines indicate the protection foil. In these OCT images the reflection of the protection foil as shown in Fig. 5.6 does not appear. However, the coating/pellet core interface of the coating layer is not clearly defined.

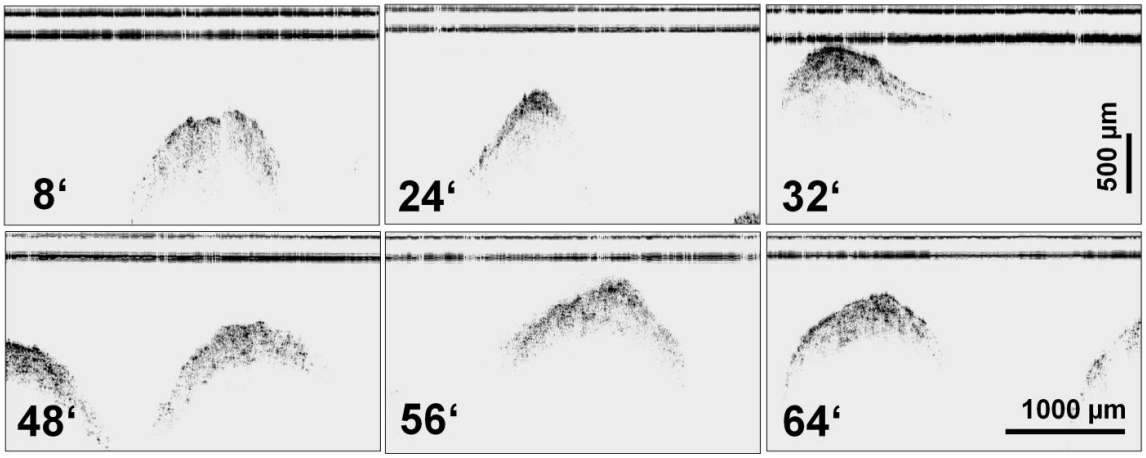

Fig. 5.7. In-line OCT images of film-coated pellets with Eudragit® L 30 D-55 at different process times (in minutes). Image dimensions (in air) are 3.13 x 1.83 mm^2 (1024 x 600 pixels).

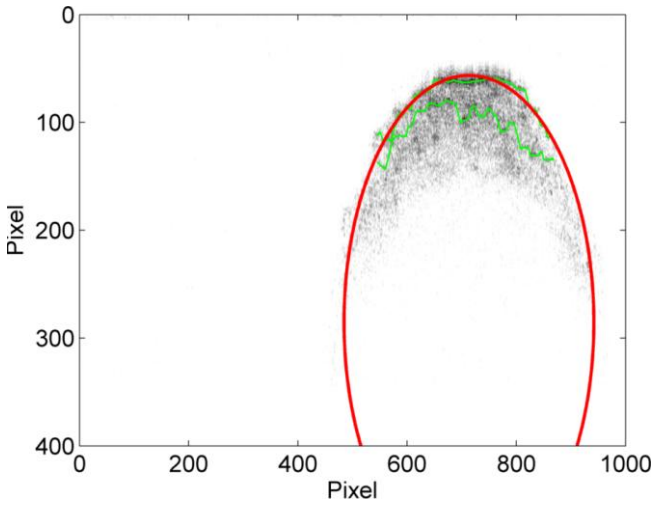

Fig. 5.8. Detected pellet (B04) with the algorithm at a process time of 62 min. Image dimensions (in air) are 3.13 x 1.22 mm^2 (1024 x 400 pixels).

Fig. 5.8 shows one automatic detected pellet with the algorithm. The upper green line indicates sufficiently the air/coating interface of the coating layer. The correction of refraction is performed by fitting a circle (red) in the air/coating interface. The detection of the coating/pellet core interface is not realisable based on the porosity and the non-uniform coating layer of the pellets.

Further experiments would be necessary to define the correct process conditions for a successful coating process with the OCT in-line monitoring. The optimisation of the in-line measurements is subject to a new research project.

6 Conclusion and Outlook

This thesis shows the off-line investigation of film-coated pellets and the in-line process monitoring of a fluid bed pellet coating process by means of OCT. The coating thickness and the homogeneity of the coating layer are key factors for the final pharmaceutical product. The off-line characterisation of pellets by OCT as explained in chapter 4 shows the algorithm for the automatic data evaluation. The automatic data evaluation of the coating thickness is compared to the theoretical coating thickness growth models, to the manual data evaluation of the OCT images and to the particle size analysis (Qicpic). In addition, the inter- and intra-pellet coating uniformity is compared to the manual data evaluation. The experiment B02 has the best coating uniformity of all three replication experiments, as explained in Table 4.4. The algorithm for the off-line characterisation can be used for further experiments to get a quick and quantitative evaluation of the coating of pellets. In addition, the algorithm is the basis for the in-line process monitoring algorithms.

For the measurement with the OCT system during the fluid bed coating process an insert was manufactured for the inspection window of the product container. Unfortunately, the quality of the in-line measured OCT images is not the same as the off-line images due to pellets movement and the protection foil. Thus, the algorithm for the minimization of the measurement errors based on the velocity of the pellets (as described in chapter 1.3.3) will be a task in a further research project. Two main problems appeared at the experiments for the in-line process monitoring of a fluid bed pellet coating process via OCT: (i) the horizontal reflection line of the protection foil as shown in Fig. 5.6 from B01-B03 and (ii) the porosity of the coating layer as illustrated in Fig. 5.8 from B04. A stable fluid bed pellet coating process increases the quality of the in-line measured OCT images.

References

Adler, D.C. et al., 2009. Three-dimensional endomicroscopy of the human colon using optical coherence tomography. *Optics express*, 17(2), pp.784–796.

Bezerra, H.G. et al., 2009. Intracoronary Optical Coherence Tomography: A Comprehensive Review. Clinical and Research Applications. *JACC: Cardiovascular Interventions*, 2(11), pp.1035–1046. Available at: http://dx.doi.org/10.1016/j.jcin.2009.06.019.

Cahyadi, C. et al., 2010. Comparative study of non-destructive methods to quantify thickness of tablet coatings. *International Journal of Pharmaceutics*, 398(1-2), pp.39–49. Available at: http://dx.doi.org/10.1016/j.ijpharm.2010.07.020.

Clayton T. Crowe, 2006. Multiphase flow handbook. In 6000 Broken Sound Parkway NW, Suite 300, Boca Raton, FL 33487: Taylor and Francis, pp. 5–1 – 5–7.

Evonik Industries AG, 2011. EUDRAGIT® L 30 D-55 Enteric coating with talc as anti-tacking agent. , pp.1–2. Available at: http://eudragit.evonik.com/product/eudragit/Documents/evonik-quickstart-eudragit-l-30-d-55-enteric-coating-with-talc-as-anti-tacking-agent.pdf [Accessed March 6, 2015].

Evonik Industries AG, 2014. EUDRAGIT® L 30 D-55 Specification and Test Methods. , pp.1–6. Available at: http://eudragit.evonik.com/sites/lists/HN/ProductSpecifications/TI-EUDRAGIT-L-30-D-55-EN.pdf [Accessed July 27, 2015].

FDA, 2004. Guidance for Industry PAT — A Framework for Innovative Pharmaceutical Development, Manufacturing, and Quality Assurance. , pp.1–19. Available at: http://www.fda.gov/downloads/drugs/guidancecomplianceregulatoryinformation/guidances/ucm070305.pdf [Accessed February 10, 2015].

Fercher, A.F., 2010. Optical coherence tomography - development, principles, applications. *Zeitschrift für medizinische Physik*, 20(4), pp.251–276.

Geldart, D., 1973. Types of Gas Fluidization. *Powder Technology*, 7, pp.285–292.

Glatt GmbH, 2014. Fluidized Bed Systems : a Review. , pp.1–24. Available at: http://www.glatt.com/fileadmin/user_upload/content/pdf_downloads/Produktbroschueren/englisch/BRO_PTPH_027_WS_2014-12_EN.pdf [Accessed February 5, 2015].

Glatt GmbH, 2011. Innovative Technologies for Granules and Pellets. , pp.1–18. Available at: http://www.glatt.com/fileadmin/user_upload/content/pdf_downloads/AB_innovative_technologies_en_111017.pdf [Accessed February 5, 2015].

IFA, 2015a. Talc (CAS-Nr. 14807-96-6) GESTIS-Stoffdatenbank. , pp.1–7. Available at: http://gestis.itrust.de/nxt/gateway.dll/gestis_de/000000.xml?f=templates$fn=default.htm$3.0 [Accessed August 11, 2015].

IFA, 2015b. Triethyl citrate (CAS-Nr. 77-93-0) GESTIS-Stoffdatenbank. , pp.1–7. Available at: http://gestis.itrust.de/nxt/gateway.dll/gestis_de/000000.xml?f=templates$fn=default.htm$3.0 [Accessed August 11, 2015].

INNOJET® Herbert Hüttlin, 2012a. *Assembly Instruction Spray Nozzle IHN-2*, Daimlerstraße 7, D-79585 Steinen.

INNOJET® Herbert Hüttlin, 2012b. *User Manual INNOJET® Hot Melt Device (IHD1)*, Daimlerstraße 7, D-79585 Steinen.

INNOJET® Herbert Hüttlin, 2008. *User Manual VENTILUS 2.5 / 1*, Daimlerstraße 7, D-79585 Steinen.

J.M. Valverde Millan, 2013. Fluidization of Fine Powders. In Dordrecht: Springer Science+Business Media, pp. 1–2.

Kessler, R.W., 2006. *Prozessanalytik: Strategien und Fallbeispiele aus der industriellen Praxis*, Weinheim: Wiley-VCH Verlag GmbH & Co. KGaA.

Knop, K. & Kleinebudde, P., 2013. PAT-tools for process control in pharmaceutical film coating applications. *International Journal of Pharmaceutics*, 457, pp.527–536. Available at: http://dx.doi.org/10.1016/j.ijpharm.2013.01.062.

Koller, D.M. et al., 2011. Non-destructive analysis of tablet coatings with optical coherence tomography. *European Journal of Pharmaceutical Sciences*, 44(1-2), pp.142–148. Available at: http://dx.doi.org/10.1016/j.ejps.2011.06.017.

Kumpugdee-Vollrath, M. & Krause, J.-P., 2011. *Easy Coating, Grundlagen und Trends beim Coating pharmazeutischer Produkte*, Vieweg+Teubner Verlag, Springer Fachmedien Wiesbaden GmbH.

Markl, D., Hannesschläger, G., Sacher, S., Leitner, M., et al., 2015. Automated pharmaceutical tablet coating layer evaluation of optical coherence tomography images. *Measurement Science and Technology*, pp.1–12.

Markl, D., Zettl, M., et al., 2014. Calibration-free in-line monitoring of pellet coating processes via optical coherence tomography. *Chemical Engineering Science*, pp.1–9. Available at: http://dx.doi.org/10.1016/j.ces.2014.05.049.

Markl, D., Hannesschläger, G., Sacher, S., Buchsbaum, A., et al., 2015. In-line Characterization of Pharmaceutical Coatings by Means of Optical Coherence Tomography. *submitted*.

Markl, D., Hannesschläger, G., et al., 2014. Optical coherence tomography as a novel tool for in-line monitoring of a pharmaceutical film-coating process. *European Journal of Pharmaceutical Sciences*, 55, pp.58–67. Available at: http://dx.doi.org/10.1016/j.ejps.2014.01.011.

Pharmatrans Sanaq AG, 2008. Cellets® Pellets from microcrystalline cellulose. , pp.1–4. Available at: http://www.cellets.org/download/cellets_english.pdf [Accessed March 6, 2015].

Pharmatrans Sanaq AG, 2013. *Certificate of Analysis Cellets® 1000*, Gewerbestrasse 12, CH-4123 Allschwil.

Radl, S., 2013. *Particle Technology I Lecture Notes*, Graz.

Recendt GmbH, 2015. Non destructive cross sectional analysis with optical coherence tomography (OCT). , pp.1–2. Available at: http://www.recendt.at/files/OCT_english.pdf [Accessed February 11, 2015].

Roblegg, E. et al., 2011. Development of sustained-release lipophilic calcium stearate pellets via hot melt extrusion. *European Journal of Pharmaceutics and Biopharmaceutics*, 79(3), pp.635–645. Available at: http://dx.doi.org/10.1016/j.ejpb.2011.07.004.

Ruotsalainen, M. et al., 2003. A novel technique for imaging film coating defects in the film-core interface and surface of coated tablets. *European Journal of Pharmaceutics and Biopharmaceutics*, 56(3), pp.381–388.

Sasol Germany GmbH, 2007. *Product Information Dynasan®*, Arthur-Imhausen-Str. 92, 58453 Witten, Germany.

Sattler, E., Kästle, R. & Welzel, J., 2013. Optical coherence tomography in dermatology. *Biomedical Optics*, 18(6), pp.1–7.

Šibanc, R. et al., 2013. Physical properties of pharmaceutical pellets. *Chemical Engineering Science*, 86, pp.50–60.

Stieß, M., 2009. *Mechanische Verfahrenstechnik - Partikeltechnologie 1*, Springer-Verlag Berlin Heidelberg.

Suzzi, D., Radl, S. & Khinast, J.G., 2010. Local analysis of the tablet coating process: Impact of operation conditions on film quality. *Chemical Engineering Science*, 65(21), pp.5699–5715. Available at: http://dx.doi.org/10.1016/j.ces.2010.07.007.

Turton, R., 2008. Challenges in the modeling and prediction of coating of pharmaceutical dosage forms. *Powder Technology*, 181, pp.186–194.

Wojtkowski, M., 2010. High-speed optical coherence tomography: basics and applications. *Applied Optics*, 49(16), pp.D30–D61.

Zeitler, J.A. & Gladden, L.F., 2008. In-vitro tomography and non-destructive imaging at depth of pharmaceutical solid dosage forms. *European Journal of Pharmaceutics and Biopharmaceutics*, 71(1), pp.2–22. Available at: http://dx.doi.org/10.1016/j.ejpb.2008.08.012.

Appendices

Appendix A: Diagrams

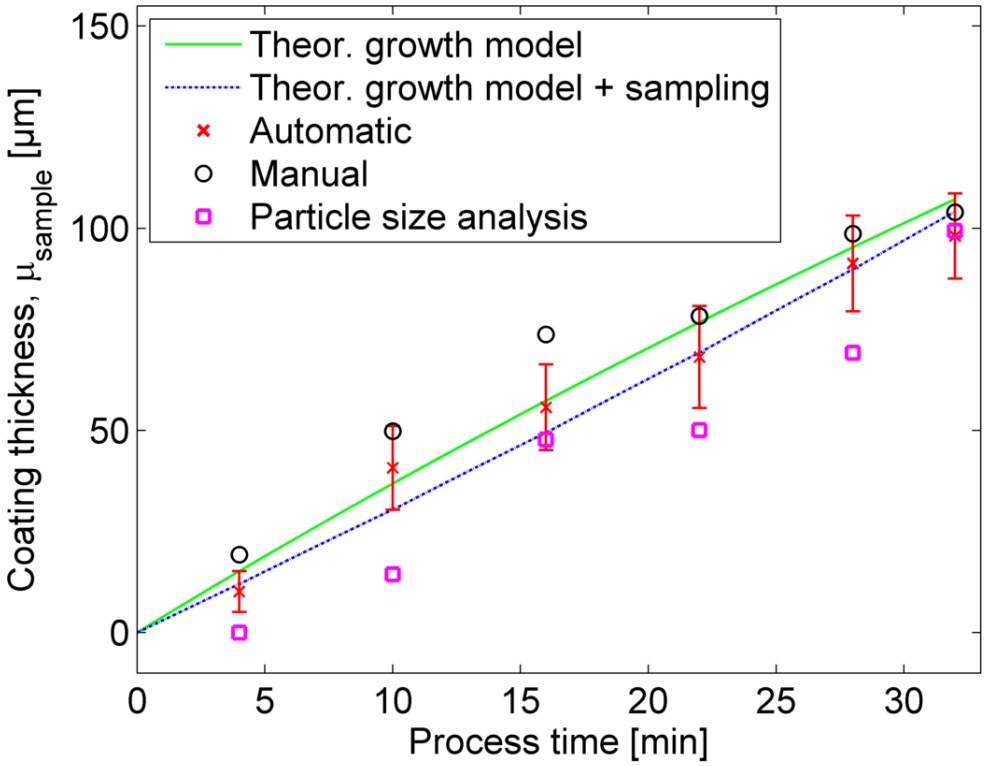

Fig. A.1. Coating thickness as a function of the process time for B01.

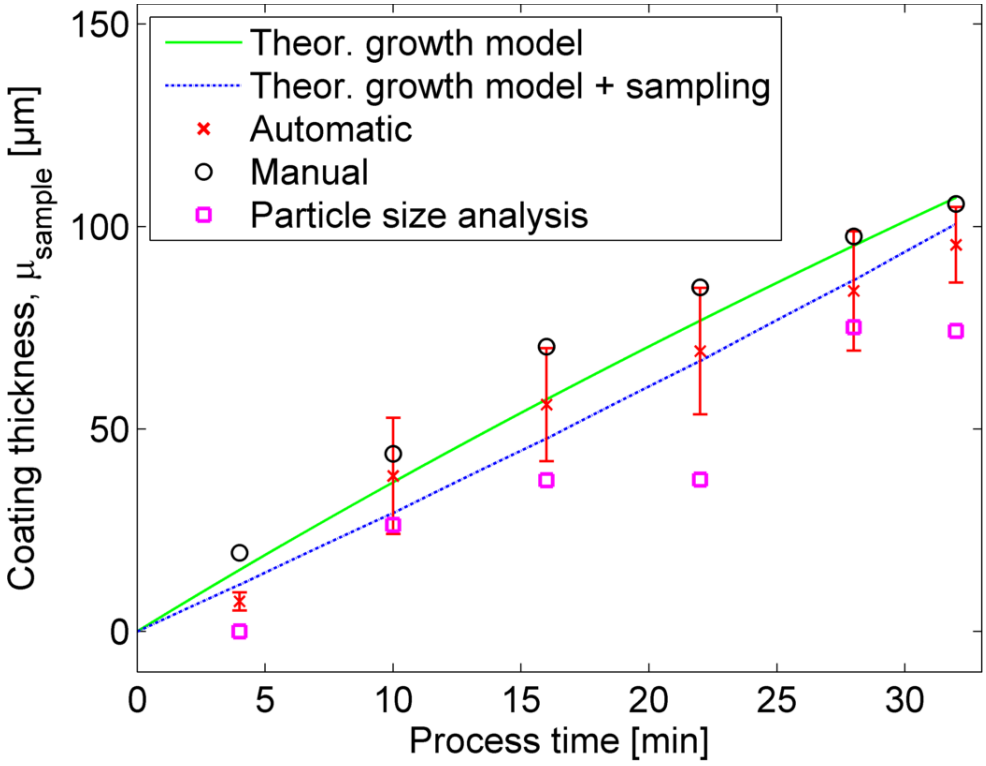

Fig. A.2. Coating thickness as a function of the process time for B03.

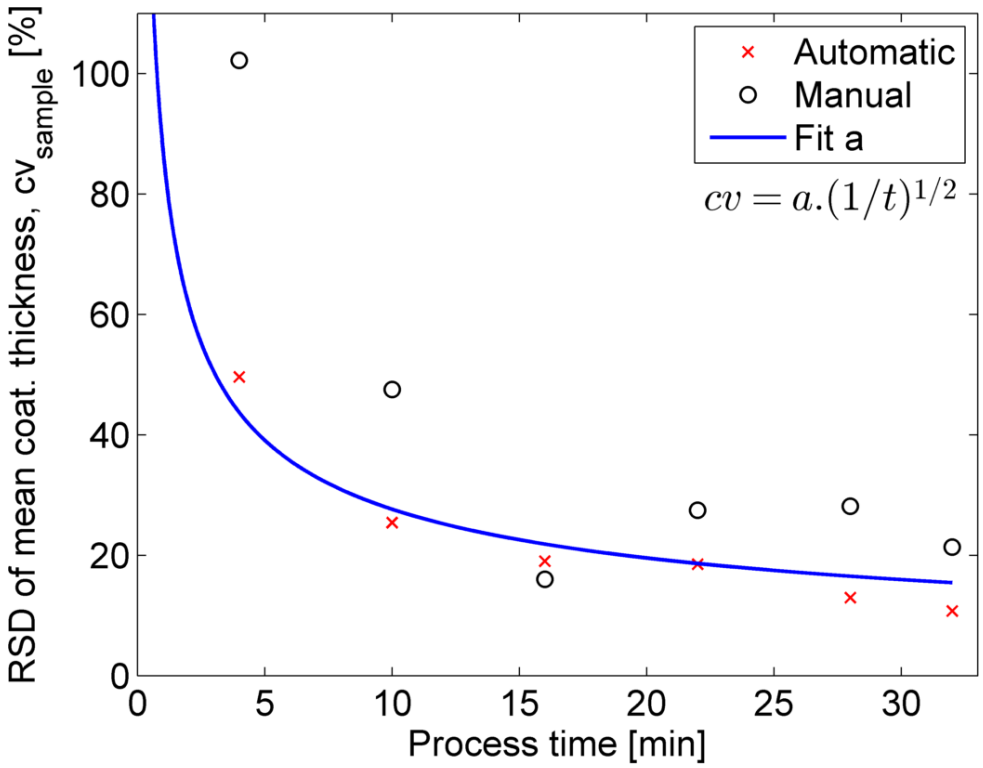

Fig. A.3. Inter-pellet coating uniformity for B01. The variable a for the blue curve was fitted with the automatic evaluated data.

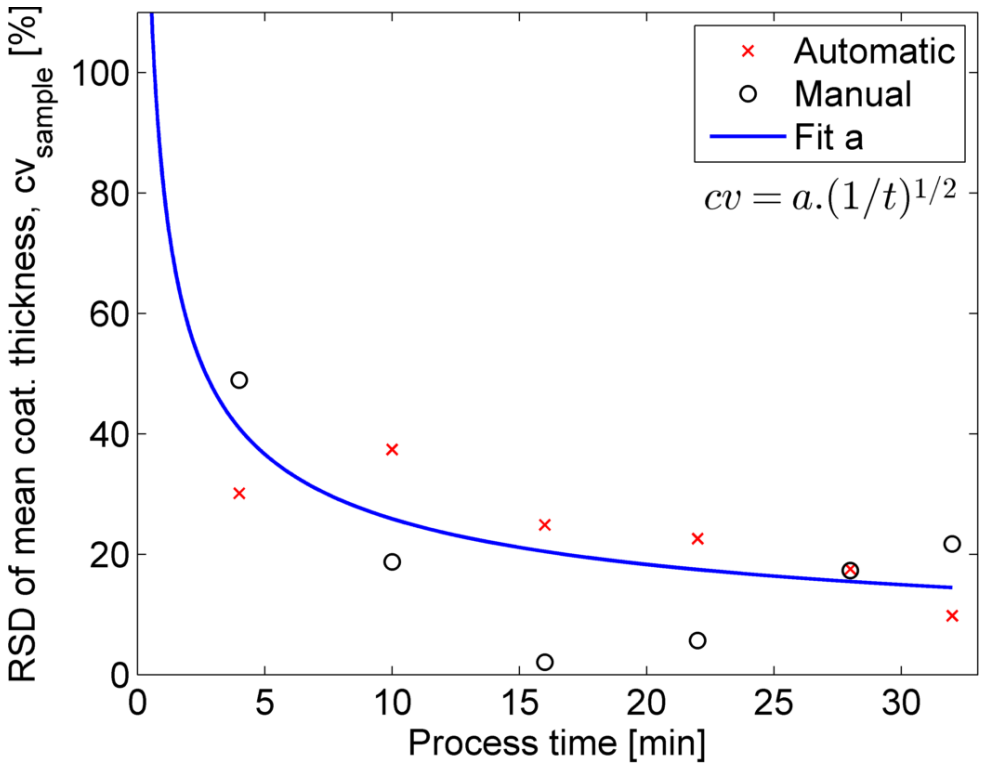

Fig. A.4. Inter-pellet coating uniformity for B03. The variable a for the blue curve was fitted with the automatic evaluated data.

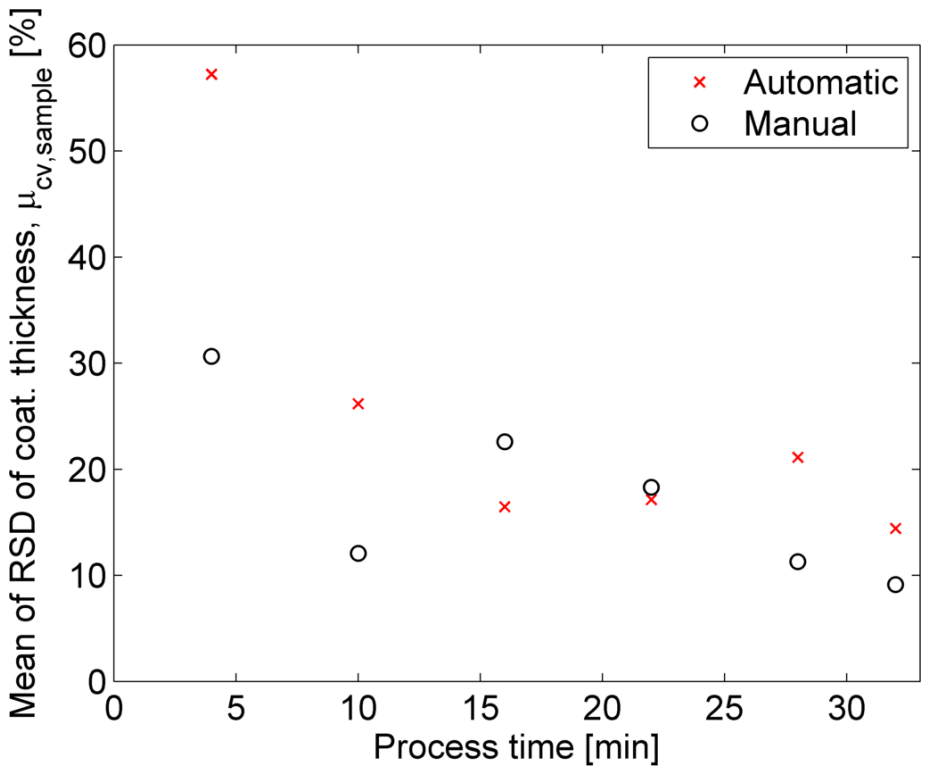

Fig. A.5. Intra-pellet coating uniformity for B01.

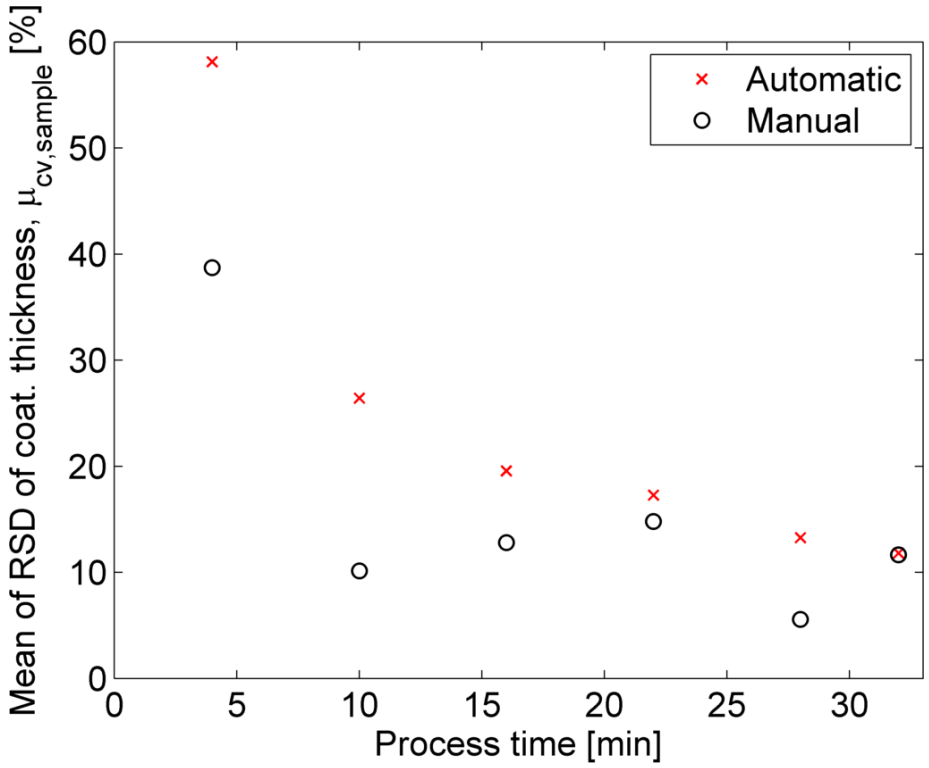

Fig. A.6. Intra-pellet coating uniformity for B03.

Appendix B: Summary of the Results

Table B.1. Summary of the results for the coating thickness (B01)

Sample index i [-]	Mean coating thickness Qicpic [µm]	Mean coating thickness Manual [µm]	Standard deviation Manual [µm]	Mean coating thickness Automatic [µm]	Standard deviation Automatic [µm]	Theor. growth model [µm]	Theor. growth model +sampling [µm]
1	0.00	19.31	19.73	10.14	5.03	15.19	12.03
2	14.45	49.85	23.70	40.74	10.36	36.84	30.41
3	47.76	73.70	11.80	55.72	10.60	57.31	49.46
4	50.08	78.31	21.54	68.13	12.62	76.75	69.26
5	69.17	98.67	27.78	91.31	11.84	95.27	89.84
6	99.34	104.00	22.20	98.06	10.53	107.20	104.10

Table B.2. Summary of the results for the coating thickness (B02)

Sample index i [-]	Mean coating thickness Qicpic [µm]	Mean coating thickness Manual [µm]	Standard deviation Manual [µm]	Mean coating thickness Automatic [µm]	Standard deviation Automatic [µm]	Theor. growth model [µm]	Theor. growth model +sampling [µm]
1	0.00	19.36	10.34	7.52	2.87	15.19	10.87
2	18.72	39.19	11.29	36.51	7.50	36.84	27.50
3	49.65	65.46	9.86	49.32	9.03	57.31	44.62
4	71.84	86.52	17.60	65.05	11.79	76.75	62.30
5	88.99	92.43	22.39	81.09	12.55	95.27	80.77
6	98.26	104.51	18.96	87.28	11.24	107.20	93.68

Table B.3. Summary of the results for the coating thickness (B03)

Sample index i [-]	Mean coating thickness Qicpic [µm]	Mean coating thickness Manual [µm]	Standard deviation Manual [µm]	Mean coating thickness Automatic [µm]	Standard deviation Automatic [µm]	Theor. growth model [µm]	Theor. growth model +sampling [µm]
1	0.00	19.41	9.49	7.42	2.23	15.19	11.55
2	26.29	43.87	8.22	38.38	14.36	36.84	29.26
3	37.31	70.30	1.45	56.00	13.94	57.31	47.66
4	37.48	84.97	4.85	69.23	15.65	76.75	66.81
5	75.12	97.56	16.90	84.08	14.74	95.27	86.78
6	74.23	105.62	22.96	95.48	9.35	107.20	100.70

Table B.4. Summary of the results for the inter- and intra-pellet coating uniformity (B01)

Sample index i [-]	RSD of mean coat. thickness Manual [%]	RSD of mean coat. thickness Automatic [%]	Mean of RSD of coat. thickness Manual [%]	Mean of RSD of coat. thickness Automatic [%]
1	102.18	49.60	30.65	57.23
2	47.54	25.42	12.09	26.17
3	16.01	19.02	22.61	16.46
4	27.51	18.52	18.32	17.13
5	28.15	12.96	11.29	21.13
6	21.35	10.73	9.14	14.42

Table B.5. Summary of the results for the inter- and intra-pellet coating uniformity (B02)

Sample index i [-]	RSD of mean coat. thickness Manual [%]	RSD of mean coat. thickness Automatic [%]	Mean of RSD of coat. thickness Manual [%]	Mean of RSD of coat. thickness Automatic [%]
1	53.41	38.17	14.09	44.43
2	28.80	20.53	16.84	36.09
3	15.06	18.31	14.00	25.15
4	20.34	18.12	14.43	18.46
5	24.23	15.47	10.34	13.70
6	18.14	12.87	10.39	15.47

Table B.6. Summary of the results for the inter- and intra-pellet coating uniformity (B03)

Sample index i [-]	RSD of mean coat. thickness Manual [%]	RSD of mean coat. thickness Automatic [%]	Mean of RSD of coat. thickness Manual [%]	Mean of RSD of coat. thickness Automatic [%]
1	48.91	30.12	38.72	58.13
2	18.74	37.40	10.14	26.42
3	2.06	24.89	12.82	19.56
4	5.70	22.60	14.80	17.27
5	17.32	17.53	5.58	13.27
6	21.74	9.79	11.67	11.81

Table B.7. Summary of the results for the coating thickness (B04)

Sample index i [-]	Mean coating thickness Automatic [µm]	Standard deviation Automatic [µm]	Theor. growth model [µm]	Theor. growth model +sampling [µm]
1	5.90	2.36	22.24	14.61
2	37.44	17.56	42.99	29.93
3	53.42	10.37	62.48	46.01
4	72.81	8.80	80.89	62.94
5	83.92	17.85	98.36	80.76
6	100.39	12.84	115.00	99.55
7	117.01	18.37	130.90	119.30
8	132.56	22.36	146.10	140.10

Table B.8. Summary of the results for the inter- and intra-pellet coating uniformity (B04)

Sample index i [-]	RSD of mean coat. thickness Automatic [%]	Mean of RSD of coat. thickness Automatic [%]
1	40.01	53.60
2	46.90	35.20
3	19.42	27.57
4	12.09	25.60
5	21.27	33.90
6	12.79	25.29
7	15.70	28.05
8	16.87	21.86

Appendix C: MATLAB® Code

```
% ========================================================================
% AUTOMATIC DATA ANALYSIS OFFLINE (FLUID BED COATING)
% ========================================================================
%   A3.12: Optical Coherence Tomography
%   Research Center Pharmaceutical Engineering GmbH
%
%   Author: Alois Herzog
%   Version: 001
%   Date: 10/07/2015
% ------------------------------------------------------------------------
%%
close all;
clear all;
clc;
%% Install init
pathtoinit = '../../'; % 2 folders back
addpath(pathtoinit);   % Add folders to search path

init;                  % Initialize framework and set default configuration

load([datapath,'options_intdet.mat']);

system = 5;

InitParamProperties;

options_intdet.weights_u = [0.6 0.3];    % weights upper interface
options_intdet.weights_l = [0.3 0.6];    % weights lower interface
options_intdet.sigma_u = 3;
options_intdet.sigma_l = 5;
options_intdet.filter = 'hessian';

options_intdet.horizont = 2;

options_intdet.delta_min = 5;
options_intdet.delta_max = 200;
%% Selection Material: (Core+Coating)
%  ParaCaSt+Dynasan= 1 or Cellets+Eudragit=2
mat = 1;

display_movie = 0;   % Show Movie B04 and save
display_circle = 1;  % Show Circle Fit and save
xyz = 1;

%% ParaCaSt+Dynasan
if mat==1

    exp_name = 'ParaCast';
    batch = 'B04';              % Insert batch name: B03,B04 or B05
    sample_idx_start = 1;
    sample_idx_end = 6;
    data_format = 0;            % bmp. data file

    param.num_ascan = 1000;
    param_detection.displacement = 2.94/param.num_ascan*10^-3;% x direction
    % [m/Pixel]
    param_detection.res_axial = 1.46/600*10^-3; % z direction [m/Pixel]
```

```
    param.res_axial = param_detection.res_axial;
    param_detection.R = 711.3*10^-6; % Radius Pellet [m]

    param.n_i = 1.4385;          % Refraction index Dynasan 118
    param_detection.n_i =  param.n_i;

    limit = 0.60;                % Contrast OCT file
    pel_min = 50;                % Minimum for pellet detection
    filter = 1.8;                % Filter for classification air/pellet

    param.error_max = 3*10^-5;  % Circle Fit error

    delta_min_vec = [5 15 35 45 60 70]*10^-6; % Initial value for
    % coating thickness [m]

    %% Movie
    if display_movie
        path_to_folder_mov = ...
            ['Z:\K1\A3.12\100_Daten\DATEN\A3_MED_FluidBedCoating\',...
            exp_name,'\Offline\B04\mov'];

        load([path_to_folder_mov,'\mov_F_B04.mat']);
        load([path_to_folder_mov,'\mov_mean_thickness_total_B04.mat']);
        load([path_to_folder_mov,'\mov_std_thickness_inter_B04.mat']);

        t_offl = [4 10 16 22 28 32];  % [min]

        mov_idx = 0;  % for show automatic evaluated data
    end
end
%% Cellets+Eudragit
if mat==2

    exp_name = 'Eudragit';
    batch = 'B04';               % Insert batch name
    sample_idx_start = 1;
    sample_idx_end = 8;
    data_format = 1;             % raw. data file

    param.num_ascan = 1024;
    param_detection.displacement = 3.13/param.num_ascan*10^-3;% x direction
    % [m/Pixel]
    param_detection.res_axial = 3.13/param.num_ascan*10^-3;   % z direction
    % [m/Pixel]
    param.res_axial = param_detection.res_axial;
    param_detection.R = 0.0006; % Radius pellet [m]

    param.n_i = 1.48;            % Refraction index Eudragit
    param_detection.n_i =  param.n_i;

    limit = 0.82;                % Contrast OCT file
    pel_min = 50;                % Minimum for pellet detection
    filter = 1.8;                % Filter for classification air/pellet

    param.error_max = 3*10^-5;  % Circle Fit error

    delta_min_vec = [5 15 25 35 45 55 65 75]*10^-6; % Initial value for
    % coating thickness [m]
end
```

```
%% Request .raw or .bmp data files
if data_format
    data_types = '*.raw';
    InitNuFFT(param);    % Fast fourier transform
else
    data_types = '*.bmp';
end
%%
mean_thickness_total = zeros(sample_idx_end-sample_idx_start+1,1);
std_thickness_inter = zeros(sample_idx_end-sample_idx_start+1,1);
rstd_thickness_inter = zeros(sample_idx_end-sample_idx_start+1,1);

std_thickness_intra = zeros(sample_idx_end-sample_idx_start+1,1);
rstd_thickness_intra = zeros(sample_idx_end-sample_idx_start+1,1);

n_pellets = zeros(sample_idx_end-sample_idx_start+1,1);

%% Movie
if display_movie
    fig = figure(1);
    set(fig,'Color',[1 1 1])
    set(fig,'Position',[100 100 850 400])

    sampling_time = 0.9;
    writerObj = VideoWriter([path_to_folder_mov,'\mov_B04.mp4'],'MPEG-4');
    writerObj.FrameRate = 1/sampling_time;
    writerObj.Quality = 100;
    open(writerObj);
    set(gcf,'Renderer','zbuffer');
    formatSpec = '%2.2f\n';
end
%% Sample file folder
for sample_idx = sample_idx_start:sample_idx_end;

    path_to_folder = ...
        ['Z:\K1\A3.12\100_Daten\DATEN\A3_MED_FluidBedCoating\',exp_name,...
        '\Offline\',...
        batch,'\Sample',num2str(sample_idx),'\imgs'];
    %% Data sorting
    current_folder = pwd;
    cd(path_to_folder);
    filelisting = dir(data_types);
    [r inx] = sort({filelisting.date});
    filelisting = filelisting(inx);
    cd(current_folder);
    %% Generate reference image
    if data_format
        sample1 = reshape(GetSingleRawFile(fullfile(path_to_folder,...
            filelisting(1).name)),...
            param.num_pixel,param.num_ascan);
        reference = repmat(EstimateReference(sample1),1,param.num_ascan);
    end
    %%
    N = length(filelisting);
    file_start_idx = 1;
    file_end_idx = N;

    if file_end_idx > N
        file_end_idx = N;
    end
```

```
mean_thickness = cell(N,1);
std_thickness = cell(N,1);
%% Initial value for coating thickness calculated in Pixel
options_intdet.delta_min = round(delta_min_vec(sample_idx)./...
    (param.res_axial)*param_detection.n_i);
%% OCT file
for file_idx = file_start_idx:file_end_idx;
    if data_format
        current_raw_file = fullfile(path_to_folder,...
            filelisting(file_idx).name);
        sample = reshape(GetSingleRawFile(current_raw_file),...
            param.num_pixel,param.num_ascan);
        reference = repmat(EstimateReference(sample),1,...
            param.num_ascan);
        stat = dir(current_raw_file);
        timestamp = stat.date;
        img = NuFFT(sample, reference);
    else
        file_name = filelisting(file_idx).name;
        cd(path_to_folder);
        img_raw = imread(file_name);
        img = double(img_raw)./255;
        cd(current_folder);
    end
    %% Prepare image data
    % -------------------------------------------------------------------
    fprintf('... Prepare data (image %i, %s, %s)\n',file_idx, ...
        filelisting(file_idx).name,filelisting(file_idx).date);
    img_disp = img;
    img_disp(img_disp>limit) = limit; % Contrast OCT file
    img_disp = img_disp./limit;
    img_cut = img_disp(30:end-500,:); % Delete reference line and
    % lower area
    %% Function for classification air/pellet
    trans = func_class(img_cut,pel_min,filter);
    %% Interface detection
    trans_n = size(trans,1);
    path_u_sp = zeros(param.num_ascan,1);
    path_l_sp = zeros(param.num_ascan,1);
    %% Movie
    if display_movie
        subplot(1,2,1);
    else
        figure(1);
    end
    %%
    imagesc(img_cut);
    colormap('gray')
    xlabel('Pixel');
    ylabel('Pixel');
    axis([0 1000 0 500]);
    set(gca,'XTick', 0:200:1000);
    set(gca,'YTick', 0:100:500);
    hold on;
    %% Detected pellet
    for ii = 1:1:trans_n

        min_trans = trans(ii,1);
        max_trans = trans(ii,2);
        img_roi_col = img_cut(:,min_trans:max_trans);%Reach of interest
        %% Function interface detection
        fprintf('... Interface Detection\n');
```

```
        [feature_vec idx_window_1] = getFeatureVector(img_roi_col,...
            25,25);

        [path_utmp,path_ltmp,~,error] = ...
            DetectInterfaces(img_roi_col, param_detection,...
            options_intdet,idx_window_1,...
            'unconstrained', 0,'display',0); % 1=show filter

        if error
            trans(ii,:) = 0;
            fprintf('DEBUG: Interface Detection failed!\n');
        else
            path_u_sp(min_trans:...
                max_trans) = path_utmp;

            path_l_sp(min_trans:...
                max_trans) = path_ltmp;
        end
        %%
    end
    if ~isempty(trans)
        trans = trans(trans(:,1)~=0,:);
    end

    %% Correct distortions
    fprintf('... Correct distortion\n');

    trans_n = size(trans,1);
    x_oct = (0:length(path_u_sp)-1)';
    x_correct = x_oct.*param_detection.displacement;
    z_correct = path_l_sp.*param_detection.res_axial;

    center_sphere_est_u = zeros(trans_n,3);
    center_sphere_est_l = zeros(trans_n,3);

    mean_thickness_est = zeros(trans_n,1);
    std_thickness_est = zeros(trans_n,1);

    error = zeros(trans_n,1);
    %% Detected pellet
    for ii = 1:1:trans_n

        % Row vector of the detected pellets upper interface
        path_u_ = path_u_sp(trans(ii,1):trans(ii,2)).*...
            param_detection.res_axial;

        % Row vector of the detected pellets lower interface
        path_l_ = path_l_sp(trans(ii,1):trans(ii,2)).*...
            param_detection.res_axial;

        % x coordinate upper interface
        x_A = x_oct(trans(ii,1):trans(ii,2)).*...
            param_detection.displacement;

        %% Circle fit upper interface
        [center_sphere_est_u(ii,:) error(ii)] = ...
            circleFitSingleTablet([x_A path_u_],param_detection);
        %%
```

```
if error(ii) > param.error_max
    center_sphere_est_u(ii,:) = 0;
    trans(ii,:) = 0;
    fprintf('DEBUG: Circle fit error too large!\n');
    fprintf('DEBUG: Error: %d\n', error(ii));
else
    center = [center_sphere_est_u(ii,1)-...
        trans(ii,1).*param_detection.displacement; ...
        center_sphere_est_u(ii,2)];
    %% Correct curvature (Snells Law)
    [ x_B z_B theta_j] = correctCurvature( x_A -trans(ii,1)*...
        param_detection.displacement, path_u_, path_l_, ...
        center, param_detection);
    %% Correct coordinates
    x_correct(trans(ii,1):trans(ii,2)) = x_B + trans(ii,1).*...
        param_detection.displacement;

    z_correct(trans(ii,1):trans(ii,2)) = z_B;
    %% Circle Fit lower Interface
    center_sphere_est_l(ii,:) = circleFitSingleTablet(...
        [x_correct(trans(ii,1):trans(ii,2))...
        z_correct(trans(ii,1):...
        trans(ii,2))],param_detection,...
        center_sphere_est_u(ii,:));
    %% Polar coordinates
    [dist_u_sp phi_u] = GetPolarCoordinates([x_A path_u_],...
        center_sphere_est_u(ii,1:2));

    [dist_l_sp phi_l] = GetPolarCoordinates(...
        [x_correct(trans(ii,1):trans(ii,2))...
        z_correct(trans(ii,1):trans(ii,2))], ...
        center_sphere_est_l(ii,1:2));
    %% Identical angle upper and lower interface
    idx_min = zeros(length(phi_u),1);
    for i = 1:length(phi_u)
        [val idx_min(i)] = min(abs(phi_u(i)-phi_l));
    end
    %% Calculating coating thickness
    thickness_est = dist_u_sp - dist_l_sp(idx_min);
    mean_thickness_est(ii) = mean(thickness_est);
    std_thickness_est(ii) = std(thickness_est);
    %% Plot Interface Detection
    plot(trans(ii,1):trans(ii,2),round(path_u_./...
        param_detection.res_axial),'g','LineWidth',2)
    plot(trans(ii,1):trans(ii,2),round(path_l_./...
        param_detection.res_axial),'g','LineWidth',2)

    if display_circle
        %Upper Interface
        height_u = 2*center_sphere_est_u(ii,3)/...
            param_detection.res_axial;
        width_u = 2*center_sphere_est_u(ii,3)/...
            param_detection.displacement;

        center_u = [center_sphere_est_u(ii,1)/...
            param_detection.displacement ...
            center_sphere_est_u(ii,2)/...
            param_detection.res_axial];
```

```
                rectangle('position',[center_u(1)-...
                    width_u/2,center_u(2)-...
                    height_u/2,width_u,height_u],...
                    'curvature',[1,1],'linestyle','-','linewidth',2,...
                    'edgecolor','r');
            end
        end
        %%
        fprintf('Mean coating thickness: %6.2f µm\n',...
            mean_thickness_est(ii)*10^6);
        fprintf('Standard deviation: %6.2f µm\n',...
            std_thickness_est(ii)*10^6);
    end

    hold off;

    %% Movie
    if display_movie
        subplot(1,2,2);

        N = length(mov_F_B04);
        t_func = 1:N;
        plot(t_func/60,mov_F_B04*10^6,'-.bl','LineWidth',1);
        xlabel('Process time [min]');
        ylabel('Coating thickness, \mu_{sample} [µm]');
        axis([0 40 0 130]);
        set(gca,'XTick', 0:10:40);
        set(gca,'YTick', 0:20:130);
        if mov_idx > 0
            hold on;
            errorbar(t_offl(1:mov_idx),...
                mov_mean_thickness_total_B04(1:mov_idx)*10^6,...
                mov_std_thickness_inter_B04(1:mov_idx)*10^6,...
                'rx','LineWidth',1);
            hold off;
        end
        if mov_idx==5 && file_idx==file_end_idx
            hold on;
            errorbar(t_offl(1:end),...
                mov_mean_thickness_total_B04(1:end)*10^6,...
                mov_std_thickness_inter_B04(1:end)*10^6,...
                'rx','LineWidth',1);
            hold off;
        end
        leg = legend('Theor. growth model','Automatic');
        set(leg,'Location','NorthWest')
        frame = getframe(gcf);
        writeVideo(writerObj,frame);
        clf;
    end
    %%  Save Plot circle fit
    if display_circle
        figpath = 'fluid_bed_coating\';
        printFig([savefigurespath,figpath,exp_name,'\',batch,...
            '\Offline'],num2str(xyz));

        xyz = xyz+1;
    end
    %%
    idx_use = mean_thickness_est~=0; % Only coating thickness unequal 0
```

```
        mean_thickness_est = mean_thickness_est(idx_use);
        std_thickness_est = std_thickness_est(idx_use);

        %% Calculation coating parameters
        mean_thickness{(file_idx)} = mean_thickness_est;
        std_thickness{(file_idx)} = std_thickness_est;

    end

    mean_all_pellets = cell2mat(mean_thickness);
    n_pellets(sample_idx) = length(mean_all_pellets);
    mean_thickness_total(sample_idx) = mean(mean_all_pellets);
    std_thickness_inter(sample_idx) = std(mean_all_pellets);
    rstd_thickness_inter(sample_idx) = std_thickness_inter(sample_idx)./...
        mean_thickness_total(sample_idx);

    std_all_pellets = cell2mat(std_thickness);
    std_thickness_intra(sample_idx) = mean(std_all_pellets);
    rstd_thickness_intra(sample_idx) = mean(std_all_pellets./...
        mean_all_pellets);

    %% Movie
    if display_movie
        mov_idx = mov_idx+1;
    end
    %%
end
%% Movie
if display_movie
    close(writerObj);
    close all;
end
%% Save data
eval(['mean_thickness_total_',sprintf(batch),' = mean_thickness_total',...
    ';']);
eval(['std_thickness_inter_',sprintf(batch),' = std_thickness_inter',...
    ';']);
eval(['rstd_thickness_inter_',sprintf(batch),' = rstd_thickness_inter',...
    ';']);
eval(['std_thickness_intra_',sprintf(batch),' = std_thickness_intra',...
    ';']);
eval(['rstd_thickness_intra_',sprintf(batch),' = rstd_thickness_intra',...
    ';']);
eval(['n_pellets_',sprintf(batch),' = n_pellets',';']);

save([datapath,exp_name,filesep,batch,'_offline'],...
    ['mean_thickness_total_',sprintf(batch)],['std_thickness_inter_',...
    sprintf(batch)],['rstd_thickness_inter_',sprintf(batch)],...
    ['std_thickness_intra_',sprintf(batch)],['rstd_thickness_intra_',...
    sprintf(batch)],['n_pellets_',sprintf(batch)]);
%%
```

```
% ========================================================================
% DATA EVALUATION OFFLINE (FLUID BED COATING)
% ========================================================================
%   A3.12: Optical Coherence Tomography
%   Research Center Pharmaceutical Engineering GmbH
%
%   Author: Alois Herzog
%   Version: 001
%   Date: 09/07/2015
% ------------------------------------------------------------------------
%%
clc;
close all;
clear all;
%% Install init
pathtoinit = '../../';
addpath(pathtoinit);
init;
%% Data define in struct
data = struct('r',[],'rho_core',[],'m_pellets',[],'rho_coat',[],'ds',[],...
    'rate',[],'cr',[],'N_sample',[]);
%% Selection Material: (Core+Coating)
%  ParaCaSt+Dynasan= 1 or Cellets+Eudragit=2
mat = 1;
%% ParaCaSt+Dynasan
if mat==1

    exp_name = 'ParaCaSt';
    batchID = '04'; % Selection batchID= 03, 04 or 05
    B03_4_5 = 0;      % 1=Evaluation B03/04/05 by B04

    %% LOAD Automatic Data
    load([datapath,exp_name,filesep,'B',batchID,'_offline']);

    eval(['mean_thickness_total = mean_thickness_total_B',...
        sprintf(batchID),';']);
    eval(['std_thickness_inter = std_thickness_inter_B',...
        sprintf(batchID),';']);
    eval(['rstd_thickness_inter = rstd_thickness_inter_B',...
        sprintf(batchID),';']);
    eval(['std_thickness_intra = std_thickness_intra_B',...
        sprintf(batchID),';']);
    eval(['rstd_thickness_intra = rstd_thickness_intra_B',...
        sprintf(batchID),';']);
    eval(['n_pellets = n_pellets_B',sprintf(batchID),';']);

    %% LOAD Manual Data
    load([datapath,exp_name,filesep,'Manual\','offlineOCT_',...
        sprintf(batchID),'.mat']);
    load([datapath,exp_name,filesep,'Manual\','Qicpic_',...
        sprintf(batchID),'.mat']);

    eval(['MittelwerteBlock_offline = MittelwerteBlock_offline_',...
        sprintf(batchID),';']);
    eval(['StandardabweichungMittelwerteBlock_offline = '...
        'StandardabweichungMittelwerteBlock_offline_',...
        sprintf(batchID),';']);
    eval(['MittelwertVMD_Qicpic = MittelwertVMD_Qicpic_',...
        sprintf(batchID),';']);
```

```
    eval(['MittelwertStandardabweichungenBlock_offline = '...
        'MittelwertStandardabweichungenBlock_offline_',...
        sprintf(batchID),';']);
    eval(['VMD_Qicpic = VMD_Qicpic_',sprintf(batchID),';']);
    %% Data of the pellet and the coating material
    data.r = 711.3*10^-6;      % Radius pellet [m]
    data.rho_core = 1110.5;    % Density of the pellet [kg/m^3]
    data.m_pellets = 450*10^-3;  % Mass of the pellets without coating [kg]
    data.rho_coat = 1056;  % Density of the coating [kg/m^3]
    data.ds = 100;             % Dry substance [%]
    %% Process parameter
    data.rate = 7.0*10^-3/60;       % Mass flow spray solution [kg/s]
    data.cr = data.rate*(data.ds/100); % Mass flow spray solution
    % dry substance [kg/s]
    data.N_sample = 6;              % Number of the samples
    T_sample = [4 10 16 22 28 32]; % Sample time [min]

    %% Mass of the samples [kg]
    if batchID=='03'
        m_sample = [4.1*10^-3,5.9*10^-3,7.2*10^-3,7.8*10^-3,4.8*10^-3,...
            4.5*10^-3];
    end
    if batchID=='04'
        m_sample = [5.4*10^-3,2.9*10^-3,5.6*10^-3,12.2*10^-3,...
            10.7*10^-3,7.0*10^-3];
    end
    if batchID=='05'
        m_sample = [6.1*10^-3,7.3*10^-3,8.7*10^-3,9.8*10^-3,5.6*10^-3,...
            10.3*10^-3];
    end
end
%% Cellets+Eudragit
if mat==2

    exp_name = 'Eudragit';
    batchID = '04';

    %% LOAD Automatic Data
    load([datapath,exp_name,filesep,'B',batchID,'_offline']);

    eval(['mean_thickness_total = mean_thickness_total_B',...
        sprintf(batchID),';']);
    eval(['std_thickness_inter = std_thickness_inter_B',...
        sprintf(batchID),';']);
    eval(['rstd_thickness_inter = rstd_thickness_inter_B',...
        sprintf(batchID),';']);
    eval(['std_thickness_intra = std_thickness_intra_B',...
        sprintf(batchID),';']);
    eval(['rstd_thickness_intra = rstd_thickness_intra_B',...
        sprintf(batchID),';']);
    eval(['n_pellets = n_pellets_B',sprintf(batchID),';']);
    %% Data of the pellet and the coating material
    data.r = 0.6*10^-3;           % Radius pellet [m]
    data.rho_core = 0.84*10^3;    % Density of the pellet [kg/m^3]
    data.m_pellets = 300*10^-3;  % Mass of the pellets without coating [kg]
    data.rho_coat = 1.585*10^3;  % Density of the coating [kg/m^3]
    data.ds = 20;                 % Dry substance [%]
    %% Process parameter
    data.rate = 12.0*10^-3/60;      % Mass flow spray solution [kg/s]
    data.cr = data.rate*(data.ds/100); % Mass flow spray solution
    % dry substance [kg/s]
```

```
    data.N_sample = 8;              % Number of the samples
    T_sample = [8 16 24 32 40 48 56 64];  % Sample time [min]

    %% Mass of the samples [kg]
    m_sample = [7.6*10^-3,8.0*10^-3,9.2*10^-3,8.9*10^-3,9.7*10^-3,...
        8.9*10^-3,8.6*10^-3,11.0*10^-3];
end

%% Theoretical coating growth model (Book Easy Coating)

d_coat = @(t) (data.r*(((data.cr*t)/data.m_pellets*(data.rho_core/...
    data.rho_coat)+1).^(1/3)-1));

%% FIT q (loss of coating material) for coating growth model with sampling:

q0 = 0.9; %Initial value

d_sample_func = @(q,t) func_coatmod_t(data,m_sample,T_sample,q,t);

q_fit = nlinfit(T_sample.*60,mean_thickness_total',d_sample_func,q0);

[d_coat_sample] = func_coatmod(data,m_sample,T_sample,q_fit);

N = length(d_coat_sample);
t_func = 1:N;

%% Fit parameter a for RSD of mean coating thickness (inter)

a0 = 1000; %Initial value

cv_t = @(a,t) (a*sqrt(1./t));

a_fit = nlinfit(T_sample.*60,rstd_thickness_inter'*100,cv_t,a0);

%% ParaCaSt+Dynasan
if mat==1

    %% Create plot coating thickness
    figure(1)
    plot(t_func/60,d_coat(t_func)*10^6,'Color','g','LineWidth',1);
    hold on;
    plot(t_func/60,d_coat_sample*10^6,'-.bl','LineWidth',1);
    errorbar(T_sample,mean_thickness_total*10^6,...
        std_thickness_inter*10^6,'rx','LineWidth',1);
    plot(T_sample, MittelwerteBlock_offline,'ko','LineWidth',1);
    plot(T_sample,MittelwertVMD_Qicpic,'ms');
    xlabel('Process time [min]');
    ylabel('Coating thickness, \mu_{sample} [µm]');
    axis([0 33 -10 155]);
    leg=legend('Theor. growth model','Theor. growth model + sampling',...
        'Automatic','Manual','Particle size analysis');
    set(leg,'Location','NorthWest')
    hold off;
    % Save Plot
    figpath = 'fluid_bed_coating\';
    printFig([savefigurespath,figpath,exp_name,'\','B',batchID,...
        '\Offline'],'coat_mod_offline');
```

```
%% Create plot RSD of mean coating thickness (inter)
figure(2)
plot(T_sample,rstd_thickness_inter*100,'rx','LineWidth',1);
hold on;
plot(T_sample,(StandardabweichungMittelwerteBlock_offline./...
    MittelwerteBlock_offline)*100,'ok','LineWidth',1);
plot(t_func./60,cv_t(a_fit,t_func));
hold off;
xlabel('Process time [min]');
ylabel('RSD of mean coat. thickness, cv_{sample} [%]');
axis([0 33 0 110]);

leg = legend('Automatic','Manual','Fit a');
text(22.25,79.00,'$cv=a.(1/t)^{1/2}$','interpreter','latex',...
    'FontSize',12);
set(leg,'Location','NorthEast');

% Save Plot
figpath = 'fluid_bed_coating\';
printFig([savefigurespath,figpath,exp_name,'\','B',batchID,...
    '\Offline'],'rsd_inter_offline');

%% Create plot mean of RSD of coating thickness (intra)
figure(3)
plot(T_sample,rstd_thickness_intra*100,'rx','LineWidth',1);
hold on;
plot(T_sample,(MittelwertStandardabweichungenBlock_offline./...
    MittelwerteBlock_offline)*100,'ok','LineWidth',1);
hold off;
xlabel('Process time [min]');
ylabel('Mean of RSD of coat. thickness, \mu_{cv,sample} [%]');
axis([0 33 0 60]);
leg = legend('Automatic','Manual');
set(leg,'Location','NorthEast')
% Save Plot
figpath = 'fluid_bed_coating\';
printFig([savefigurespath,figpath,exp_name,'\','B',batchID,...
    '\Offline'],'rsd_intra_offline');

%% Evaluation B03/04/05
if B03_4_5==1

    load([datapath,exp_name,filesep,'B03_offline']);
    load([datapath,exp_name,filesep,'B04_offline']);
    load([datapath,exp_name,filesep,'B05_offline']);

    %% Create plot coating thickness
    figure(4)
    plot(t_func/60,d_coat(t_func)*10^6,'Color','g','LineWidth',1);
    hold on;
    plot(t_func/60,d_coat_sample*10^6,'-.bl','LineWidth',1);
    plot(T_sample,mean_thickness_total_B03*10^6,'rs','LineWidth',1);
    plot(T_sample,mean_thickness_total_B04*10^6,'mo','LineWidth',1);
    plot(T_sample,mean_thickness_total_B05*10^6,'k+','LineWidth',1);
    xlabel('Process time [min]');
    ylabel('Coating thickness, \mu_{sample} [µm]');
    axis([0 33 -10 155]);
    leg = legend('Theor. growth model',...
        'Theor. growth model + sampling','Automatic B01',...
        'Automatic B02','Automatic B03');
```

```
        set(leg,'Location','NorthWest')
        hold off;
        % Save Plot
        figpath = 'fluid_bed_coating\';
        printFig([savefigurespath,figpath,exp_name,'\','B',batchID,...
            '\Offline'],'coat_mod_offline_B01_2_3');

        %% Create plot RSD of mean coating thickness (inter)
        figure(5)
        plot(T_sample,rstd_thickness_inter_B03*100,'rs','LineWidth',1);
        hold on;
        plot(T_sample,rstd_thickness_inter_B04*100,'mo','LineWidth',1);
        plot(T_sample,rstd_thickness_inter_B05*100,'k+','LineWidth',1);
        plot(t_func./60,cv_t(a_fit,t_func));
        hold off;
        xlabel('Process time [min]');
        ylabel('RSD of mean coat. thickness, cv_{sample} [%]');
        axis([0 33 0 110]);

        leg = legend('Automatic B01','Automatic B02','Automatic B03',...
            'Fit a');
        text(21.00,72.00,'$cv=a.(1/t)^{1/2}$','interpreter','latex',...
            'FontSize',12);
        set(leg,'Location','NorthEast');

        % Save Plot
        figpath = 'fluid_bed_coating\';
        printFig([savefigurespath,figpath,exp_name,'\','B',batchID,...
            '\Offline'],'rsd_inter_offline_B01_2_3');

        %% Create plot mean of RSD of coating thickness (intra)
        figure(6)
        plot(T_sample,rstd_thickness_intra_B03*100,'rs','LineWidth',1);
        hold on;
        plot(T_sample,rstd_thickness_intra_B04*100,'mo','LineWidth',1);
        plot(T_sample,rstd_thickness_intra_B05*100,'k+','LineWidth',1);
        hold off;
        xlabel('Process time [min]');
        ylabel('Mean of RSD of coat. thickness, \mu_{cv,sample} [%]');
        axis([0 33 0 60]);
        leg = legend('Automatic B01','Automatic B02','Automatic B03');
        set(leg,'Location','NorthEast')
        %Save Plot
        figpath = 'fluid_bed_coating\';
        printFig([savefigurespath,figpath,exp_name,'\','B',batchID,...
            '\Offline'],'rsd_intra_offline_B01_2_3');

    end
end
%% Cellets+Eudragit
if mat==2
    %% Calculate the porosity of the coating layer
    q_min=0.60;
    q_max=0.70;

    eps_min=1-(q_min/q_fit);

    eps_max=1-(q_max/q_fit);

    eps_mean=(eps_min+eps_max)/2;
```

```
q_new=q_fit*(1-eps_mean);

% Density of the coating with porosity [kg/m^3]
data.rho_coat = 1.585*10^3*(1-eps_mean);

%% Theoretical coating growth model (Book Easy Coating)

d_coat = @(t) (data.r*(((data.cr*t)/data.m_pellets*(data.rho_core/...
    data.rho_coat)+1).^(1/3)-1));

%% Coating growth model with sampling

[d_coat_sample] = func_coatmod(data,m_sample,T_sample,q_new);

N = length(d_coat_sample);
t_func = 1:N;

%% Create plot coating thickness
figure(1)
plot(t_func/60,d_coat(t_func)*10^6,'Color','g','LineWidth',1);
hold on;
plot(t_func/60,d_coat_sample*10^6,'-.bl','LineWidth',1);
errorbar(T_sample,mean_thickness_total*10^6,...
    std_thickness_inter*10^6,'rx','LineWidth',1);
xlabel('Process time [min]');
ylabel('Coating thickness, \mu_{sample} [µm]');
axis([0 65 -10 200]);
leg = legend('Theor. growth model','Theor. growth model + sampling',...
    'Automatic');
set(leg,'Location','NorthWest')
hold off;
% Save Plot
figpath = 'fluid_bed_coating\';
printFig([savefigurespath,figpath,exp_name,'\','B',batchID,...
    '\Offline'],'coat_mod_offline');

%% Create plot RSD of mean coating thickness (inter)
figure(2)
plot(T_sample,rstd_thickness_inter*100,'rx','LineWidth',1);
hold on;
plot(t_func./60,cv_t(a_fit,t_func));
hold off;
xlabel('Process time [min]');
ylabel('RSD of mean coat. thickness, cv_{sample} [%]');
axis([0 65 0 150]);

leg = legend('Automatic','Fit a');
text(43.75,118.00,'$cv=a.(1/t)^{1/2}$','interpreter','latex',...
    'FontSize',12);
set(leg,'Location','NorthEast');

% Save Plot
figpath = 'fluid_bed_coating\';
printFig([savefigurespath,figpath,exp_name,'\','B',batchID,...
    '\Offline'],'rsd_inter_offline');

%% Create plot mean of RSD of coating thickness (intra)
figure(3)
plot(T_sample,rstd_thickness_intra*100,'rx','LineWidth',1);
```

```
    xlabel('Process time [min]');
    ylabel('Mean of RSD of coat. thickness, \mu_{cv,sample} [%]');
    axis([0 65 0 60]);
    leg = legend('Automatic');
    set(leg,'Location','NorthEast')
    % Save Plot
    figpath = 'fluid_bed_coating\';
    printFig([savefigurespath,figpath,exp_name,'\','B',batchID,...
        '\Offline'],'rsd_intra_offline');

end
```

```
% ========================================================================
% AUTOMATIC DATA ANALYSIS INLINE (FLUID BED COATING)
% ========================================================================
%   A3.12: Optical Coherence Tomography
%   Research Center Pharmaceutical Engineering GmbH
%
%   Author: Alois Herzog
%   Version: 002
%   Date: 30/07/2015
% ------------------------------------------------------------------------
%%
close all;
clear all;
clc;
%% Install init
pathtoinit = '../../'; % 2 folders back
addpath(pathtoinit);   % Add folders to search path

init;                  % Initialize framework and set default configuration

load([datapath,'options_intdet.mat']);

system = 5;

InitParamProperties;

options_intdet.weights_u = [0.6 0.3];   % weights upper interface
options_intdet.weights_l = [0.3 0.6];   % weights lower interface
options_intdet.sigma_u = 3;
options_intdet.sigma_l = 5;
options_intdet.filter = 'hessian';

options_intdet.horizont = 2;

options_intdet.delta_min = 5;
options_intdet.delta_max = 200;
%% Selection Material: (Core+Coating)
%  ParaCaSt+Dynasan= 1 or Cellets+Eudragit=2
mat = 1;

display_circle = 1;  % Show Circle Fit and save
xyz = 1;

%% ParaCaSt+Dynasan
if mat==1

    exp_name = 'ParaCast';
    batch = 'B03_Show';     % Insert batch name
    data_format = 0;        % bmp. data file

    param.num_ascan = 1000;
    param_detection.displacement = 2.94/param.num_ascan*10^-3; %x direction
    % [m/Pixel]
    param_detection.res_axial = 1.46/600*10^-3; % z direction [m/Pixel]
    param.res_axial = param_detection.res_axial;
    param_detection.R = 711.3*10^-6; % Radius Pellet [m]

    param.n_i = 1.4385;         % Refraction index Dynasan 118
    param_detection.n_i =  param.n_i;
```

```
    limit = 0.60;               % Contrast OCT file
    pel_min = 50;               % Minimum for pellet detection
    filter = 1.8;               % Filter for classification air/pellet

    param.error_max = 3*10^-5;  % Circle Fit error

    delta_min_vec = [5 15 35 45 60 70]*10^-6; % Initial value for
    % coating thickness [m]
end
%% Cellets+Eudragit
if mat==2

    exp_name = 'Eudragit';
    batch = 'B04_Show';      % Insert batch name
    data_format = 1;         % raw. Datei

    param.num_ascan = 1024;
    param_detection.displacement = 3.13/param.num_ascan*10^-3; %x direction
    % [m/Pixel]
    param_detection.res_axial = 3.13/param.num_ascan*10^-3; % z direction
    % [m/Pixel]
    param_detection.R = 0.0006; % Radius pellet [m]

    param.n_i = 1.48;           % Refraction index Eudragit
    param_detection.n_i =  param.n_i;

    limit = 0.82;                % Contrast OCT file
    pel_min = 50;                % Minimum for pellet detectionn
    filter = 1.8;                % Filter for classification air/pellet

    param.error_max = 3*10^-5;   % Circle Fit error

    delta_min_vec = [5 15 30 45 55 70 85 95]*10^-6; % Initial value for
    % coating thickness [m]

end
%% Request .raw or .bmp data files
if data_format
    data_types = '*.raw';
    InitNuFFT(param);   % Fast fourier transform
else
    data_types = '*.bmp';
end

%%
path_to_folder = ...
    ['Z:\K1\A3.12\100_Daten\DATEN\A3_MED_FluidBedCoating\',exp_name,...
    '\Inline\',batch];

%% Data Sorting
current_folder = pwd;
cd(path_to_folder);
filelisting = dir(data_types);
[r inx] = sort({filelisting.date});
filelisting = filelisting(inx);
cd(current_folder);

N = length(filelisting);
```

```
file_start_idx = 1;
file_end_idx = N;

if file_end_idx > N
    file_end_idx = N;
end

mean_thickness = cell(N,1);
std_thickness = cell(N,1);
elapsed_time_sec = zeros(N,1);

%%
mean_thickness_total = zeros(N,1);
std_thickness_inter = zeros(N,1);
rstd_thickness_inter = zeros(N,1);

std_thickness_intra = zeros(N,1);
rstd_thickness_intra = zeros(N,1);

n_pellets = zeros(N,1);

%% Generate Reference Image
if data_format
    sample1 = reshape(GetSingleRawFile(fullfile(path_to_folder,...
        filelisting(1).name)),...
        param.num_pixel,param.num_ascan);
    reference = repmat(EstimateReference(sample1),1,param.num_ascan);
end
%% OCT file
for file_idx = file_start_idx:file_end_idx;
    if data_format
        current_raw_file = fullfile(path_to_folder,...
            filelisting(file_idx).name);
        sample = reshape(GetSingleRawFile(current_raw_file),...
            param.num_pixel,param.num_ascan);
        reference = repmat(EstimateReference(sample),1,param.num_ascan);
        stat = dir(current_raw_file);
        timestamp = stat.date;
        img = NuFFT(sample, reference);
    else
        file_name = filelisting(file_idx).name;
        cd(path_to_folder);
        img_raw = imread(file_name);
        img = double(img_raw)./255;
        cd(current_folder);
    end
    %% Prepare image data
    % ---------------------------------------------------------------------
    fprintf('... Prepare data (image %i, %s, %s)\n',file_idx, ...
        filelisting(file_idx).name,filelisting(file_idx).date);
    img_disp = img;
    img_disp(img_disp>limit) = limit;   % Contrast OCT file
    img_disp = img_disp./limit;
    img_cut = img_disp(30:end-500,:);   % Delete reference line and
    % lower area
    %% Function for detection the reach of interest
    [img_roi] = func_roi(img_cut);
    %% Function for classification air/pellet
    trans = func_class(img_roi,pel_min,filter);
    %% Interface Detection
    trans_n = size(trans,1);
```

```
path_u_sp = zeros(param.num_ascan,1);
path_l_sp = zeros(param.num_ascan,1);

figure(1);
imagesc(img_roi);
colormap('gray')
xlabel('Pixel');
ylabel('Pixel');
axis([0 1000 0 400]);
set(gca,'XTick', 0:200:1000);
set(gca,'YTick', 0:100:400);
hold on;
%% Detected pellet
for ii = 1:1:trans_n

    min_trans = trans(ii,1);
    max_trans = trans(ii,2);
    img_roi_col = img_roi(:,min_trans:max_trans); % Reach of interest
    %% Function Interface Detection
    fprintf('... Interface Detection\n');

    [feature_vec idx_window_1] = getFeatureVector(img_roi_col,...
        25,25);

    [path_utmp,path_ltmp,~,error] = ...
        DetectInterfaces(img_roi_col, param_detection,...
        options_intdet,idx_window_1,...
        'unconstrained', 0,'display',0); % 1=show filter

    if error
        trans(ii,:) = 0;
        fprintf('DEBUG: Interface Detection failed!\n');
    else
        path_u_sp(min_trans:...
            max_trans) = path_utmp;

        path_l_sp(min_trans:...
            max_trans) = path_ltmp;
    end
    %%

end
if ~isempty(trans)
    trans = trans(trans(:,1)~=0,:);
end

%% Correct distortions
fprintf('... Correct distortion\n');

trans_n = size(trans,1);
x_oct = (0:length(path_u_sp)-1)';
x_correct = x_oct.*param_detection.displacement;
z_correct = path_l_sp.*param_detection.res_axial;

center_sphere_est_u = zeros(trans_n,3);
center_sphere_est_l = zeros(trans_n,3);

mean_thickness_est = zeros(trans_n,1);
std_thickness_est = zeros(trans_n,1);
```

```
error = zeros(trans_n,1);
%% Detected pellet
for ii = 1:1:trans_n

    % Row vector of the detected pellets upper interface
    path_u_ = path_u_sp(trans(ii,1):...
        trans(ii,2)).*param_detection.res_axial;

    % Row vector of the detected pellets lower interface
    path_l_ = path_l_sp(trans(ii,1):...
        trans(ii,2)).*param_detection.res_axial;

    % x coordinate upper interface
    x_A = x_oct(trans(ii,1):...
        trans(ii,2)).*param_detection.displacement;

    %% Circle Fit upper interface
    [center_sphere_est_u(ii,:) error(ii)] = ...
        circleFitSingleTablet([x_A path_u_],...
        param_detection);
    %%
    if error(ii) > param.error_max
        center_sphere_est_u(ii,:) = 0;
        trans(ii,:) = 0;
        fprintf('DEBUG: Circle fit error too large!\n');
        fprintf('DEBUG: Error: %d\n', error(ii));
    else
        center = [center_sphere_est_u(ii,1)-...
            trans(ii,1).*param_detection.displacement; ...
            center_sphere_est_u(ii,2)];
        %% Correct Curvature Snells Law
        [ x_B z_B theta_j] = ...
            correctCurvature( x_A -...
            trans(ii,1)*...
            param_detection.displacement, path_u_, path_l_, ...
            center, param_detection);
        %% Correct Coordinates
        x_correct(trans(ii,1):trans(ii,2)) = x_B + ...
            trans(ii,1).*param_detection.displacement;

        z_correct(trans(ii,1):trans(ii,2)) = z_B;
        %% Circle Fit lower interface
        center_sphere_est_l(ii,:) = circleFitSingleTablet(...
            [x_correct(trans(ii,1):trans(ii,2)) ...
            z_correct(trans(ii,1):...
            trans(ii,2))],param_detection,center_sphere_est_u(ii,:));
        %% Polar Coordinates
        [dist_u_sp phi_u] = GetPolarCoordinates([x_A path_u_], ...
            center_sphere_est_u(ii,1:2));

        [dist_l_sp phi_l] = GetPolarCoordinates(...
            [x_correct(trans(ii,1):trans(ii,2))...
            z_correct(trans(ii,1):trans(ii,2))], ...
            center_sphere_est_l(ii,1:2));
        %% Identical angle upper and lower interface
        idx_min = zeros(length(phi_u),1);
        for i = 1:length(phi_u)
            [val idx_min(i)] = min(abs(phi_u(i)-phi_l));
        end
        %% Calculating coating thickness
        thickness_est = dist_u_sp - dist_l_sp(idx_min);
```

```
            mean_thickness_est(ii) = mean(thickness_est);
            std_thickness_est(ii) = std(thickness_est);
            %% Plot Interface Detection
            plot(trans(ii,1):trans(ii,2),round(path_u_./...
                param_detection.res_axial),'g','LineWidth',1)
            plot(trans(ii,1):trans(ii,2),round(path_l_./...
                param_detection.res_axial),'g','LineWidth',1)

            if display_circle
                % Upper Interface
                height_u = 2*center_sphere_est_u(ii,3)/...
                    param_detection.res_axial;
                width_u = 2*center_sphere_est_u(ii,3)/...
                    param_detection.displacement;

                center_u = [center_sphere_est_u(ii,1)/...
                    param_detection.displacement ...
                    center_sphere_est_u(ii,2)/...
                    param_detection.res_axial];

                rectangle('position',[center_u(1)-...
                    width_u/2,center_u(2)-...
                    height_u/2,width_u,height_u],...
                    'curvature',[1,1],'linestyle','-','linewidth',2,...
                    'edgecolor','r');
            end
        end
        %%
        fprintf('Mean coating thickness: %6.2f µm\n',...
            mean_thickness_est(ii)*10^6);
        fprintf('Standard deviation: %6.2f µm\n',...
            std_thickness_est(ii)*10^6);
    end

    hold off;

    %% Save Plot mit circle
    if display_circle
        figpath = 'fluid_bed_coating\';
        printFig([savefiguresPath,figpath,exp_name,'\',batch,...
            '\Inline'],num2str(xyz));

        xyz = xyz+1;
    end
    %%
    idx_use = mean_thickness_est~=0; % Only coating thickness unequal 0

    mean_thickness_est = mean_thickness_est(idx_use);
    std_thickness_est = std_thickness_est(idx_use);

    %% Calculation coating parameters
    mean_thickness{(file_idx)} = mean_thickness_est;
    std_thickness{(file_idx)} = std_thickness_est;
    %%
end
```

```
function [img_roi] = func_roi(img)
% ========================================================================
% FUNCTION FOR DETECTION THE REGION OF INTEREST (FLUID BED COATING)
% ========================================================================
%   A3.12: Optical Coherence Tomography
%   Research Center Pharmaceutical Engineering GmbH
%
%   Author: Alois Herzog
%   Version: 001
%   Date: 14/07/2015
% ------------------------------------------------------------------------
%%  Input:
%   img         OCT file
%
%%  Output:
%   img_roi     OCT file without the protection foil
%%

img_mean=mean(img,2);       % Mean value of the A-scan per row

foil_offset = 10;           % Offset protection foil
[val idx]= min(img_mean);   % Detect minimum
idx_roi = idx + foil_offset;

img_mean_part = img_mean(idx(1):end);

r_xx_corr = acf(img_mean_part,100);  % Autocorrelation function

[val idx_max] = max(r_xx_corr(20:end));

if val > 0.34
    idx_roi = idx_roi + idx_max + 19;
end

img_roi = img(idx_roi:end,:); %Region of interest

end
```

```
function [trans_reshape] = func_class(img_roi,pel_min,filter)
% ========================================================================
% FUNCTION FOR CLASSIFICATION AIR/PELLET (FLUID BED COATING)
% ========================================================================
%   A3.12: Optical Coherence Tomography
%   Research Center Pharmaceutical Engineering GmbH
%
%   Author: Alois Herzog
%   Version: 001
%   Date: 13/07/2015
% ------------------------------------------------------------------------
%%  Input:
%   img_roi         OCT file
%   pel_min         Minimum for the pellet detection
%   filter          Filter for classification air/pellet
%
%%  Output:
%   trans_reshape   Vector with the classified pellets
%%
[size_z size_x] = size(img_roi);

w_size = 150;
[feature_vec idx_window_1] = getFeatureVector(img_roi,w_size,w_size);

img_mean_col = idx_window_1;

idx_col=round(size_x/2);
val_col=img_mean_col(idx_col);

mean_filt = zeros(size_x,1);
mean_filt(idx_col) = val_col;

idx_filt_savg = savGol(idx_window_1, 5, 5, 1); % Filter "Savitzky Golay"

diff_filt = savGol(diff(idx_filt_savg(1:1:end)), 15, 15, 1);

class = zeros(size_x,1);

class(abs(diff_filt)<filter) = 1;

%% Plot Filter for classification air/pellet
% figure(111)
% plot(idx_filt_savg)
%
% figure(112)
% plot(diff_filt)
%
% figure(113)
% plot(img_mean_col)
% hold on;
% plot(mean_filt,'r')
% hold off;
%%
transitions_tmp = class(2:end) - class(1:end-1);

if  mean(class(1:5))== 1
    transitions_tmp(1) = 1;
end
```

```
if mean(class(end-5:end)) == 1
    transitions_tmp(end) = 1;
end

trans = find(transitions_tmp)';

N = length(trans);

if mod(N,2)==0 % Check if even
    trans_reshape = reshape(trans,2,N/2)';
    trans_reshape(:,1) = trans_reshape(:,1)+50;
    trans_reshape(:,2) = trans_reshape(:,2)-50;
    idx_trans = trans_reshape(:,2) - trans_reshape(:,1) > pel_min;
    trans_reshape = trans_reshape(idx_trans,:);
else
    trans_reshape=[];
    fprintf('Error Pellet Detection');
end

end
```

```
function [d_coat_sample_t] = func_coatmod_t(data,m_sample,T_sample,q,t)
% ========================================================================
% FUNCTION FOR CALCULATING THE THEOR. COATING THICKNESS (FLUID BED COATING)
% ========================================================================
%   A3.12: Optical Coherence Tomography
%   Research Center Pharmaceutical Engineering GmbH
%
%   Author: Alois Herzog
%   Version: 001
%   Date: 10/07/2015
% ------------------------------------------------------------------------
%%  Input:
%   data       Data of the pellet and the coating material
%   m_sample   Mass of the samples [kg]
%   T_sample   Sample time [min]
%   q          Loss of coating []
%   t          Time vektor [s]
%%  Output:
%   d_coat_sample_t     Theoretical coating thickness+sampling [m]
%%
d_coat_sample = func_coatmod(data,m_sample,T_sample,q);
d_coat_sample_t = d_coat_sample(t)';
end
```

```
function [d_coat_sample] = func_coatmod(data,m_sample,T_sample,q_fit)
% ========================================================================
% FUNCTION FOR CALCULATING THE THEOR. COATING THICKNESS (FLUID BED COATING)
% ========================================================================
%   A3.12: Optical Coherence Tomography
%   Research Center Pharmaceutical Engineering GmbH
%
%   Author: Alois Herzog
%   Version: 002
%   Date: 22/09/2015
% ------------------------------------------------------------------------
%%  Input:
%   data       Data of the pellet and the coating material
%   m_sample   Mass of the samples [kg]
%   T_sample   Sample time [min]
%   q_fit      Loss of coating []
%%  Output:
%   d_coat_sample   Theoretical coating thickness+sampling [m]
%%
r = data.r;
rho_core = data.rho_core;
rho_coat = data.rho_coat;
m_pellets = data.m_pellets;
N_sample = data.N_sample;
cr = data.cr;
%%
func = @(r,K) (r*((K.*(rho_core/rho_coat)+1).^(1/3)-1));
d_coat_sample = zeros(T_sample(end)*60,1);

for i=1:N_sample

    if i==1
        delta_T_sample = T_sample(i);
    else
        delta_T_sample = T_sample(i)-T_sample(i-1);
    end

    xdata = 0:(delta_T_sample*60-1);

    K = q_fit*cr.*xdata./m_pellets;

    if i==1
        d_coat_sample(1:T_sample(i)*60) = func(r,K);
    else
        d_coat_sample(T_sample(i-1)*60+1:T_sample(i)*60) = ...
            d_coat_sample(T_sample(i-1)*60) + ...
            func(r+d_coat_sample(T_sample(i-1)*60),K);
    end

    if i==1
        m_coat = 0;
    end

    m_pellets_coat = m_pellets+cr*(delta_T_sample*60-1)+m_coat;

    m_sample_coat = (m_sample(i)/m_pellets_coat)*...
        (cr*(delta_T_sample*60-1)+m_coat);

    m_pellets = m_pellets-(m_sample(i)-m_sample_coat);
```

```
    m_coat = m_coat-m_sample_coat+cr*(delta_T_sample*60-1);

end
end
```